Transport into fungal haustoria; ultrastructure, autoradiography and cytochemistry.

Peter Tyrell Nelson Spencer-Phillips.

Ph.D. Thesis

Imperial College of Science and Technology

University of London

To my family ; past, present and future.

ERECTUS SED NON ELATUS

Abstract.

The thesis is arranged in three sections:

1. The distribution and ultrastructure of Phyllactinia guttata within leaves of Corylus avellana and Betula pendula are described. Caffeine improved fixation by restricting osmiophilic phenolic material to the vacuoles of uninfected cells but was less effective in cells which were necrotic or contained haustoria.

2. Electron microscope autoradiography was carried out on haustorial complexes isolated from leaves of Pisum sativum infected with Erysiphe pisi and exposed to $^{14}CO_2$. The distribution of ^{14}C was related to the volumes estimated by morphometry. Three classes of complex were distinguished by isotope concentration, ultrastructure and U.V. fluorescence microscopy. All components of one class in particular were labelled, haustorial lobes and extrahaustorial membranes showing the highest densities. The ultrastructure of necrotic regions of infected leaves is also described.

3.Sites of phosphatase activity were determined by a lead precipitation technique and electron microscopy in leaves of P. sativum and Phaseolus vulgaris infected with E. pisi and Uromyces appendiculatus respectively.

In both plants ATPase activity was higher at plasma membranes of epidermal, phloem transfer and companion cells than in other cells. Extrahaustorial regions of host plasma membranes showed no enzyme activity but infection did not otherwise alter the

distribution of activities. Transition of activities always occurred at haustorial neckbands. Only E. pisi haustoria showed phosphatase activity at their haustorial plasma membranes.

Sub-cellular fractionation indicated that infection of stem epidermis of P. sativum by E. pisi increased Mg^{2+}-ATPase activity at plasma membranes whereas Peronospora pisi infections reduced activities in leaves. Attempts to localise ATPase in leaves of Hordeum vulgare infected with Erysiphe graminis were unsuccessful.

Results are discussed with special regard to the factors influencing translocation through infected cells and a mechanism of solute transport into haustoria is proposed.

Acknowledgements.

Special thanks are due to Dr. John Gay for his guidance, encouragement and patience without which this work would not have been initiated or completed.

I am also indebted to many others in London, Liverpool and elsewhere for their advice and friendship. In particular the staff of the E.M. Unit at Imperial College, Chris Makepeace and Wendy Thompson are gratefully acknowledged.

Table of Contents. Page Numbers.

Title. 1

Dedication. 2

Abstract. 3

Acknowledgements. 5

Table of contents. 6

List of tables. 11

List of figures. 12

List of plates. 13

Introduction. 17

MATERIALS AND METHODS. 20

1. Hosts and fungi. 20

1.1. Species. 20

1.2. Cultivation. 20

1.2.1. Powdery mildews. 20

a. *Erysiphe pisi*/*Pisum sativum*. 20

b. *Erysiphe graminis*/*Hordeum vulgare*. 21

c. *Phyllactinia guttata*/*Corylus avellana* and *Betula pendula*. 22

1.2.2. Rust. *Uromyces appendiculatus*/*Phaseolus vulgaris*. 22

1.2.3. Downy mildew. *Peronospora pisi*/*Pisum sativum*. 22

2. Preliminary preparative procedures. 23

2.1. Isolation of haustorial complexes. 23

2.2. Isolation of cuticle. 25

3. Transmission electron microscopy. 26

3.1. Fixation and embedding. 26

3.1.1. Routine schedule. 26

3.1.2. Manipulation of specimens at fixation. 28

a. Leaves. 28

b. Haustorial complexes. 28

c. Epidermis. 29

d. Cuticle. 29

3.1.3. Caffeine fixation for phenol-containing cells. 29

3.2. Sectioning and staining. 30

3.3. Microscopes. 31

4. Light microscopy. 31

4.1. Bright field and phase contrast microscopy. 31

4.1.1. Leaves. 31

4.1.2. Epidermes. 31

a. Neutral red. 32

b. Evans blue. 32

4.1.3. Isolated haustorial complexes. 32

4.2. Fluorescence microscopy. 33

4.2.1. Acetamido-isothiocyanato-stilbene (SITS). 33

4.2.2. Aniline blue. 33

5. Electron microscope autoradiography. 35

5.1. $^{14}CO_2$ labelling. 35

5.2. Preparation of autoradiograms. 36

5.2.1. Membrane method. 36

5.2.2. Flat substrate method. 37

5.3. Quantitative analysis of autoradiograms. 39

6. Localization of phosphatases (ATPase, alkaline and acid phosphatase). 42

6.1. Fixation of specimens. 42

6.2. Incubation with substrate. 43

7. Assay of adenosine triphosphatase activity. 44

7.1. Preparation of samples. 44

7.1.1. Specimens. 44

a. Leaves. 44

b. Haustorial complexes. 44

c. Epidermes. 45

7.1.2. Homogenisation. 45

7.1.3. Preparation of fractions. 46

7.2. Incubation with substrate. 46

7.3. Analytical techniques. 47

7.3.1. Assay of inorganic phosphate. 47

7.3.2. Assay of protein. 48

CHAPTER 1. 49

Ultrastructure of leaves of Corylus avellana and Betula pendula and infection by Phyllactinia guttata. 49

1. Introduction. 49

2. Results. 51

2.1. The effect of caffeine on fixation and ultrastructure. 51

2.2. Organization and ultrastructure of leaves. 52

2.3. Distribution and morphology of electron dense deposits. 54

2.4. Ultrastructure of Phyllactinia guttata and infected leaves. 55

2.4.1. Organization of intercellular hyphal system and distribution of haustoria. 55

2.4.2. Ultrastructure of haustoria and associated structures. 56

2.4.3. Ultrastructure of cells with electron dense cytoplasms. 59

3. Discussion. 61

3.1. Characterization and distribution of the osmiophilic deposits. 61

3.2. Morphology of Phyllactinia in relation to the structure of infected leaves. 63

3.3. Responses to infection and effect of phenolics on haustorial function. 65

CHAPTER 2. 80

Electron microscope autoradiography of ^{14}C photosynthate distribution at the haustorium-host interface and ultrastructure of necrotic tissues in powdery mildew of Pisum sativum. 80

1. Introduction. 80

2. Results. 82

2.1. Isolated fraction. 82

2.2. Infected leaves. 85

2.3. Isotope distribution in the isolated fraction 88

2.4. Isotope distribution among the classes of haustorial complexes. 88

2.5. Isotope distribution among components of healthy haustorial complexes. 89

2.6. Light microscopy and staining with SITS and aniline blue. 90

3. Discussion. 91

3.1. Assimilate distribution in the compatible interaction. 92

3.2. Structure of the extrahaustorial membrane and ^{14}C accumulation. 94

3.3. Mechanism of haustorial necrosis. 96

3.4. Necrosis of infected cells and the nature of wall appositions in mesophyll cells. 99

CHAPTER 3. 122

Phosphatase activity in tissues infected by rust, powdery and downy mildew fungi. 122

1. Introduction. 122

2. Experimental procedures. 126

3. Results. 130

3.1. Phosphatase cytochemistry. 130

3.1.1. Distribution of precipitates in pea and bean leaves. 130

3.1.2. Effect of infection on the distribution of precipitates. 134

3.1.3. Isolation of epidermis from Pisum sativum; phosphatase localization and infection with Erysiphe pisi. 137

3.2. Assays of phosphatase activities. 139

3.2.1. Infections of Erysiphe pisi. 139

a. Activities of ATPase in crude extracts from leaves, epidermes and haustorial complexes. 139

b. Activities of Mg^{2+}-ATPase in fractions from stem epidermis. 142

c. Inhibition of Mg^{2+}-ATPase by NaF. 143

3.2.2. Infections of Peronospora pisi. 144

4. Discussion. 145

4.1. Interpretation of precipitates in phosphatase cytochemistry of pea and bean leaves. 145

4.2. Phosphatase activities and translocation in powdery mildew and rust infected tissues. 147

4.3. Domains of ATPase in plasma membranes and transport in powdery mildew and rust infected cells. 151

4.4. ATPase activities in leaves of Pisum sativum infected with Peronospora pisi. 159

Appendix. Purity of glutaraldehyde used for phosphatase cytochemistry. 201

Plate labels. 202

References. 203

List of tables. Page numbers.

CHAPTER 1.

1.1. Frequency of haustoria and intercellular hyphae of P. guttata in Betula and Corylus leaves. 71

CHAPTER 2.

2.1. Distribution of silver grains in haustorial complex fractions. 103

2.2. Distribution of silver grains in healthy, pre-necrotic and necrotic classes of haustorial complexes. 105

2.3. Distribution of silver grains in haustorial complexes classified by grain density. 106

2.4. Distribution of silver grains in components of healthy haustorial complexes. 107

2.5. Correction indices for component diffuseness of healthy haustorial complexes. 108

2.6. Distribution of silver grains allocated to components of healthy haustorial complexes. 109

CHAPTER 3.

3.1. Locations of lead-phosphate precipitates in leaves of P. sativum and P. vulgaris. 162

3.2. Phosphatase activities of plasma membranes of leaf cells of P. vulgaris. 163

3.3. Phosphatase activities of plasma membranes of leaf cells of P. sativum. 164

3.4. Phosphatase activities of plasma membranes of U. appendiculatus and infected leaf cells of P. vulgaris. 165

3.5. Phosphatase activities of plasma membranes of E. pisi and infected leaf cells of P. sativum. 166

3.6. Germination of conidia of E. pisi on water and epidermis of P. sativum. 167

3.7. ATPase activities in crude extracts of epidermis and leaves of P. sativum uninfected and infected with E. pisi. 168

3.8. ATPase activities in crude extracts of stem epidermis of P. sativum uninfected and infected with E. pisi. 169

3.9. ATPase activities of haustorial complexes isolated from P. sativum infected with E. pisi. 170

3.10. ATPase activities of crude extracts of epidermis and leaves of P. sativum; effect of Mg^{2+} and NaF. 171

3.11. Mg^{2+}-ATPase activities in fractions of stem epidermis of P. sativum. 172

3.12. Mg^{2+}-ATPase activities in fractions of stem epidermis of P. sativum uninfected and infected with E. pisi. 173

3.13. ATPase activities in fractions of stem epidermis of P. sativum uninfected and infected with E. pisi; effect of Mg^{2+}. 174

3.14. Inhibition by NaF of ATPase activities in epidermes, leaves and haustorial complexes. 174

3.15. Mg^{2+}-ATPase activities in fractions from leaves of P. sativum uninfected and infected with P. pisi. 175

List of figures.

MATERIALS AND METHODS.

1. Flow diagram for isolation of haustorial

complexes from pea leaves infected with E. pisi. 24

CHAPTER 2.

2.1. Distribution of silver grains in classes of haustorial complexes. 110

CHAPTER 3.

3.1. Frequencies of flocculent precipitates at plasma membranes of epidermal cells in leaves of P. vulgaris infected with U. appendiculatus. 176

3.2. Frequencies of flocculent precipitates at plasma membranes of mesophyll cells in leaves of P. vulgaris infected with U. appendiculatus. 177

3.3. Frequencies of flocculent precipitates at plasma membranes of minor veins in leaves of P. vulgaris infected with U. appendiculatus. 178

3.4. Diagram of proposed mechanisms of solute transport through pea epidermal cells infected with E. pisi. 179

Appendix.

Absorption spectra of glutaraldehyde solutions. 201

List of plates.

CHAPTER 1.

1.1. Sections of leaves of C. avellana; with and without caffeine treatment. 72

1.2. Transverse section through leaf of C. avellana in region of minor vein. 73

1.3. Light micrographs of lower surface of C. avellana leaves infected with P. guttata. 74

1.4. Sections of leaves of C. avellana infected with P. guttata; stomatal aperture and mesophyll cell inclusion. 75

1.5. Sections of leaf cells of *C. avellana* with healthy and necrotic haustoria of *P. guttata*. 76

1.6. Adjacent sections of haustorium and intercellular hyphae. 77

1.7. Sections of haustorial neck. 78

1.8. Section through haustorium and interfacial structures. 79

CHAPTER 2.

2.1. Section through pellet of haustorial complex fraction. 111

2.2. Longitudinal section of healthy haustorial complex. 112

2.3. Longitudinal sections through neck regions of healthy haustorial complexes. 113

2.4. Sections of healthy, pre-necrotic and necrotic haustorial complexes. 114

2.5. Extrahaustorial membranes of haustorial complex classes. 115

2.6. Sections of necrotic regions of infected leaves. 116

2.7. Sections of epidermal regions of necrotic leaves. 117

2.8. Sections of epidermal cells in necrotic regions of leaves. 118

2.9. Sections of walls of mesophyll and epidermal cells in necrotic regions of leaves. 119

2.10. Point of penetration of epidermal wall and light micrographs of epidermal peels with aniline blue. 120

2.11. Autoradiograms of haustorial complex fraction and light micrographs of haustoria of *E. pisi* and *E. graminis* with SITS. 121

CHAPTER 3.

3.1. Sections of minor veins in leaves of P. vulgaris: ATP and Mg^{2+} ±NaF at pH7.2. 180

3.2. Sections of minor veins in leaves of P. vulgaris: ATP and Mg^{2+}; β-GP and NaF; both at pH 7.2. 181

3.3. Sections of epidermal and mesophyll cells in leaves of P. vulgaris: ATP, Mg^{2+} ±NaF at pH 7.2. 182

3.4. Sections of lower epidermal cells in leaves of P. vulgaris: ATP and Mg^{2+} at pH 7.2. 183

3.5. Section of minor vein in leaf of P. sativum: β-GP and NaF at pH 5.5. 184

3.6. Section of minor vein in leaf of P. sativum: ATP, Mg^{2+} and NaF at pH7.2. 185

3.7. Sections of transfer cells of minor veins in leaves of P. sativum: β-GP and Mg^{2+} at pH 7.2; β-GP at pH 5.5. 186

3.8. Adjacent sections of transfer cell and sieve element of minor vein in leaf of P. sativum: ATP and Mg^{2+} at pH 7.2. 187

3.9. Sections in region of upper epidermis in leaves of P. sativum: ATP and Mg^{2+} ±NaF at pH 7.2; β-GP and NaF at pH 5.5. 188

3.10. Sections of epidermal cell and minor vein in leaf of P. sativum infected with E. pisi: β-GP at pH 5.5; ATP and Mg^{2+} at pH 7.2. 189

3.11. Sections of epidermal cells of P. sativum infected with E. pisi: No substrate control; ATP, Mg^{2+} and NaF; both at pH 7.2. 190

3.12. Sections of epidermal cells in leaves of P. sativum infected with E. pisi: β-GP or ATP and Mg^{2+} at pH 7.2. 191

3.13. Section of epidermal cell infected by

E. pisi in region of haustorial neck: ATP and Mg^{2+} at pH 7.2. 192

3.14. Sections of mesophyll and epidermal cells in leaves of *P. vulgaris* infected with *U. appendiculatus*: No substrate control; ATP and Mg^{2+}; both at pH 7.2. 193

3.15. Sections of mesophyll cells of *P. vulgaris* infected with *U. appendiculatus*: ATP and Mg^{2+}; β-GP and NaF; both at pH 7.2. 194

3.16. Serial sections of neck of haustorium of *U. appendiculatus*: ATP and Mg^{2+} at pH 7.2. 195

3.17. Sections of mesophyll cells of *P. sativum* infected with *P. pisi*: ATP and Mg^{2+} $\pm$NaF at pH 7.2. 196

3.18. Sections of necrotic haustorium in mesophyll cell of *P. sativum* infected with *P. pisi*: ATP and Mg^{2+} at pH 7.2. 197

3.19. Adjacent sections of epidermal cell of *H. vulgare* infected with *E. graminis* (ATP, Mg^{2+} and NaF) and section of epidermal peel from stem of *P. sativum*: ATP and Mg^{2+}; all at pH 7.2. 198

3.20. Sections of leaf of *H. vulgare* (no substrate control) and of cuticle from upper epidermis of *P. sativum*. 199

3.21. Light micrographs of epidermes from leaves and stems of *P. sativum* uninfected or infected with *E. pisi*. 200

Introduction.

Early investigations of haustoria (DeBary, 1870; Smith, 1900) revealed by light microscopy most of the structures which were subsequently confirmed by electron microscopy. Indeed when the present study was initiated the ultrastructure of a wide variety of parasitic interfaces between pathogens and infected plant cells had been described in detail (Bracker and Littlefield, 1973). The most significant progress towards indicating the function of haustoria was probably the demonstration that the extrahaustorial membrane is formed, or at least initiated, by invagination of the host plasma membrane and that the two remain continuous throughout the functional duration of the parasitic interface. However, the structural investigations did not provide evidence that nutrients were transferred from the host via haustoria of biotrophic fungi and consequently there was little indication of the mechanisms by which transport was effected.

Subsequent advances in haustorial physiology have come mainly from ectophytic powdery mildew fungi (Bushnell and Gay, 1978; Gay and Manners, 1981). Extensive studies with powdery mildew of pea have confirmed the circumstantial evidence provided by Ellingboe and co-workers (Martin and Ellingboe, 1978; Slesinski and Ellingboe, 1971) that assimilates are absorbed by haustoria. Moreover the major translocates have been identified as sucrose and glycerol and the biochemistry of their fate in the infecting structures and surface mycelium has been documented (Manners, 1979;

Manners and Gay, 1982). These investigations depended on a procedure for isolating haustorial complexes (Gil and Gay, 1977) which effectively constitute the parasitic interface and include haustoria, the invaginating portion of host plasma membrane and the intervening structures.

Biochemical studies also suggested evidence of mechanisms involved in nutrient transfer. It seems likely that transport across the interface would be favoured by a concentration gradient of translocates maintained by their removal on the haustorial aspect. Thus invertases and conversion to strictly fungal metabolites may contribute to transport (Manners, 1979; Manners and Gay, 1982); however in view of the high rate of assimilate movement that occurs (Manners, 1979) active transport processes seem most probable.

Powdery mildews which form endophytic as well as ectophytic mycelia have largely been neglected. Species of the genera Leveillula and Phyllactinia are of particular interest as they share several features typical of both rust and epiphytic powdery mildew fungi. Consequently, endophytic powdery mildews are potentially useful in comparative studies of the physiology of endo- and ectophytic biotrophic fungi. Before such work can be initiated it is essential that the structural relationships of pathogen and host are determined and therefore the ultrastructure of infections by Phyllactinia guttata were investigated and are reported in the first chapter of this thesis.

The remainder of the thesis is concerned with the distribution of photoassimilates at the parasitic

interface of Erysiphe pisi infections (Chapter 2) and the means by which nutrients are obtained by the pathogen. The latter investigations have concentrated on the role of phosphatases and transport mechanisms in powdery mildew, downy mildew and rust infections (Chapter 3).

Some of the work described here has been published (Spencer-Phillips and Gay, 1980a, b and c; 1981).

MATERIALS AND METHODS.

1.Hosts and fungi.

1.1.Species.

The fungi used in experiments include powdery mildew, rust and downy mildew species. All are obligate pathogens of higher plants and are listed below with their respective hosts.

Pathogen	Host
1.Powdery mildews (Erysiphales)	
Erysiphe pisi DC ex Saint-Amans	*Pisum sativum* L. cv. Onward (Pea)
Erysiphe graminis DC ex Merat	*Hordeum vulgare* L. cv. Golden Promise (Barley)
Phyllactinia guttata (Wallr. ex Fr.)Lev.	*Corylus avellana* L. (Hazel)
Phyllactinia guttata (Wallr. ex Fr.)Lev.	*Betula pendula* Roth. (Birch)
2.Rust (Uredinales)	
Uromyces appendiculatus (Pers.)Unger.	*Phaseolus vulgaris* L. cv. Pinto (French bean)
3.Downy mildew (Peronosporales)	
Peronospora pisi Sydow.	*Pisum sativum* L. cv. Onward (Pea)

1.2.Cultivation.

1.2.1.Powdery mildews.

a.*Erysiphe pisi* / *Pisum sativum*.

Five week old plants of *Pisum sativum* were

inoculated with conidia of Erysiphe pisi by shaking over them plants which had been similarly infected 14 days previously. The pea cultivar Onward was used throughout as it has a high degree of susceptibility and large leaflets and stipules which facilitate isolation of haustorial complexes (Gil,1976). When infected stems were required for experiments large clouds of conidia were released to ensure adequate infection.

Plants were grown in a glasshouse at the University of London Botanical Supply Unit, Egham and at the age of three weeks were removed to the Departmental glasshouse. This was at approximately 22^{o}C and the natural light was supplemented when necessary with artificial light (Mercury vapour lamps, Philips Ltd.) to maintain a minimum daylength of 17h.

Seven days after infection when the upper surfaces of the leaves or the stems were covered with a uniform, confluent mycelium with conidia the material was used for isolation of haustorial complexes and all other experiments requiring infected leaves or stems.

b.Erysiphe graminis / Hordeum vulgare.

Seeds of the susceptible barley cultivar Golden Promise were sown in vermiculite and ten days later the plants were inoculated with conidia of Erysiphe graminis f.sp.hordei (Race Ao) by shaking similarly infected plants over them. Infected and uninfected plants were grown at room temperature and in daylight. Seven days after inoculation infected leaves showing characteristic individual colonies with conidia were used in experiments.

c.Phyllactinia guttata/Corylus avellana and Betula pendula.

Specimens of Corylus avellana with some leaves naturally infected with Phyllactinia guttata were collected at Broadclyst, Devon in late August (1978). Similarly infected specimens of Betula pendula were collected at Gulworthy, Devon. In both plants the superficial mycelium was restricted to the lower surface of the leaves, and cleistothecia at varying stages of development were abundant.

1.2.2.Rust.

Uromyces appendiculatus/Phaseolus vulgaris.

Bean plants were grown from seed in John Innes potting compost (No.2) under glasshouse conditions. Twenty days after sowing both surfaces of the leaves were inoculated by spraying with uredospores suspended in 0.01% Tween 20 at a concentration of $10^4 ml^{-1}$. Plants were kept at 100% relative humidity (under a polyethylene cover) for 16 hours. Uredospores had been collected from similarly infected plants and stored at -20^oC until required. After thawing they were washed several times by centrifugation in distilled water to remove self-inhibitors of germination (Bell and Daly,1962). Seven days after inoculation non-eruptive lesions were visible as chlorotic flecks approximately 1mm in diameter.

1.2.3.Downy mildew.

Peronospora pisi/Pisum sativum.

Plants of Pisum sativum were grown from seed in pots of John Innes potting compost (No.2) in daylight

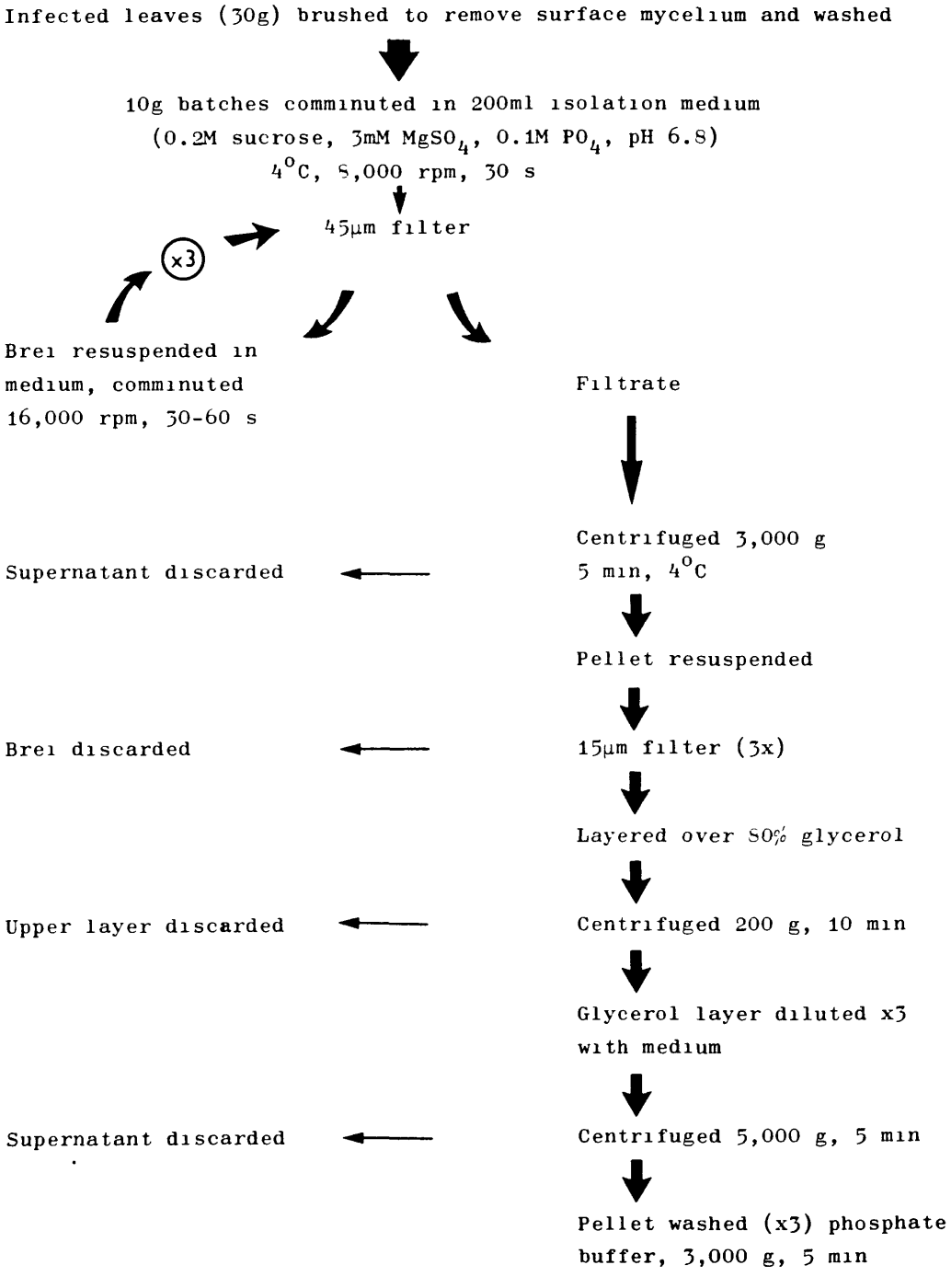
supplemented with artificial light where neccessary and at approximately 22°C. When 3-4 weeks old the plants were inoculated and maintained in conditions described by Pegg and Mence (1970) for the successful infection, growth and sporulation of the fungus. Plants were inoculated with a sporangial suspension prepared by shaking sporulating infections on leaf, tendril and stem pieces in distilled water, filtering through a double layer of gauze and applied with a Shandon spray gun. Pots of inoculated plants were placed in a closed propagator covered with black polythene to maintain a saturated atmosphere for 20h in darkness at 12-16°C. The polythene cover was then removed, the ventilators of the propagator opened and the plants kept at 12-16°C in a growth room for eight days with a 12h photoperiod and a light intensity of 13 watts m^{-2} produced by a bank of warm-white fluorescent tubes. Sites of infection were located by returning the plants to darkness and a saturated atmosphere for 1-3 days to induce sporulation. Uninfected control plants were treated similarly.

2.Preliminary preparative procedures.

2.1.Isolation of haustorial complexes.

Haustorial complexes were isolated from pea plants infected with powdery mildew by the method described by Manners (1979). This is a modification of the method of Gil (1976) who adapted the technique for isolating haustoria from cucumber leaves infected with Sphaerotheca fuliginea (Dekhuijzen,1966).

Figure 1. Flow diagram for isolation of haustorial complexes from pea leaves infected with Erysiphe pisi.



All stages of the isolation procedure outlined in fig. 1 were at 4°C. The surface mycelium was removed by brushing with a cotton buffing mop rotated by a small electric motor, and the leaves washed in three changes of tap water followed by three changes of distilled water. The final pellet of haustorial complexes was layered over a discontinuous sucrose density gradient (50% and 70% w/w) and centrifuged at 100xg for 10min. if contamination by chloroplasts, starch grains and other crystals was considerable. Chloroplasts remained in the surface layer, crystals passed through both sucrose concentrations and haustorial complexes were removed by aspiration from the 50-70% interface. They were washed in buffer three times by centrifugation.

2.2. Isolation of cuticle.

Fully expanded leaves of pea were excised and their lower epidermes removed with fine forceps. The leaves were floated in glass petri dishes with the exposed mesophyll in contact with a filter sterilised mixture of 0.8% w/v cellulase (Onozuka R-10) and 0.2% w/v Macerozyme R-10 in an aqueous solution of 0.4% w/v mannitol at pH 5.6. After an incubation period of 20h in darkness and at 25°C, residual debris was removed by gentle agitation of the enzyme solution.

3.Transmission electron microscopy.

3.1.Fixation and embedding.

3.1.1.Routine schedule.

The routine procedure for material to be examined by transmission electron microscopy was as follows:

(a) Fixation: glutaraldehyde (2.5% $^{v}/v$) in 0.1M phosphate or cacodylate buffer, pH 7, 2-3h.

(b) Wash: buffer as previously, 3 x 10min.

(c) Post-fixation: OsO_4 (1% $^{w}/v$) in the buffer, 1h.

(d) Wash: buffer as previously, 3 x 5min.

(e) Dehydration: acetone or ethanol 10% $^{v}/v$ in water, 5min.
" " " 20% " " " 5min.
" " " 30% " " " 5min.
" " " 45% " " " 10min.
" " " 60% " " " 10min.
" " " 75% " " " 10min.
" " " 95% " " " 30min.
" " " 100% " " " 3x30min.

(f) Infiltration: with either Epon or Spurr resin:

Epon	Spurr

Stages in sealed containers.

Epoxypropane:ethanol
(50:50 $^{v}/v$), 15min.

Epoxypropane:ethanol
(75:25 $^{v}/v$), 15min.

Epoxypropane (100%), 2x20min.

Epoxypropane:resin (70:30 $^{v}/v$), 2h.

Acetone:resin (50;50 $^{v}/v$), 2h.

Stages in open containers.

Epoxypropane:resin (70:30% $^{v}/v$), overnight, 4^{o}C.

Acetone:resin (50:50% $^{v}/v$), 2h.

Resin (100%), 24h, (2 changes).

Resin (100%), overnight, 4^{o}C.

Resin (100%), 8h, (2 or 3 changes).

Polymerisation.

Resin (100%), 60^{o}C, 2 days.

Resin (100%), 60^{o}C, 8h.

Material at all stages was kept at room temperature unless stated otherwise. The glutaraldehyde used was electron microscope grade supplied as a 25% ($^{v}/v$) solution (EM-scope). Fixation was occasionally overnight at 4^{o}C, and fixed specimens were frequently stored overnight at 4^{o}C at the end of the dehydration series in pure (100%) ethanol or acetone. Most specimens were dehydrated in acetone and embedded in Spurr resin as this reduced the total preparation time to three days whereas embedding in Epon increased the period to a minimum of five days.

Resins were prepared to the following recipes:

Epon 812, 1A : 1B mixture (Luft,1961).

A mixture :	Epon 812	46g
	Duodecenyl succinic anhydride	61.8g
	Benzyl dimethylamine	2ml
B mixture :	Epon 812	69g
	Methyl nadic anhydride	57g
	Benzyl dimethylamine	2ml

Spurr, standard hardness (Spurr,1969).

Vinyl cyclohexene dioxide	10g
Diglycidyl ether polypropylene glycol	6g
Nonenyl succinic anhydride	26g
Dimethyl amino ethanol	0.4g

3.1.2.Manipulation of specimens at fixation.

a.Leaves.

Infected and uninfected leaves were removed from plants and immediately cut under fixative solution into 1mm squares with a razor blade.

b.Haustorial complexes.

Isolated haustorial complexes were suspended in a small volume of fixative solution (2.5% ^{v}/v glutaraldehyde in 0.1M phosphate buffer, pH 7) for 30min. in a small tapered plastic centrifuge tube. An equal volume of bovine plasma albumin (10% ^{w}/v, fraction V, Armour Products) in the phosphate buffer was added and the mixture immediately centrifuged for 5min. at 3,000×g. This procedure produced a coherent pellet and avoided the heating applied when agar

is used (Gil,1976). After a further 30min. the tip of the plastic tube was cut off with a razor blade and the pellet extracted and divided into pieces approximately $1mm^3$. These were processed further as detailed in the schedule for routine fixation and embedding.

c.Epidermes.

Epidermis of pea leaf and stem were stripped directly onto the surface of the fixative solution. Epidermis that had been brushed with a camel hair brush or rotary cotton mop prior to stripping could be immersed in the solution, but un-brushed epidermis floated on the surface.

d.Cuticle.

Cuticles of pea leaves isolated by enzymic digestion and floating on liquid medium were transfered to the surface of a small volume of molten agar (1.2% $^{w}/v$, Difco Oxoid Bacto) with a small piece of filter paper. After solidification, the agar was cut into 3mm squares and pieces, approximately 1mm thick, were transfered to the fixative solution for microscopy as before. This method both protects the fragile cuticle from physical damage during processing and facilitates orientation during microscopy.

3.1.3.Caffeine fixation for phenol containing cells.

Leaves of hazel (Corylus avellana) uninfected or infected with Phyllactinia guttata, and leaves of Pisum sativum infected with Erysiphe pisi and showing necrotic flecking were fixed according to the routine schedule with the addition of 0.5% $^{w}/v$ caffeine (Sigma) to the

glutaraldehyde solution and the first series of washes in buffer. Post-fixation and embedding was by the procedure outlined in the routine schedule.

3.2.Sectioning and staining.

Resin blocks were trimmed with razor blades to expose the embedded specimens. Thick sections (ca. 10μm) were routinely cut by hand and their examination assisted in subsequent specimen orientation. They were stained in 1% $^{w}/_{v}$ toluidine blue in 1% $^{w}/_{v}$ borax with gentle heating over a bunsen flame and observed with the light microscope.

Thin sections were cut with a diamond knife (I.V.I.C.) and a LKB Ultratome 1 and collected on formvar coated, 100 mesh copper grids. Formvar films were prepared by placing cleaned glass slides in a separating funnel containing a 0.8% $^{w}/_{v}$ solution of formvar in chloroform. The tap of the funnel was then opened and the formvar solution drained away. The film was floated off the slide onto the surface of double glass distilled water when grids were placed on the film and the raft collected on strips of parafilm.

Sections were routinely double stained with uranyl actate and lead citrate. Grids were floated in drops of 2% $^{w}/_{v}$ aqueous uranyl acetate for 30min. at 60°C, washed in double distilled water and transferred to lead citrate (Reynolds,1963) for 10min. at room temperature in an atmosphere kept free from CO_2 by a filter paper soaked in a saturated NaOH solution. Finally the grids were washed in double distilled water and air dried. Sections were also stained in either uranyl acetate or lead alone, and others

were viewed unstained.

3.3.Microscopes.

All thin sections were examined on either an AEI EM6B or a Philips 301G transmission electron microscope. The micrographs presented were made with the Philips microscope operating at an accelerating voltage of 80KV and Agfa FOTIP automatic processing 70mm film. Developed negatives were printed using a "Prefect" enlarger with 135mm Comparon lens on Agfa Rapidoprint paper.

4.Light microscopy.

4.1.Bright field and phase contrast microscopy.

4.1.1.Leaves.

Simple observations of leaf pieces were made with bright field optics. Specimens were prepared as sections or pieces (2-3mm^2) either untreated or cleared for several days in lactophenol or chloral hydrate (25g in 10ml H_2O). Sections were made (10-15µm) from fresh material with a freezing microtome or as described earlier (Section 3.2) from material fixed and embedded for electron microscopy.

4.1.2.Epidermes.

Pieces of epidermis stripped as before (Section 3.1.2.c) from pea leaves and stems infected with powdery mildew were routinely examined with bright field optics before isolation of haustorial complexes and all preparations for electron microscopy. Usually surfaces of the leaves and stems were brushed before stripping to

remove conidia, mycelia and surface waxes which interfere with observation. The frequency of haustoria was estimated by mounting the strips in water over a haemocytometer grid and counting the number of haustoria per unit area.

Epidermal strips from leaves and stems of P. sativum were stained with the vital dyes neutral red and Evans blue by the procedures below:

a.Neutral red.

Immediately after stripping, epidermes from leaves and stems were placed on drops of 0.005% ($^{w}/v$) aqueous neutral red (BDH Chemicals Ltd.) on a glass microscope slide. After 5-10min. the excess stain was removed and replaced by drops of 0.8M aqueous KCl. The strips were covered with a glass cover slip and examined with bright field optics.

b.Evans blue.

Epidermal strips from stems were immersed in an aqueous solution of 0.5% (w/v) Evans blue (BDH Chemicals Ltd.) for 5 min. and mounted under cover slips on glass slides for observation by bright field microscopy. Excess stain was removed with filter paper to ensure the space between slide and coverslip was completely filled by the specimen and differential uptake was not masked by extracellular stain.

4.1.3.Isolated haustorial complexes.

These were suspended in water or isolation medium and a drop placed on a microscope slide and covered with a coverslip. Observations were made without staining by bright field and phase contrast microscopy. Estimates of numbers of haustorial complexes were made with a

haemocytometer slide (0.1mm depth).

4.2.Fluorescence microscopy.

4.2.1.Acetamido-isothiocyanato-stilbene (SITS).

Epidermis from leaves of pea and barley with powdery mildew infections and isolated haustorial complexes of *E. pisi* were prepared for microscopy as described above (Section 4.1) and mounted on glass slides in a freshly made solution of 100µm disodium 4-acetamido-4'-isothiocyanato-stilbene-2,2'-disulphonate (SITS; BDH Chemicals Ltd.) in 0.05M phosphate buffer (pH 7). Controls were mounted in buffer alone and all specimens left at least 5min. before examination. Observations were made with a Reichert Zetopan microscope with visible and ultraviolet illumination provided by tungsten and high pressure mercury vapour (Osram HBO 200W) lamps respectively. For fluorescence microscopy exciter filter E4 (peak transmission 360nm) and absorption filter Sp1 (transmission above 400nm) were used. Under these conditions reaction with SITS was seen as a bluish-white fluorescence.

4.2.2.Aniline blue.

Powdery mildew infected and non-infected epidermis stripped from leaves of pea and sections of leaves made with a freezing microtome were floated in drops of 0.05% ($^{w}/v$) aniline blue (BDH Chemicals Ltd.) in 0.1M phosphate buffer at pH 8.5 on a glass slide and covered with a coverslip. Isolated haustorial complexes were suspended in a small volume of phosphate buffer at pH 8.5 and one drop mixed with one of the aniline blue solution on a slide and

then covered with a coverslip. Control specimens were mounted in buffer alone as autofluorescence of some plant components (eg. phenolic substances) is enhanced at the alkaline pH required to maximise aniline blue fluorescence (Smith and McCully, 1978a). Observations were made with the same microscope and filters as for SITS and reaction with aniline blue was seen as a yellow-green fluorescence.

5.Electron microscope autoradiography.

5.1. $^{14}CO_2$ labelling.

Plants of Pisum sativum with a seven day infection of Erysiphe pisi were exposed to 5mCi $^{14}CO_2$ for 2h in the light as described by Manners and Gay (1978). Plants were trimmed with a razor blade to remove all leaves without confluent mildew colonies on their upper surface and those showing etiolation or browning. The selected stems were then cut at their bases with a wet razor blade and 30g of leaves still attached to stem segments were arranged on a perforated perspex plate over a tray of water. The stems projected through the perforations and their cut ends were immersed in the water. The tray assembly was then placed in a rectangular perspex exposure chamber (55 l) and the apparatus sealed and placed in a fume cupboard. A solution of $NaH^{14}CO_3$ (2.5ml, 5mCi, 60mCi/mmol) was injected through a rubber seal into a shallow container and $^{14}CO_2$ released by subsequent injection of 2ml of 50% lactic acid. Air was circulated in the chamber by a small electric fan and the whole apparatus illuminated by two Atlas tungsten reflector lamps (each 150W) providing 13,000 lux at the surface of the chamber. A perspex tray of cold water immediately beneath the lamps prevented overheating and the temperature within the chamber was $25\pm1^{o}C$. After exposure for 2h, 4ml of 2N KOH was injected into the chamber and air passed through for 1min. The plants were removed and the leaves detatched and placed in a cold room at $4^{o}C$. They were removed a few at a time for brushing and washed 5 times in an ice-water mixture and twice in

distilled water at 4°C. Haustorial complexes were isolated and prepared for electron microscopy as described previously. Fractions prepared similarly but without exposure to $^{14}CO_2$ were used as controls for positive chemography.

5.2.Preparation of autoradiograms.

5.2.1.Membrane method.

Perspex slides (the same dimensions as conventional glass microscope slides) with 7mm diameter holes were made to the specifications of Budd and Pelc (1964). Formvar films were prepared as previously described and floated onto the surface of double distilled water. Films were picked up either by immersing a Perspex slide in the water and raising it underneath the film to cover the holes on one side only (Budd and Pelc,1964), or by placing one end of a vertical slide in the centre of a film and pushing down into the water. The latter results in both sides of the holes being covered and is advantageous since it restricts access of the emulsion to one side of each formvar film when it is applied by the "dipping technique". After single side coating, the liquid emulsion was applied by pipette and the excess allowed to drain. Concentric interference colours of emulsion layers prepared by both these procedures indicated a progressive decrease in thickness away from the centres of the formvar covered holes. This condition was due to slight sagging of the formvar film and was not significantly improved by increasing the thickness of the film (to an extent where resolution in the electron microscope was seriously

impaired).

5.2.2.Flat substrate method.

Ribbons of pale gold sections (c 100nm thick) were placed, with a platinum wire loop 2mm in diameter, at predetermined positions on formvar coated slides. The slides had previously been cleaned in 2% RBS 25 (Chemical Concentrates (RBS) Ltd., London) and rinsed in tap water, double distilled water and finally ethanol. Four ribbons of sections were spaced at the end one third of each slide. Three of the ribbons were of labelled haustorial complexes and the fourth was unlabelled. The sections were stained, on the slides, under drops of uranyl acetate and lead. After each treatment the slides were washed with a stream of double glass distilled water (DDW). The stained sections still attached to the slides were then coated by vacuum evaporation with a 5-6nm layer of carbon (equivalent to a slight greying of a glazed white porcelain surface), to protect the emulsion from chemography.

The slides were coated with Ilford L4 nuclear emulsion under an Ilford 902 safelight in a darkroom at 40-50% relative humidity and 18-20^{o}C. The emulsion is supplied in pellicle form and was prepared as a liquid by the following procedure. Emulsion was transfered in the darkroom by spatula to a graduated plastic beaker (50ml) which was filled to the 10ml mark. This was placed in a waterbath at 43^{o}C and the emulsion stirred very gently (to avoid frothing) until melted. The liquid emulsion was diluted with 30ml DDW at 43^{o}C, mixed by gentle stirring, and cooled to 25^{o}C. Preliminary experiments showed that

when the beaker containing 40ml of dilute emulsion at 43°C was transfered to a waterbath at 20°C, the emulsion took 3min. of gentle stirring to reach 25°C (reading a thermometer was impossible under safelight conditions). The cooled emulsion was slowly poured into the dipping jar, which was in an insulated chamber held at 25°C by an oil bath, and left to stand for approximately 2min. until all the bubbles had dispersed. Test slides showed that the four fold dilution of the emulsion gave a uniform film of purple interference colour (equivalent to a close packed monolayer of silver halide crystals c 150nm thick, (Bachmann and Salpeter,1965)) when the slides were withdrawn mechanically from it at 83mm/min. The experimental slides were drained vertically at room temperature for 30min., transferred to open slide boxes for a further 1 hour and placed overnight in a desiccator in the darkroom. The slide boxes were then protected from the light and desiccated during storage for nine weeks at 4°C. The exposure period required was determined by processing and examining replicate autoradiograms at intervals of 2 weeks. The autoradiograms were developed in full-strength D-19 (Ilford) for 2min., washed in DDW for 30s , placed in a stopbath of 1% acetic acid for 10s , washed in DDW for 30s and fixed in 30% ($^{w}/v$) sodium thiosulphate for 3min. Final washing was by three 90s changes of DDW. All stages of development were carried out at 20°C and all processing solutions were freshly prepared. Negative chemography controls were exposed to an unfiltered tungsten lamp before development.

Autoradiograms were floated off the slides on to the surface of DDW emulsion side uppermost. Copper grids (100

mesh) placed over the sections were collected for microscopy on strips of parafilm. Separation from the glass slides was aided by releasing drops of 10% hydrofluoric acid on to the water surface near the slides (Salpeter and Bachmann,1972).

Electron micrographs of the autoradiograms were made and print montages were prepared at a magnification of 6,600. Randomization was ensured by the technique itself; all areas of section not obscured by extraneous particles, folding or grid bars were recorded.

5.3.Quantitative analysis of autoradiograms.

The distribution of ^{14}C in constituents (haustorial complexes and various contaminant fragments) of the isolated fraction was assessed by counting silver grains in areas determined by overlaying a transparency of equidistant points drawn to the specifications of the "multipurpose test system" (Freere and Weibel, 1967; Weibel et al., 1966). Each point of the transparency represented 2.742μm^2 at a print magnification of 6,600. A grain was assigned to a constituent when completely or partially overlaying it.

The distribution of ^{14}C within haustorial complexes was similarly analysed except that a transparency of equidistant points each representing 0.428μm^2 at print magnification of 6,600 was used. In this analysis each silver grain was scored as either exclusive to the directly underlying component or as shared by two or more components which underlay any part of the grain (Levine, 1977 in Bergeron et al.,1979). Shared grains were

subsequently alloted to individual components (n) by the procedure described by Nadler (1971) and outlined below:

The ratio of exclusive grains of each component (${}_nE$) to the sum of exclusive grains of all components (Σ_nE) is taken to be in proportion to the ratio of the true grain count for each component (${}_nC$) to the total grains counted (T_{EM});

$$\text{or} \quad \frac{{}_nE}{\Sigma_nE} = \frac{{}_nC}{T_{EM}}$$

and therefore a rough approximation (${}_nC_1$) which does not take into account component diffuseness (discussed below) of the true grain count (${}_nC$) can be determined where:

$${}_nC_1 = T_{EM}\,\frac{{}_nE}{\Sigma_nE}$$

If shared grains were alloted according to the ratio found for exclusive grains, the proportion of all grains shared by, for example, components n_1, n_2 and n_3 which could be attributed to n_1 alone would be:

$$\frac{{}_{n_1}C}{{}_{n_1}C + {}_{n_2}C + {}_{n_3}C}$$

When component diffuseness (${}_nV_p/{}_nV_o$) is considered this equation becomes:

$$\frac{{}_{n_1}C({}_{n_1}V_p/{}_{n_1}V_o)}{{}_{n_1}C({}_{n_1}V_p/{}_{n_1}V_o) + {}_{n_2}C({}_{n_2}V_p/{}_{n_2}V_o) + {}_{n_3}C({}_{n_3}V_p/{}_{n_3}V_o)}$$

The values determined for ${}_nC_1$ can be substituted in the equation above and multiplied by the number of grains shared by the components n_1, n_2 and n_3 for every combination. Thus the shared grains are allocated to

components and a second approximation ($_nC_2$) of the true grain count made. If for each component $_nC_1$ is less than 5% different from $_nC_2$ then $_nC_2$ is accepted as the true grain count. If there is more than 5% difference for any component then $_nC_2$ is substituted for $_nC$ in the above equation. Ultimately the results yield statistical values for $_nC$ for all components.

Because silver grains are not infinitesimal the correction index ($_nV_p/_nV_o$) for component diffuseness was calculated (Nadler,1971). The relative area of each component was determined both by counting points of the transparent grid ($_nV_p$) and by scoring randomly distributed probability circles drawn on the transparent grid at the average grain frequency experimentally determined for healthy haustorial complexes ($_nV_o$). These probability circles were drawn with a diameter equivalent to the average maximum silver grain dimension (355nm), which corresponds closely to the 50% probability circle, estimated from the data of Salpeter and Bachmann (1972). This takes into account the average track length for ^{14}C, section thickness and the particular developer used and assumes a point source with the 50% probability circle equivalent to 1.7 half distance. Thus the actual and hypothetical sources, with a 50% probability, lay under the silver grains or within the circles respectively.

The percentage sampling error of the grain density values, where N_1= number of silver grains counted and N_2= number of points counted for area estimations, is given by $\sqrt{\frac{1}{N_1} + \frac{1}{N_2}} \times 100$ (Salpeter and Bachmann,1972).

6.Localisation of phosphatases (ATPase, alkaline and acid phosphatase).

Phosphatase activity was localised in leaf tissue of the following infected plants and uninfected controls:- pea with *Erysiphe pisi* or *Peronospora pisi* ; barley with *Erysiphe graminis* ; french bean with *Uromyces appendiculatus*.

6.1.Fixation of specimens.

Portions of leaves were excised under fixative solution and cut into small pieces (0.5-1 mm squares). The lower epidermis of pea leaves with powdery mildew infections of the upper epidermis was removed by stripping with fine forceps prior to cutting. This facilitated permeation of the tissue by the several solutions employed. Fixation was by one of the following solutions:

(a) Glutaraldehyde (0.5 or 1 % ^{v}/v) prepared from 25% aqueous solutions supplied by Taab (EM-grade) or EM-scope (ultrapure) with or without 4% ^{v}/v formaldehyde (Taab; supplied as a 36% aqueous solution) in 0.1M sodium cacodylate buffer, pH 7.2.

(b) Glutaraldehyde (0.5% ^{v}/v) prepared from 8% aqueous solutions supplied by Polysciences (EM-grade; stored in 10ml aliquots in nitrogen filled glass ampoules at 4^{o}C) and 4% formaldehyde in 0.1M sodium cacodylate buffer, pH 7.2. Formaldehyde was prepared as an 8% ^{w}/v aqueous solution by alkaline hydrolysis of paraformaldehyde (Taab, EM-grade). Eight grammes of paraformaldehyde were dissolved in 92ml distilled water at 60-70^{o}C. Drops of NaOH (1M) were added to the stirred solution until it cleared.

Approximately four drops were usually required.

The purity of the glutaraldehyde was determined spectrophotometrically (see appendix).

The leaf pieces were fixed for 1-2h at room temperature and then thoroughly washed for 2-3h in several changes of 0.1M Tris-maleate at $4^{o}C$ and at the pH of the incubation medium.

6.2.Incubation with substrates.

The pieces were subsequently incubated for 2-3h at $22^{o}C$ in media containing 0.1M Tris-maleate, 0.002M $Mg(NO_3)_2$, 0.002M substrate and 0.002M $Pb(NO_3)_2$. All these constituents were initially prepared as fresh stock solutions at x10 working strength except Tris-maleate which was double strength. Media were prepared immediately before use by mixing 1ml of each of the required constituents with 5ml Tris-maleate and made up to 10ml with double distilled water. They were added in the order listed above in order to minimise hydrolysis of the substrate by lead. The addition of substrate immediately after $Mg(NO_3)_2$ favours formation of a complex between substrate and Mg^{2+} in preference to Pb^{2+} (Winter-Sluiter et al,1977). In addition, preliminary experiments showed that mixing stock solutions of $Pb(NO_3)_2$ and ATP resulted in the immediate appearance of a white precipitate. This was presumably a lead-ATP complex or lead phosphate formed as a result of the instantaneous hydrolysis of ATP by the very high concentration of lead.

Adenosine triphosphatase (ATPase) was localised at pH 7.2 with the sodium salts of adenosine triphosphate

(ATP, Sigma) or β-glycerophosphate (β-GP, Sigma) as substrates. β-GP was used at pH 5.5 for acid phosphatase. Control specimens were incubated in the same media but without substrate or with substrate in the presence of the inhibitor sodium fluoride (0.01M). All specimens were washed for 1h in 0.1M sodium cacodylate buffer, pH 7.2. Post-fixation in OsO_4 and subsequent preparation for sectioning and examination in the electron microscope was as before.

7.Assay of adenosine triphosphatase activity.

7.1.Preparation of samples.

7.1.1.Specimens.

a.Leaves.

Uninfected leaves of Pisum sativum and leaves with colonies of Erysiphe pisi on their upper epidermes were detatched from petioles and immediately brushed with a camel hair brush to remove waxes and the surface mycelium. Midveins were excised and the pieces of lamina were washed in 3 changes of distilled water at $4^{o}C$ and transferred to the homogenisation medium (also at $4^{o}C$) described below.

For Peronospora pisi infections leaves were detatched and areas of the laminae bearing sporangiophores excised without brushing and washed as above. Uninfected controls were treated similarly.

b.Haustorial complexes.

Haustorial complexes were isolated by the

procedure described previously except that Tris-maleate was used instead of phosphate to buffer the isolation and washing media. They were stored overnight in 0.1M Tris-maleate buffer (pH 7.2) at 4°C prior to homogenisation.

c.Epidermes.

Epidermes of leaves and stems of P. sativum were brushed to remove waxes and powdery mildew mycelia and detatched as before. They were immediately placed in the homogenisation medium at 4°C and washed in several fresh changes. Particular care was taken to reject epidermes showing necrotic flecking.

The area of stem epidermis collected was determined by measuring the width and length of the stem pieces from which it had been stripped. Pea stems have an approximately square cross section and the surface area can be calculated by multiplying the product of width and length by 4.

7.1.2.Homogenisation.

Homogenisation of samples followed procedures adapted from Leonard and Hodges (1973). Specimens were homogenised in an aqueous solution of sucrose (0.15M), EDTA (3mM), dithiothreitol (2.5mM) and Tris-maleate (0.1M) buffered to pH 7.2 in the following quantities and proportions: whole leaf tissue, 2g in 10ml; epidermis, 8,000-10,000mm^2 ($\triangleq$0.3g) in 10ml; haustorial complexes ($8-10 \times 10^6$) at 2×10^6 ml^{-1}.

Specimens were disrupted either with a mortar and pestle or with 50 strokes of a tight-fitting Potter homogeniser at 4°C. Homogenates of leaf and epidermis were

filtered through a double layer of gauze and the brei resuspended and subjected to further disintegration. The filtrates from both homogenates were combined and designated "crude extract". Homogenates of isolated haustorial complexes were not filtered.

7.1.3.Preparation of fractions.

The crude extracts from homogenates of stem epidermes were centrifuged at 1,500 x g for 10min., and the supernatants obtained further centrifuged for 30min. at 4°C. The precipitate from each centrifugation and the final supernatant were designated 1,500 x g precipitate, 10,000 x g precipitate and 10,000 x g supernatant respectively. Precipitates were resuspended in 1ml Tris-maleate buffer (0.1M, pH 7.2) at 4°C and 0.3ml was taken for assay of protein. The remainder was made up to 4ml with buffer.

7.2.Incubation with substrate.

Samples were incubated at pH 7.2 for 30min. in glass test-tubes held in a waterbath at 37°C. The reaction mixture contained 2mM $Mg(NO_3)_2$, 3mM ATP (sodium salt, Sigma), 0.1M Tris-maleate buffer and 0.2 or 0.4ml test sample depending on the activity of the preparation. Controls were incubated without substrate, in the absence of Mg^{2+} and in the presence of NaF (10mM). The assay mixture was prepared from solutions of ATP, $Mg(NO_3)_2$ and NaF made in Tris-maleate buffer (0.1M) at ten times their working concentration and added as 0.1ml aliquots. The mixture was made up to 1ml with buffer solution. Preliminary experiments showed that it was necessary to

adjust the Tris-maleate buffer to pH 7.4 to compensate for the acidity of the ATP solution and maintain the reaction mixture at pH 7.2. The reaction was initiated by adding 0.1ml of ATP solution and was stopped after incubation by adding 0.5ml ammonium molybdate (2.5% $^{w}/_{v}$) in H_2SO_4 (5N). Duplicate samples were incubated without substrate which was subsequently added immediately after molybdate for estimation of constitutive inorganic phosphate.

7.3.Analytical techniques.

7.3.1.Assay of inorganic phosphate.

Inorganic phosphate was determined by the Fiske and SubbaRow (1925) procedure as adapted by Stanton (1968) for use in the presence of biological material and ATP. The incubated reaction mixtures (with molybdate) were made up to 4ml with distilled water and the time was noted when 0.2ml Fiske-SubbaRow reducer (Sigma) was added and mixed vigorously with a vortex mixer (Whirlimix, Fisons). The mixtures from incubations with crude extract and the 1,500 x g pellet were centrifuged for 5min. in a bench centrifuge (approx. 1,500 x g) to remove particulate matter. After 20 and 40min. at room temperature their optical densities were measured at 700nm with distilled water as reference sample.

A standard phosphate curve was determined in the range 0-20µg Pi by diluting a stock solution of KH_2PO_4 (4.39g/100ml ≡ 10µg Pi/µl) to 1µg Pi/10µl. Aliquots of multiples of 10µl were transferred to glass test-tubes to give the desired quantities of Pi and made up to 4.3ml

with distilled water and assayed as above.

7.3.2.Assay of protein.

Protein was determined by the method of Lowry et al (1951). Samples containing 60-150µg protein were measured into test-tubes with a microlitre syringe and made up to 100µl with water. To all samples 0.4ml of 5% ($^{w}/v$) sodium deoxycholate was added to solubilise protein (eg. membrane components). Then 5ml of Na_2CO_3 (2% $^{w}/v$) in 0.1N NaOH, 50µl $CuSO_4.5H_2O$ (1% $^{w}/v$) and 50µl sodium-potassium tartrate (2% $^{w}/v$) was added, mixed thoroughly and left to stand for 10min. at room temperature. A 0.5ml quantity of a mixture of 1 part Folin-Ciolcalteau phenol reagent with 2 parts water was added whilst mixing vigorously with a vortex mixer (Whirlimix, Fisons). When the tubes had stood for 30min. at room temperature, optical densities were estimated at 600nm. The constitutive absorbance of each protein sample was similarly determined with duplicates containing water instead of Folin-Ciolcalteau reagent. Bovine serum albumin was used as a standard.

CHAPTER 1.

Ultrastructure of leaves of *Corylus avellana* and *Betula pendula* and infection by *Phyllactinia guttata*.

1.Introduction.

The ultrastructure of the association of the powdery mildew *Phyllactinia guttata* with any host has not been described before. Previous studies have mostly been concerned with epidemiology (Butt,1978) and all morphological examinations have been restricted to light microscopy for taxonomic purposes (e.g. Blumer,1967) and the description of cleistocarp development and dehiscence (Cullum and Webster,1977). *Phyllactinia spp.* infect a large range of trees and shrubs (Blumer,1967; Burchill, 1978) and are widely distributed in the north temperate zone. *P. guttata* commonly occurs on *Corylus avellana* (hazel) where it may cause severe defoliation (Brown,1968) but injury to this host and others is usually slight and it is not considered to be a serious disease. However *Phyllactinia spp.* are unusual in that they form haustoria from an intercellular mycelium whereas most of the *Erysiphales* have epiphytic mycelium with haustoria restricted to cells of the epidermis. *Leveillula* is the only other genus of the group normally developing intercellular hyphae.

Leaves of the *Betulaceae* and *Corylus avellana* in particular contain large quantities of phenolics and tannins[+] (Bate-Smith and Lerner,1954). Intracellular

[+]Although tannins and phenolics are biochemically distinct (Anderson,1968) for the purposes of the current study the term "phenolics" includes any substances containing phenolic hydroxy groups.

phenolics are mostly confined to the vacuole of plant cells (Ledbetter and Porter,1970) but other organelles may contain phenolics and have been implicated as possible sites of synthesis of the vacuolar deposits. These include amyloplasts (Wardrop and Cronshaw,1962), dictyosomes (Amelunxen and Gronau,1969), smooth endoplasmic reticulum and vesicles (Baur and Walkinshaw,1973) and rough endoplasmic reticulum (Parham and Kaustein,1977). Many electron microscope studies of the ultrastructure of plant cells with high phenolic content have hitherto proved very unsatisfactory (Mueller and Beckman,1974; 1976). Cytoplasmic detail of these cells prepared by conventional fixation with glutaraldehyde and osmium is usually obscured by electron opacity presumably due to leaching, during fixation, of phenolic compounds from the vacuoles. The tonoplast of these phenol storing cells seems to be very fragile and indeed this membrane is particularly susceptible to damage during fixation (Lawton and Harris,1978). Phenolic compounds are strongly osmiophilic and cytoplasm affected by leached vacuolar phenolics is essentially tanned and becomes similar in appearance to that of necrotic cells (Bell,1981).

In studies of disease in phenol containing plants the problem is accentuated because it is necessary to distinguish between necrotic cells and those normally containing phenolics. This becomes especially difficult where additional phenolic compounds are developed in response to infection (Kosuge,1969; Kuc,1972; Swain, 1977; Vance *et al.*, 1980). There are many published, and probably even more unpublished, micrographs which illustrate this effect (e.g. Perera and Gay,1976; Robb

et al,1975b).

This problem has been approached in cotton root endodermis and phenol storing cells by including nicotine, cinchonine or caffeine (Mueller and Rodehorst,1977) and caffeine (Mueller and Greenwood,1978) in the glutaraldehyde fixative solutions respectively. They found this caused phenolics to condense in the vacuoles and the degree of cytoplasmic detail observed was typical of that in conventionally fixed cells lacking vacuolar phenolics. Caffeine also stabilises the structure of membranes (Juniper and Lawton,1979) but its effect on the permeability of the tonoplast to phenolics is not known.

In the current study caffeine was employed during fixation to investigate the distribution and ultrastructure of Phyllactinia guttata within leaves of Corylus avellana and Betula pendula and this is preceded by a description of the ultrastructure of the uninfected leaves. In addition, the effect of infection by P. guttata on the distribution of phenolic compounds is described.

2.Results.

2.1.The effect of caffeine on fixation and ultrastructure.

In the absence of caffeine, glutaraldehyde and osmium fixation of C. avellana and B. pendula leaf pieces resulted in dense osmiophilic cytoplasms in which almost all details of ribosomes, membranes and organelles were obscured (plate 1.1a). In addition the vacuoles contained varying amounts of osmiophilic deposits which often became dislodged during sectioning and caused considerable problems similar to those

experienced by Beckman and Mueller (1970) and Mueller and Beckman (1974). These included section tearing and fragmentation which subsequently had a detrimental effect due to redeposition as particles on the sections. Increasing the duration of treatment with glutaraldehyde to 24h did not significantly improve fixation. However, occasional cells showed considerable cytoplasmic detail and in these the dense osmiophilic deposits were either absent or confined as distinct aggregates to the vacuole.

In contrast, treatment of leaf pieces of C. avellana with caffeine during fixation restricted the osmiophilic material to the vacuoles of most uninfected cells (plates 1.1b,c;1.2), and alleviated the problems associated with sectioning material which was fixed with glutaraldehyde and osmium alone. Thus the descriptions that follow are restricted to observations on caffeine-treated leaves of Corylus avellana unless stated otherwise.

2.2.Organisation and ultrastructure of leaves.

Leaves of both C. avellana and B. pendula show the typical dorsi-ventral organisation of dicotyledonous angiosperms (Esau,1953) with their internal tissue differentiated into palisade and spongy mesophylls (plate 1.2). Elongated cells of the palisade (plates 1.1b,c) were arranged as a distinct layer one or more cells deep immediately below the upper epidermis and with their long axes at right angles to the leaf surface. The spongy mesophyll was a tissue of irregular, loosely arranged cells separated by large air spaces and lay between the palisade and lower epidermis. Vascular bundles of minor veins (plate

1.2) were situated within the spongy mesophyll and phloem seive elements, companion cells, xylem vessels and parenchyma were recognisable. There were no cells with wall thickenings characteristic of transfer cells. Around the bundle was a layer of larger cells which comprised the bundle sheath. Intercellular spaces were usually absent between adjoining cells of the bundle sheath and those of the vascular tissues. The bundles were often connected to the upper epidermis by a compact tissue with few intercellular spaces (plate 1.2) which is also present in other species (Fahn,1974; Wylie,1952). Cells of this tissue have thickened walls (plate 1.2) but otherwise their ultrastructure was similar to bundle sheath cells. Their large central vacuoles were surrounded by a thin peripheral layer of cytoplasm which contained a full complement of organelles including chloroplasts. Darkly staining nucleoli were often observed near the centre of nuclei in these and in other cell types. Epidermal cells had an even thinner peripheral layer of cytoplasm around their vacuoles (plates 1.2; 1.5b). Each cell contained an elongate nucleus and occasional small chloroplasts with starch grains and a few unstacked thylakoids. The cell walls were thick and their outer surfaces sculptured into finger-like projections which were particularly frequent on the upper epidermis. A thick cuticle closely followed the contour of these projections and was continuous over the junctions of adjacent cells.

In mesophyll cells the peripheral cytoplasm was thicker and the vacuoles occupied a smaller proportion of the cell volume. Mitochondria, golgi bodies and free

ribosomes were abundant throughout the cytoplasm and there was an extensive system of endoplasmic reticulum. The nucleus was located centrally and usually spherical. Chloroplasts with well developed thylakoids organised into stacks of grana occurred adjacent to the plasma membrane. Starch grains were often present and osmiophilic droplets especially frequent. The latter had the same electron density as the vacuolar deposits in unstained sections (plate 1.1b) but their density did not increase to the same extent after staining with lead and uranyl acetate (plate 1.1c).

2.3.Distribution and morphology of electron dense deposits.

After fixation in the presence of caffeine the contents of vacuoles and the droplets in chloroplasts represented the only conspicuous osmiophilic features in leaf sections (plate 1.1b). The cytoplasm of necrotic cells was also osmiophilic, often fragmented and shrunken from the cell walls which were infolded (plate 1.1c). Without caffeine the whole cytoplasm was almost uniformly dense in all cells.

Osmiophilic deposits were present in the vacuoles of most cell types fixed in the presence of caffeine (plate 1.2). They were frequent in cells of the bundle sheath, spongy and palisade mesophylls and the upper and lower epidermes including guard cells. Only cells of the phloem and xylem elements were always devoid of the deposits which were also infrequent in the associated parenchyma (plate 1.2). Deposits usually filled most of the vacuole and had a foam-

like/reticulate structure (plate 1.1b). Sometimes, particularly in epidermal cells, they were condensed away from the tonoplast as dense globules (plates 1.2; 1.5b) with spherical or irregularly lobed outlines and located either centrally in a single mass or scattered as smaller droplets throughout the vacuole. Other deposits were intermediate in form and comprised an amorphous layer next to the tonoplast with strands dividing the vacuole into one or two smaller compartments (plate 1.5b).

2.4.Ultrastucture of Phyllactinia guttata and infected leaves.

2.4.1.Organisation of intercellular hyphal system and distribution of haustoria.

The present study confirms previous observations (e.g. Blumer,1967) that Phyllactinia forms an epiphytic mycelium on the lower epidermis of infected leaves and also that hyphae penetrate the leaf via stomata (plate 1.3). Light microscopy of cleared infected leaves (plate 1.3) and electron microscopy of thin sections (plates 1.5b; 1.6) have elucidated the organisation of the intercellular system. On occasion, more than one hypha penetrated a single stoma (plate 1.3c) and each swelled in the substomatal cavity to form a structure similar to the substomatal vesicle of rust fungi (plate 1.3b,d). The substomatal cell was separated from the surface hypha by a septum in the region of the stomatal aperture (plate 1.4a). From each substomatal cell a single intercellular hypha (plate 1.3b,d) extended towards the spongy mesophyll and vascular bundles in particular. These hyphae were unbranched and showed no signs of passing

between host cells which were not already separated by intercellular spaces. Hyphal cells each contained a single nucleus and were separated by perforate septa.

Haustoria were difficult to distinguish by light microscopy from the dense vacuolar deposits in preparations of leaf tissue cleared in lactophenol or chloral hydrate. Electron microscopy showed they occurred very infrequently (table 1.1). Only six were found in sections of at least 4,250 distinct cells (seventy three grids of sections prepared from 24 samples infected with Phyllactinia were examined, each grid carrying a ribbon of serial sections and each section an average of 180 cells). Sections with haustoria also showed profiles of intercellular hyphae and sections from a further eight samples showed profiles of hyphae alone. All haustoria were located in spongy mesophyll cells either directly underlying the palisade layer or associated with bundle sheath cells. Never more than one haustorium was seen to be associated with each intercellular hypha; however the hyphae extended beyond the infected cells (plate 1.6) and thus the possibility that additional haustoria occurred further along them cannot be excluded.

2.4.2.Ultrastructure of haustoria and associated structures.

Each haustorium was connected by a neck to an appressorium-like structure which arose as a branch from an adjacent cell of the intercellular hypha (plates 1.5b; 1.6a; 1.7a,b). The wall of the neck was continuous with both the wall of the body and the inner layer of the wall of the intercellular appressorium (plate 1.7b). A septum

occurred between the neck and body regions of the haustoria (plate 1.5a) and slender lobes, which arose from the body, were mostly attached near the neck (plates 1.5; 1.6) and were sometimes branched. In some haustoria they were reflexed to form a compact layer over the body (plate 1.5a) whilst in others they extended away from the body (plate 1.6). The haustorial cytoplasm was bounded by a plasma membrane and cell wall which were continuous over the body and lobes. A single nucleus was located centrally in the cytoplasm of the body (plate 1.5a). Small vacuoles were conspicuous throughout the cytoplasm and their lumens often showed profiles of membranes and osmiophilic globules (plate 1.8). Elements of rough and smooth endoplasmic reticulum were infrequent and randomly dispersed whilst mitochondria and free ribosomes were abundant throughout the cytoplasm of body and lobes. Mitochondria in haustoria and intercellular hyphae were elongate (plate 1.7b) and, as in other ascomycetes, had plate-like cristae. Small areas within the cytoplasm (plate 1.8) were devoid of ribosomes and groundplasm and contained faintly staining granules which resembled glycogen in size and arrangement. These were particularly frequent in lobes as were osmiophilic droplets of lipidic material (plate 1.8). The cytoplasm of the neck (plate 1.7a) contained free ribosomes and osmiophilic droplets associated with the plasma membrane but neither a nucleus nor mitochondrion was present.

Haustoria were enveloped by an extrahaustorial membrane which was highly convoluted (plate 1.8). Between the extrahaustorial membrane and the haustorial wall was an extrahaustorial matrix containing dense granules in a

random or reticulate arrangement and small osmiophilic droplets (plate 1.8). The latter were usually close to the extrahaustorial membrane.

Around the neck was a small collar which was attached to the host cell wall (plates 1.5a; 1.7a). In contrast to collars formed in other powdery mildew infections it did not taper from a particularly wide base on the host wall but extended more as a cylinder with walls approximately 0·5μm thick along its whole length. The structure of the collar differed from that of the host wall so that a distinct boundary occurred at their junction (plate 1.7a). The collar was electron lucent and electron dense granules and fragments of membrane were randomly dispersed within it. The host wall showed a characteristic fibrillar structure except for a distinct, more electron dense zone immediately adjacent to the site of penetration (plate 1.7b). The outer edge was incurved and the inner portion closely adpressed to the wall of the haustorial neck which suggested that penetration involved both chemical modification and mechanical pressure. Examination of serial sections showed the collar and neck were separated by a narrow channel which was continuous with the cytoplasm of the host cell. The host plasma membrane was seen closely adpressed over most of the irregular surface of the collar but an annulus of osmiophilic material obscured it at the junction of the wall-lining and extrahaustorial regions of the plasma membrane so that continuity was not confirmed. Although the wall of the neck was more electron dense in this region than elsewhere there was no definite evidence of neckbands similar to those around the necks of haustoria in other powdery mildew

infections. However as the present descriptions are based on sections through only two neck regions, one of which was sectioned at an oblique angle (plate 1.7) and the other longitudinally but with detail obscured by osmiophilic material (plate 1.5a), the evidence should not be taken as proof that neckbands do not exist in this infection.

2.4.3.Ultrastructure of cells with electron dense cytoplasms.

Despite treatment with caffeine, the cytoplasms of cells containing haustoria were more electron dense than in uninfected cells. This may have been due to increased numbers of ribosomes but because the general increase of density made these and other cytoplasmic particles difficult to resolve (plate 1.8), the presence of additional osmiophilic material is a more likely cause. Large deposits of osmiophilic material were still present in the vacuoles of these cells (plate 1.5b) as is to be expected where caffeine was included in the fixative solutions. It seems unlikely therefore that the osmiophilic material in the cytoplasm had leached from the vacuoles during fixation. Furthermore, the extrahaustorial matrices and cytoplasms associated with these haustoria (plates 1.7; 1.8) were less electron dense than in material fixed without caffeine (plate 1.5a). Indeed the cytoplasms of caffeine-treated haustoria were similar in opacity to those of hyphae of both the intercellular and epiphytic mycelia (plates 1.5b; 1.7). These observations suggest that phenolic compounds are normally present in the cytoplasm of cells with haustoria.

The walls of body and lobes of two haustoria took

up angular outlines (plate 1.5a) and their cytoplasms were shrunken. Although nuclei could be identified by the outline of the nuclear envelope and their central position, other organelles were difficult to distinguish. The extrahaustorial matrices of these haustoria were thinner and more densely staining than normal. The intercellular appressorium of one haustorium was detached from the neck and the cytoplasm of the neck extruded (plate 1.5a) although it was retained in the body and lobes. These haustoria were considered necrotic.

A further structure was tentatively identified as either an encased haustorium or a deposit formed in response to attempted penetration of the cell wall (plate 1.4b). It was situated in a spongy mesophyll cell directly adjacent to the palisade layer (as were most haustoria) and the profile of an intercellular hypha was closely associated. The cytoplasms of the infected cell and hypha were electron dense and their walls infolded in a manner suggesting that turgor had been lost. Within the cytoplasm of the host cell was a structure with two distinct components. A central zone contained amorphous deposits of varying electron density and formed an irregular boundary with the encasing material. The latter was continuous with an apposition lining the cell wall and similar to deposits in mesophyll cells with otherwise normal ultrastructure but adjacent to cells with necrotic cytoplasm and infolded cell walls (plate 1.1a).

3.Discussion.

3.1.Characterisation and distribution of the osmiophilic deposits.

The present study corroborates previous evidence that caffeine causes condensation of phenolics at their *in vivo* sites in plant cells (Mueller and Greenwood,1978; Mueller and Rodehorst,1977). Without caffeine, interpretation of the distribution of phenolics in healthy and infected leaves of *Corylus avellana* and *Betula pendula* would not have been possible. The inclusion of caffeine in the fixative solution is now recommended for all ultrastructural studies of infection of woody plants since there is a correlation of the tannin content of leaves and woodiness in plant species (Bate-Smith and Metcalfe,1957).

Identification of the osmiophilic deposits in vacuoles of leaf cells of *C. avellana* and *B. pendula* with the phenolics present in extracts of leaves (Bate-Smith and Lerner,1954) is based on the following comparative evidence:
1.) the osmiophilic properties of the deposits suggest they could contain either phenolic (Czanisky and Catesson,1974), lipidic or proteinaceous material (Hayat,1975);
2.) the appearance of cells fixed without caffeine was typical of phenol storing cells where the vacuolar phenolics had leached through the tonoplast and tanned the cytoplasm (Mueller and Beckman,1976). Differences in the intensity of cytoplasmic darkening probably reflect the degree of tonoplast integrity and initial quantity of phenolics present in each cell;
3.) the precipitation and restriction of osmiophilic material

in cells of Corylus by caffeine is characteristic of its effect on phenolics and tannins (Mueller and Greenwood,1978; Mueller and Rodehorst,1977);

4.) the form of the vacuolar deposits was similar to those in other plant species where their identity has been confirmed by cytochemical and chemical tests for phenolics (Baur and Walkinshaw,1973; Beckman and Mueller,1970; Beckman et al,1972; Mueller and Beckman,1976).

Although osmiophilic deposits in cells of x-ray treated fern prothalli were described as lipidic (Allen and Haigh,1973), the evidence above indicates these too contained phenolics. However all the deposits including those in C. avellana and B. pendula, probably also contain proteins since poly-phenols are protein precipitants (Anderson,1968; Withers,1976).

In C. avellana and B. pendula the vacuole alone seems to be the site of synthesis and storage of phenolics. Plastids have been implicated (as possible synthesis sites) by ultrastructural studies of other species (Mueller and Beckman,1974; Wardrop and Cronshaw,1962) and the polyphenol oxidase activity of thylakoids has been correlated with phenolic formation (e.g. in cotton roots, Mueller and Beckman,1978). However thylakoids were absent or considerably reduced in number in the plastids described by those authors but in leaves of C. avellana and B. pendula they were organised as chloroplasts which are concerned primarily with photosynthesis (Gunning and Steer,1975). Although osmiophilic droplets were frequent throughout the stroma, their appearance after poststaining was different from the deposits in the vacuoles and thus they are most

probably lipidic. This does not preclude chloroplasts or indeed any other organelle as sites of synthesis of phenolic precursors, but their osmiophilic properties are only apparent when the phenolics are sequestered in the vacuoles.

3.2.Morphology of *Phyllactinia* in relation to the structure of infected leaves.

The present work also confirms the presence of endophytic hyphae in *P. guttata* infections in addition to the epiphytic mycelium characteristic of other powdery mildews. This distinct morphology was described by Blumer (1967) as hemi-endophytic and reflects the requirements of *P. guttata* for nutrition and sporulation and its adaptation to the structure and organisation of the infected tissue in the following ways:

Upper epidermes of *C. avellana* leaves have highly sculptured surfaces and thick cuticles which probably hinder formation of appressoria and subsequent penetration (Campbell *et al*, 1980). The lower epidermis is less sculptured and the cuticle thinner but there are also many stomata through which access to the leafs' interior is relatively easily attained. This provides an opportunity which powdery mildews infecting upper epidermes do not usually encounter.

The advantages of an intercellular mycelium are exploited by many other pathogenic fungi but only *Phyllactinia* and *Leveillula* spp. amongst the powdery mildews (Blumer,1967). Benefits include protection from environmental stresses (particularly desiccation)

prevalent on the leaf surface and the opportunity to select tissues and cells which will provide rich nutrient sources. Haustoria of P. guttata situated in cells of the bundle sheath are suitably positioned to intercept photosynthates en route to the phloem. Similar associations are reported for rust fungi (Al-Khesraji et al, 1980) where hyphae penetrate to the vascular elements themselves. In contrast hyphae of P. guttata were restricted to pre-existing intercellular spaces and did not seem capable of penetration beyond the bundle sheath.

Haustoria of P. guttata show the organisation typical for powdery mildews with morphological differences which reflect the variation of shape and orientation of infected cells. Lobes mostly arise from the neck end of the body and are arranged so that the shape of the haustorial complex conforms to the shape of the infected cell. Thus lobes extend directly away from the body and lie parallel to the long axis of elongated cells but are recurved over the body to form a compact structure in cells that have a more spherical shape. The orientation of lobes with respect to the body is typically constant for all the haustoria of a particular species of powdery mildew and variation between species is restricted to two distinct forms (Hirata and Kojima,1962). Haustoria in graminaceous hosts are elongate with the lobes extending away from the body (Bracker,1968) whilst in non-graminaceous hosts they are compact pear-shaped structures (e.g.Gil and Gay,1977; Perera and Gay, 1976). Thus the ability of haustoria of P. guttata to conform to the shape of individual host cells is an adaptation which is not shown by other

powdery mildew species.

In addition to the benefits of an intercellular mycelium, the stomatal connection to the epiphytic mycelium enables P. guttata to sporulate freely without causing the disruption of host tissues associated with erumpent pustules of rust fungi (Littlefield and Heath,1979). The elegant mechanisms for the detachment of cleistocarps from the lower surface of infected leaves and subsequent ascospore discharge (Cullum and Webster,1977) complete the structural adaptations shown by P. guttata.

3.3.Responses to infection and effect of phenolics on haustorial function.

Infections of P. guttata elicit host responses characteristic of powdery mildew infections including envelopement of haustoria by an extrahaustorial membrane and the formation of an extrahaustorial matrix. A collar of material deposited around the neck region is also typical and although in P. guttata and other powdery mildew infections it usually remains small, it may extend to encase the haustorium in certain circumstances (Gil and Gay,1977; Perera and Gay,1976; Stavely et al.,1969). The incidence of necrotic haustoria in cells with osmiophilic cytoplasms indicates that hypersensitivity (Kiraly,1980) might be expressed by a proportion of infected cells and the role of the vacuolar phenolics in this response is of particular interest.

The possible functions of plant phenolics in relation to wound healing and defense mechanisms are well documented (see Introduction to this chapter; Beckman et al., 1972; Mueller and Beckman,1976). These phenolics can be

classed as "constitutive" or "induced" respectively according to whether they are present in healthy, uninfected cells and tissues or are only formed in response to adverse stimuli such as infection. The phytoalexins are included in the latter group and are the subject of many studies (see reviews by Kosuge,1969; Kuc,1972). A role for constitutive phenolics in resistance to infection has also been suggested (Beckman *et al*,1972; Mace,1963; Mueller and Beckman,1976; Schlösser,1980; Swain,1977) and is considered below.

Although infection by *P. guttata* may cause vacuolar phenolics to leach into the cytoplasm of cells containing haustoria it seems likely that phenolics are formed directly in the cytoplasm as the vacuoles still contain large volumes of osmiophilic material. If the latter had contributed significantly to cytoplasmic darkening, it is expected that their volume would be diminished and they would show a similar ultrastructure to the deposits remaining in vacuoles of cells fixed without caffeine (compare plates 1.5b and 1.1a). Evidence that synthesis *de novo* may occur in the cytoplasm is provided by studies of other plant species where phenolics appear as distinct globules in the cytoplasm (Obukowicz and Kennedy,1981). Additionally, in epidermal cells of *Pisum sativum* infected with *Erysiphe pisi* caffeine does not alter the distribution of osmiophilic material (presumably phenolic) which occurs throughout the cytoplasm during necrosis without first accumulating in the vacuole or other specific sites (Chapter 2, section 2.2).

In contrast to the evidence above that following infection phenolics arise in the cytoplasm, constitutive

phenolics stored in vacuoles are released into the cytoplasm in other infections and in response to various physical and chemical stimuli (Beckman et al,1972) which include damage to the tonoplast during fixation. Similar effects also occur in tissues which accumulate vacuolar phenolics during senescence (Baur and Walkinshaw,1973; Robb et al,1975a) and during physiological and infectious diseases (Robb et al,1975a; Syrop,1975a and b). Changes in the distribution of constitutive phenolics brought about by infection may be expected to be detrimental to the activities of affected cells. Phenoloxidases in the cytoplasm oxidise phenolics to quinones and tannins which inactivate enzymes and organelles by specifically inhibiting enzyme activity and precipitating proteins (Anderson,1968; Bell,1981; Loomis and Battaile ,1966). The degree of inactivation will probably depend on the quantity of phenolics and activity of the phenoloxidases present in the cytoplasm. Phenoloxidases require high partial pressures of O_2 for maximal activity which are not prevalent whilst the plasma membrane remains intact (Anderson,1968). Thus in cells where only the tonoplast is ruptured, oxidation products will accumulate at a slow rate and cellular activities decline gradually. Individual enzymes are inhibited by phenolics to different degrees (Loomis and Battaile,1966) and therefore some processes would cease before others. In particular, ATPases are inhibited by low concentrations of several phenolic compounds (Balke and Hodges,1975 and 1979) and reduced activity of these enzymes would have a detrimental effect on transport of solutes across the parasite interfaces

where ATPases are thought to play an essential role (Chapter 3, section 4.3; Spencer-Phillips and Gay,1981). In addition to the reduced transport resulting from the presence of phenolics in the cytoplasm of infected cells, haustoria are infrequent and a high proportion necrotic. These observations question the importance of haustoria as interfaces for nutrient transfer in infections of P. guttata. Considerable evidence indicates that haustoria of other powdery mildews are essential for transfer of photosynthates (Manners,1979; Manners and Gay,1978 and 1982) and inorganic ions (Martin and Ellingboe,1978; Slesinski and Ellingboe,1971). These species lack intercellular hyphae and haustoria are restricted to epidermal cells of their host. In contrast the role of haustoria in infections of rust fungi is not certain and accumulation of assimilates by intercellular hyphae cannot be discounted particularly as these pathogens can be grown in axenic culture where they do not form haustoria (Scott, 1976) and growth of intercellular hyphae continues after the death of haustoria in infected tissue (Ogle and Brown, 1971). Thus the intercellular hyphae of P. guttata, although not extensive, may also provide an interface for nutrient uptake and play an important role in the absence of healthy haustoria.

On the other hand it should be noted that most haustoria of P. guttata were extensively lobed and completely enveloped by an extrahaustorial membrane. This indicates that early stages of haustorium development and establishment of the parasitic interface are not inhibited by phenolics and transport of assimilates

probably occurs during initial phases of infection. In addition phenolics may not pass through the extrahaustorial membrane even when the host cytoplasm is affected as the haustorium does not become osmiophilic until later. Haustoria may therefore accumulate metabolites by mechanisms that are independent of an active host cytoplasm and essentially similar to those of necrotrophic pathogens before the cytoplasms of haustoria and intercellular appressoria become osmiophilic and necrotic. Initial exclusion of phenolics reflects the specific permeability properties of the extrahaustorial membrane (Gay and Manners,1984) which have been shown by swelling experiments with isolated haustorial complexes to be retained for several days after the host cytoplasm has been removed (Gil and Gay,1977).

Whether phenolics enter haustoria at any stage is not certain since the cytoplasm of necrotic haustoria was less osmiophilic than affected host cytoplasm. Soluble phenolics would be oxidised by phenoloxidases and precipitated in the host cytoplasm leaving less to permeate the extrahaustorial region. Phenolics that enter haustoria may be compartmentalised before they affect cellular activity. The osmiophilic globules in vacuoles within the haustorial cytoplasm (plate 1.8) are possibly phenolic and the similar appearance of vacuoles in necrotic haustoria with those in the host cytoplasm (see plate 1.5a) suggests their phenolic contents were lost during sectioning. Tolerance to phenolics including phytoalexins is exhibited by many other pathogenic fungi (Higgins and Millar,1976; Pueppke and Van Etten,1976; Shiraishi *et al*,1977; Ward *et al*,

1973) but the mechanisms have not been unequivocally established. Evidence for vacuoles as suitable sites for storage is provided by plants such as Corylus and Betula spp. which accumulate large quantities of constitutive phenolics.

In conclusion the present study provides ultrastructural evidence which indicates that whilst phenolics undoubtedly have antifungal properties their primary effect in infections of P. guttata is to inactivate the host cytoplasm. This would essentially starve the haustorium as a healthy host cytoplasm is prerequisite for substantial transport of photosynthates to haustoria of powdery mildews (Chapter 2, section 3.3; Spencer-Phillips and Gay,1980a).

Table 1.1. Frequency of profiles of haustoria and intercellular hyphae of Phyllactinia guttata in thin sections of Betula and Corylus leaves fixed in glutaraldehyde in the presence or absence of caffeine.

Specimen	Treatment with caffeine	Number of samples (leaf pieces)	Number of grids examined	Number of intercellular hyphae	Number of haustoria with healthy appearance	Number of haustoria with necrotic appearance
Corylus (uninfected)	+	3	5	0	0	0
	-	2	6	0	0	0
Corylus and Phyllactinia	+	16	46	8	2	0
	-	6	20	5	0	2
Betula and Phyllactinia	-	2	7	2	0	2

Plate 1.1.

Sections of leaves of Corylus avellana.

a. Representative field of mesophyll cells fixed without caffeine; section stained with uranyl acetate and lead. Cytoplasmic detail is largely obscured by phenolic material leached from vacuoles (v). Note deposits (large arrows) at cytoplasmic face of walls adjacent to cells with infolded cell walls (arrowed, w) and disrupted cytoplasms. Is = intercellular space. Neg. no. 8008, x 6,300.

b. Palisade mesophyll cell fixed with caffeine, section not post-stained. Contents of vacuoles (v) and lipid droplets in chloroplasts (Cl) alone are strongly osmiophilic. Cy = cytoplasm. Neg. no. 7737, x 9,600.

c. Epidermis and palisade mesophyll cells (centre) fixed with caffeine; post-stained as in (a). Cytoplasm (Cy) of one cell is osmiophilic and disrupted whilst the nucleus (n) and other organelles within the cytoplasm of its neighbour are clearly distinguished. Neg. no. 7727, x 3,750.

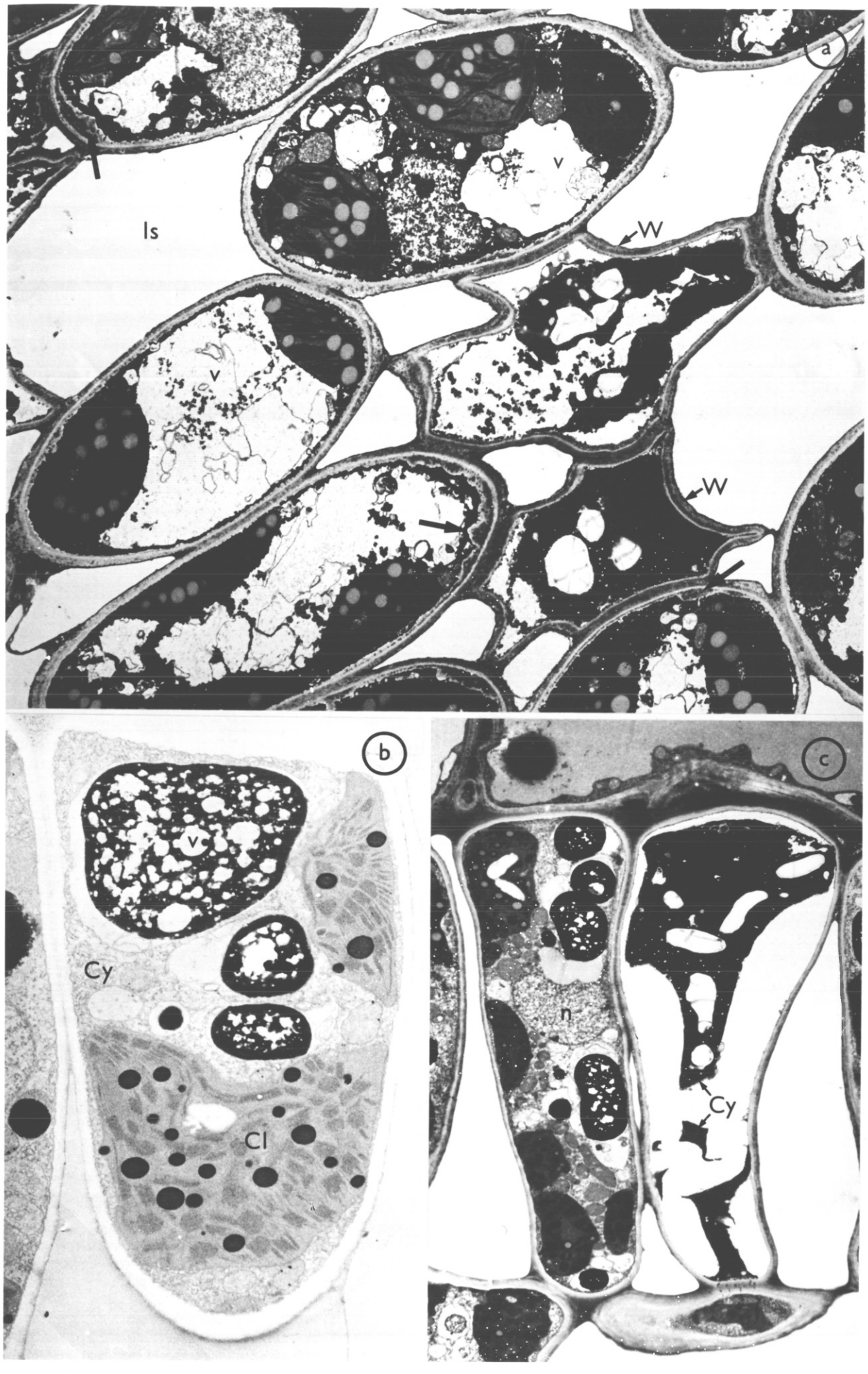

a
ls
v
v
W
W
b
v
Cy
Cl
c
n
Cy

Plate 1.2.

Section through leaf of C. avellana prepared as in plate 1.1.c. The upper epidermis has a convoluted outer surface (cf smooth lower epidermis) and one cell contains phenolic material as a large spherical globule in its vacuole. Cells of the bundle sheath (Bs) delimit the vascular tissue which is connected to the upper epidermis by cells with thickened walls (W) and no intercellular spaces (Is). Neg. nos. 7744 and 7745, x 2,600.


W
Bs
Is

Plate 1.3.

Light micrographs of the lower surface of leaves of Corylus avellana infected with Phyllactinia guttata. Tissue pieces cleared and mounted in lactophenol, viewed with bright field optics. x 1,850.

a,c. Focused on surface of leaf, showing surface mycelium (hy; conidium asterisked) and hyphae (arrows) penetrating via stomata.

b,d. Focused on substomatal cavity, showing swollen cells of infecting hyphae each with a single intercellular hypha extending towards the internal tissues of the leaf.

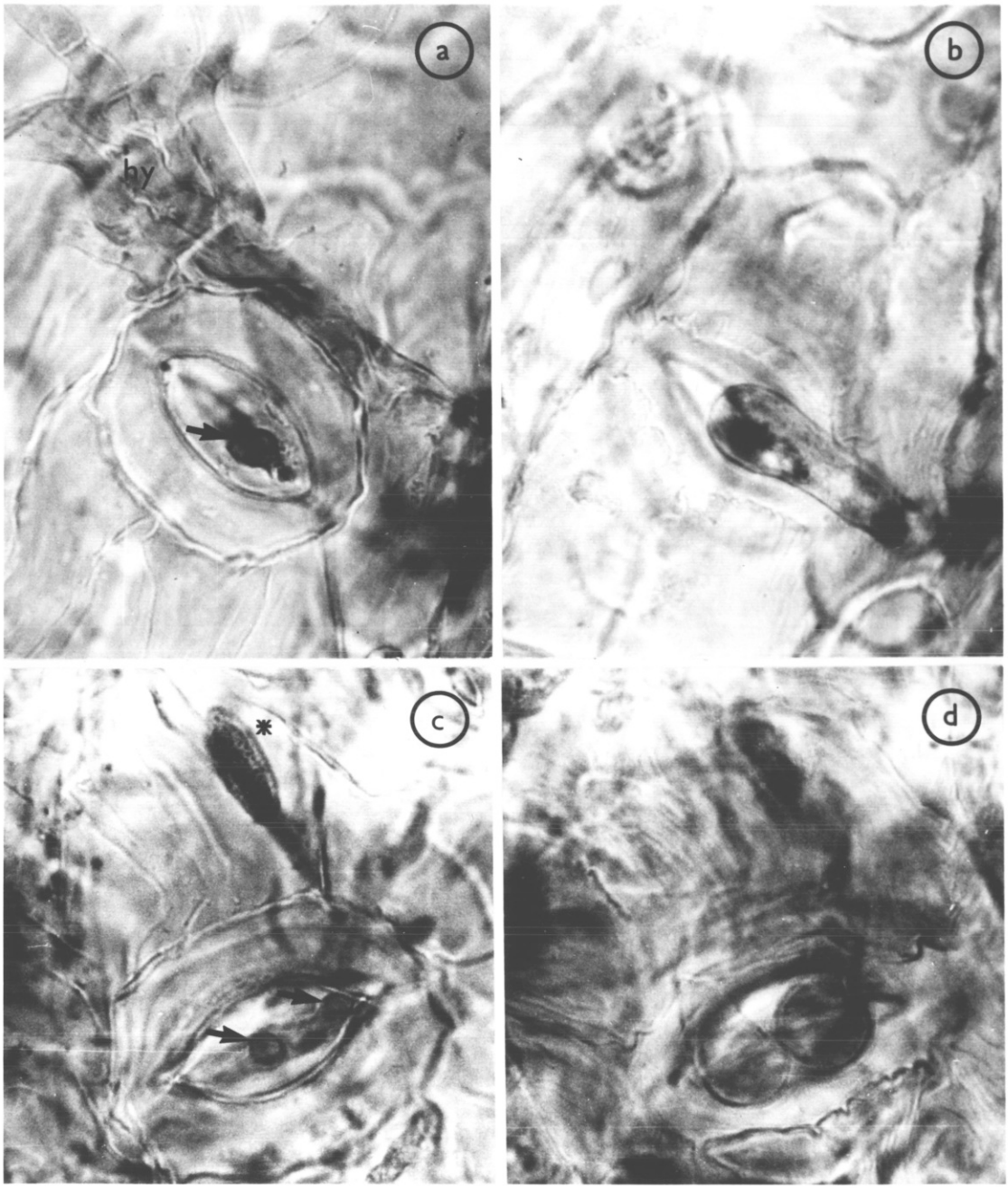
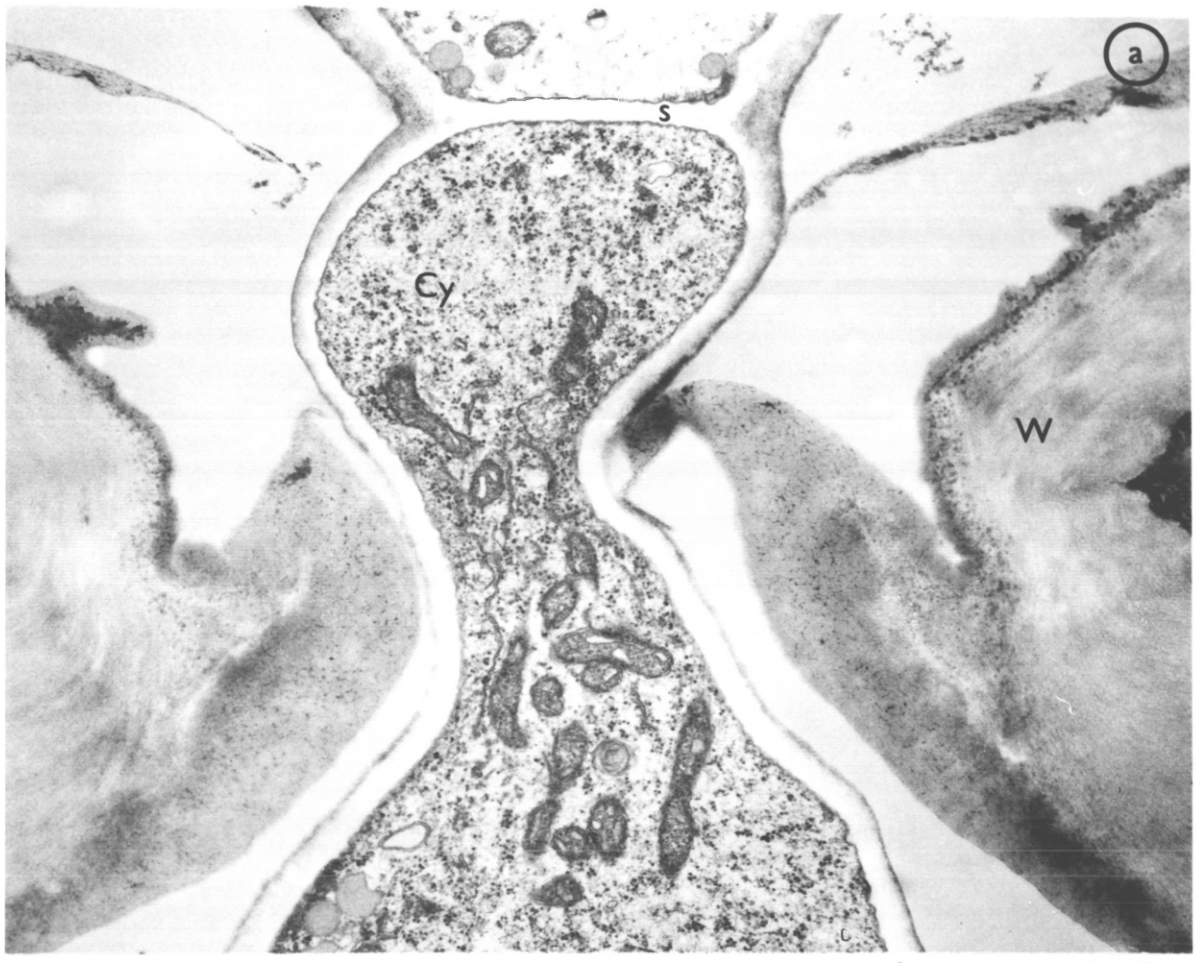

a
hy
b
c
*
d

Plate 1.4.

Leaves of C. avellana infected with P. guttata.

a. Section through stomatal aperture. The surface hypha is separated from the substomatal cell (cy = cytoplasm) by a septum (s). W = guard cell wall. Neg. no. 5315, x 20,100.

b. Spongy mesophyll cell and intercellular hypha both with electron dense cytoplasms (Cy and cy respectively). The structure in the mesophyll cell has a central zone (arrow) surrounded by a layer of less electron dense material (asterisk) continuous with an apposition lining the cell wall (W). Neg. no. 8128, x 15,600.


a
S
Cy
W

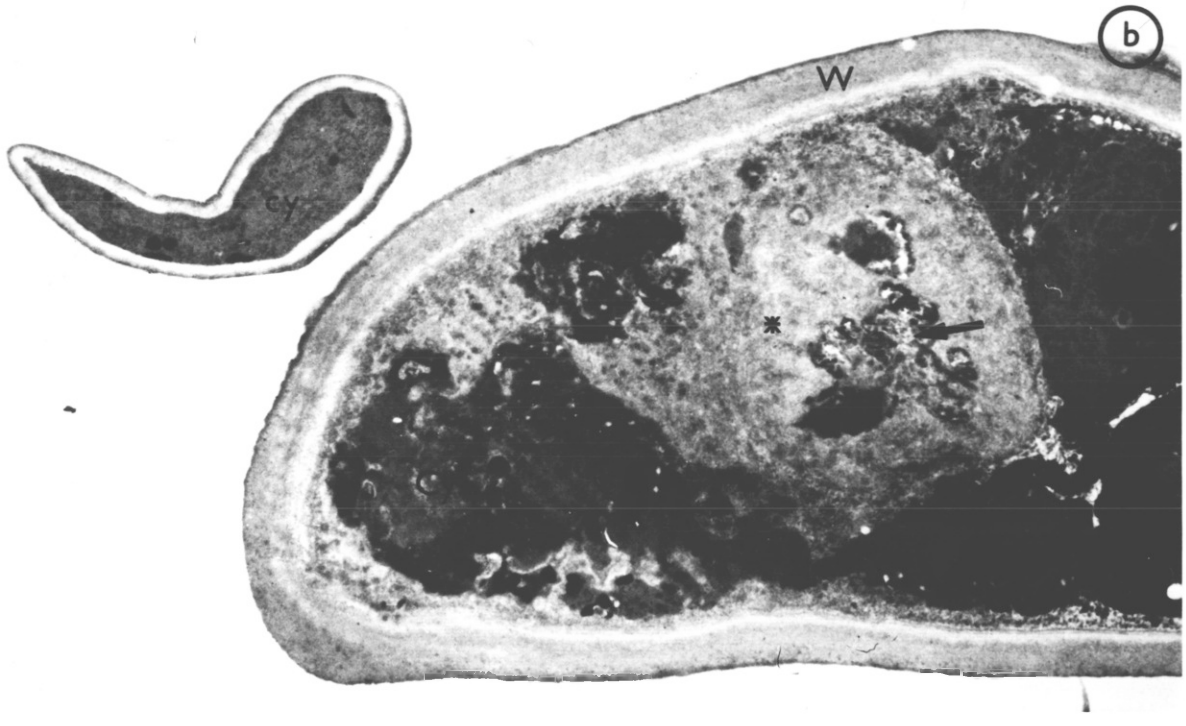

b
W
Cy

Plate 1.5.

a. Section of mesophyll cell with necrotic haustorium, prepared as in plate 1.1.a. The cytoplasm of the infected cell (Cl = chloroplast) is electron dense and the appearance of vacuoles (v) suggests their contents were lost during sectioning. A nucleus (n) is positioned centrally in the haustorial body which is separated from the neck (hn) by a septum (s). The appressorium is detatched and cytoplasm (cy) extruded to the intercellular space. Haustorial lobes are mostly attached to the neck end of the body. The haustorium has an angular outline and the extrahaustorial matrix (Ma) is reduced in volume and electron dense. Neg. no. 8015, x 9,600.

b. Lower epidermis and mesophyll of infected leaf; section prepared as in plate 1.1.c. The thin layers of cytoplasm in epidermal cells surround vacuoles containing phenolic material in the form of irregularly lobed globules. A vacuole (v) containing condensed phenolics is also present in the infected mesophyll cell whose cytoplasm (Cy) is more electron dense than in the haustorium (h) and hyphae (hy) in the intercellular space (Is) and on the leaf surface. See plates 1.6, 1.7, 1.8 for adjacent sections. Neg. no. 8238, x 3,400.

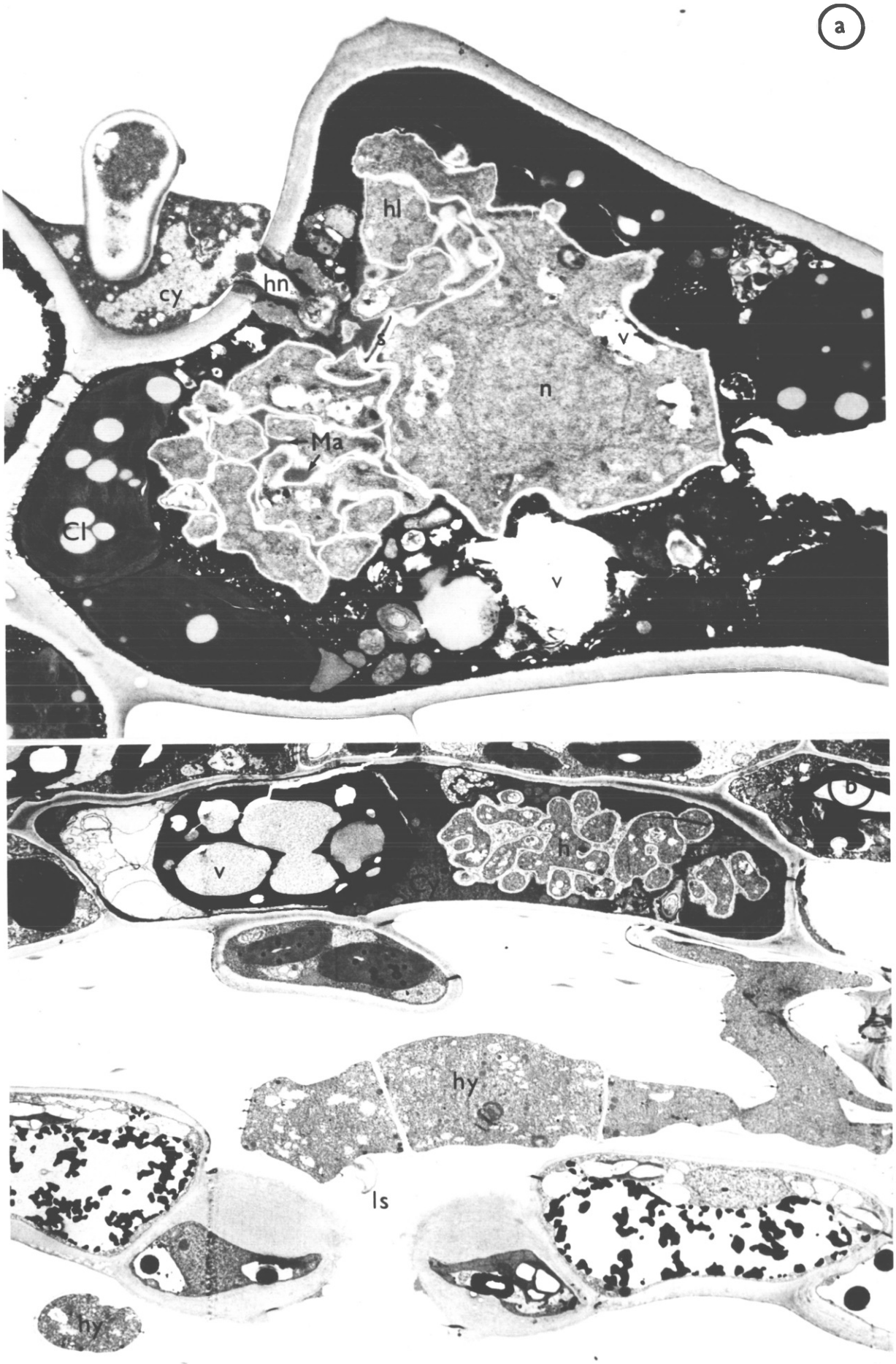

a
hl
cy
hn
s
v
n
Ma
cl
v
v
n
b
hy
ls
hy

Plate 1.6.

Adjacent sections through haustorium in plate 1.5. The intercellular hypha (hy in a) is connected via an appressorium (ap) to the haustorium. The latter (in b) has a central body (hb) with lobes (hl), sometimes branched and extending in parallel with the long axis of the infected cell. Note the hypha (hy in b,c,d) extending beyond the cell containing the haustorium. Neg. nos. 8237, 8245, 8244 and 8363, x 5,300.

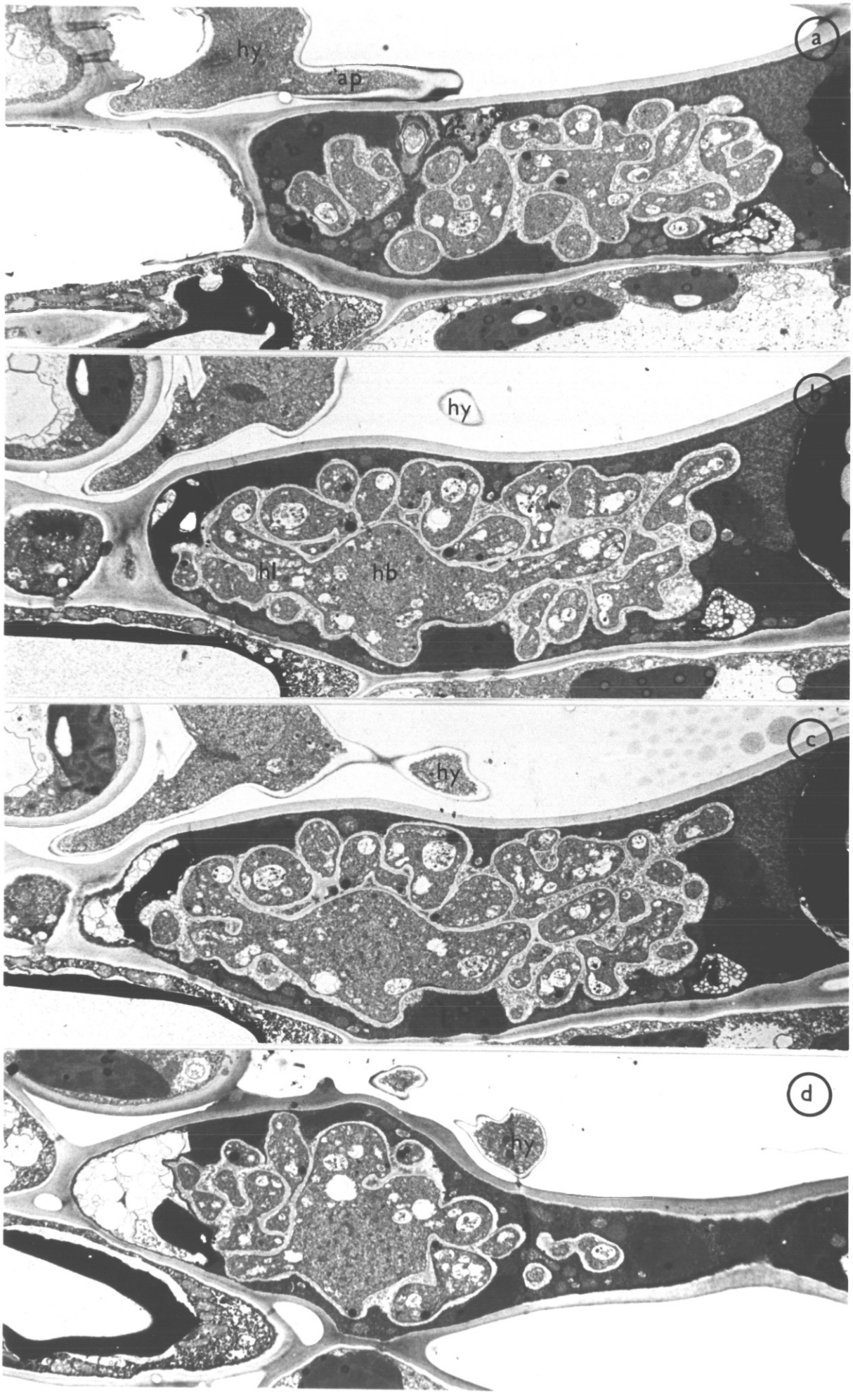

a
hy
ap
b
hy
hl
hb
c
hy
d
hy

Plate 1.7.

a,b. Oblique sections through neck region of haustorium in plate 1.5. The wall of the neck (hn) is continuous with the inner layer (arrows in b) of the wall of the appressorium (ap). The wall (W) of the infected cell is more electron dense directly adjacent to the point of penetration and a collar (C) extends from this region to surround the neck of the haustorium (hn). hl = haustorial lobe; m = mitochondrion; Ma = extrahaustorial matrix.
a, neg. no. 8239; b, neg.no. 8135, x 20,100.


a
ap
W
C
hn
Ma
hl
b
m
W

Plate 1.8.

Section of haustorium in mesophyll cell shown in plate 1.5. Lobes are separated from the host cytoplasm by an extrahaustorial membrane (Em) and matrix (Ma). The latter contains small osmiophilic droplets (asterisks). Vacuoles (v) in the cytoplasm of the haustorium show profiles of membranes and osmiophilic globules. Electron lucent areas (arrows) in the cytoplasm resemble glycogen. Note the increased electron density of the cytoplasm of the infected cell in comparison with the adjacent cell (bottom of micrograph) and the haustorium and appressorium (ap). Neg. no. 8132, x 37,200.


ap
Em
Ma
v

CHAPTER 2.

Electron microscope autoradiography of ^{14}C photosynthate distribution at the haustorium-host interface and ultrastructure of necrotic tissues in powdery mildew of Pisum sativum.

1.Introduction.

Haustoria are specialised intracellular structures characteristic of fungi that are obligate plant pathogens (Bracker and Littlefield,1973). However, only recently has evidence of their function in translocating nutrients from host to pathogen become available. Experiments supplying host tissue with inorganic isotopes (Martin and Ellingboe, 1978; Slesinski and Ellingboe,1971), mechanically damaging haustoria (Bushnell et al,1967) or simply correlating hyphal extension rates with haustorium development (Hirata,1971) provide indirect evidence for this role. Further, isotopes applied to the host either as radio-labelled amino acids (Andrews,1975; Manocha,1975; Mendgen, 1977) or $^{14}CO_2$ (Manners and Gay,1978; Takahashi et al, 1977) have been detected in haustoria. Manners and Gay showed that photosynthates were both translocated into haustoria and subsequently metabolised.

The latter experiments (Manners and Gay,1978) depended on isolation of haustorial complexes from pea leaves infected with Erysiphe pisi (Gil and Gay,1977) and subsequent physiological and biochemical analyses. The haustorial complex comprises the haustorium, the portion of host plasma membrane invaginated around it (the

extrahaustorial membrane), and the intervening structures (mainly the extrahaustorial matrix). Since the results of Manners and Gay were averages for all the constituents of the fraction, light microscope autoradiographic analyses were subsequently carried out (Manners and Gay,1980). These showed considerable variation in the quantity of isotope in individual haustorial complexes. This was not correlated with age and remained unexplained.

The present study has employed electron microscope autoradiography and the increased resolution provides a more detailed analysis of photosynthate incorporation and permits labelling of the fungal components of haustorial complexes to be distinguished from that in other interfacial structures. In particular, the status of the extrahaustorial matrix is explored. It is characteristic of the host interface with powdery mildew haustoria and of many other intracellular pathogenic fungi (Bracker and Littlefield,1973). It is sealed between the haustorium surface and the extrahaustorial membrane by annular structures in the necks of powdery mildew haustoria (Gay and Gil,1975; Gil and Gay,1977; Manners and Gay,1977) and rust haustoria (Heath,1976) and host translocates are thus assumed to be directed across the extrahaustorial membrane and matrix to the haustorium. The origin and function of the matrix is unknown (Bushnell and Gay,1978), but the zone characteristically increases in volume as haustoria age and development in rusts may be associated with host resistance (Bracker and Littlefield,1973). The present study indicates the origin of the matrix and

extrahaustorial membrane. As in the autoradiography carried out by Manners and Gay (1980) isolated haustorial complexes have been employed. This has facilitated the autoradiographic analysis by providing the necessary large number of haustoria with their host interfaces.

The autoradiography is complemented by an investigation of the ultrastructure of infected leaves. In particular, necrotic regions are described in detail.

2.Results.

2.1.Isolated fraction.

Isolated haustorial complex fractions include several species of particles (constituents) and to assist interpretation of the autoradiographic results these are qualitatively and quantitatively described. To analyse the results further, components of the haustorial complexes are also recognised; these are the haustorial body, haustorial lobes, extrahaustorial matrix and extrahaustorial membrane.

Area analysis of the fraction constituents (table 2.1) shows that approximately 62% of its volume consisted of haustorial complexes and the remainder of host cell wall fragments, organelles and cytoplasm which were both free and adhering to haustorial complexes, occasional E. pisi conidia, starch grains and crystalline inclusions (plate 2.1). Starch grains were recognised by their rounded outline and charateristic concentric layered structure whereas the crystalline inclusions were trapezoid (described as rhomboid from light microscopy by

Manners,1979) and completely electron translucent within the background of the bovine plasma albumin (plate 2.1). The latter were sometimes as large as haustoria and occur in bundle sheath cells of the leaf.

The haustorial complexes were considered as three classes, healthy, necrotic and pre-necrotic (plate 2.4a,b). These occurred in the proportion 3.25: 1.25: 1 but the values would probably vary with the degree of necrotic flecking shown by leaves used to prepare the fraction. Healthy complexes (plates 2.2; 2.4a) clearly showed an organised haustorial cytoplasm with organelles which were retained by a plug in the pore of the neck septum (plates 2.2; 2.3), an haustorial wall, extrahaustorial matrix and highly convoluted extra-haustorial membrane similar to those described by Gil and Gay (1977). Their necks were devoid of cytoplasm but the osmiophilic inclusions which were present before isolation of haustorial complexes (plates 3.11a; 3.13) remained in situ (plate 2.3). The neck of one haustorium contained fibrils which were shown by examination of serial sections to fill the lumen. Occasionally necks of other isolated haustorial complexes contained small groups of fibrils. The extrahaustorial membrane was completely free from adherent host cytoplasm (plates 2.2; 2.5a).

Necrotic complexes (plate 2.4) differed from the healthy both in the appearance of the haustorial cytoplasm and in changes to the extrahaustorial membrane and the matrix. An adherent layer of host cytoplasm was always apparent. Occasionally cytoplasmic membranes were

visible in the fungal and adherent host cytoplasms but they had lost their integrity and organelles were not distinguishable. The cytoplasms were very electron dense and the fungal cytoplasm was often shrunken from the haustorial wall. The extrahaustorial matrix was considerably narrower and with greater electron density than in a healthy complex (plate 2.4). The extra-haustorial membrane lacked the characteristic convolutions and highly electron dense globules were associated with it (plates 2.5b; 2.6b) often giving a beaded appearance. The latter are described more fully in the next paragraph. The adherent host cytoplasm often retained the shape of the collapsed necrotic epidermal cell (plate 2.4b). The free fragments of host cytoplasm and organelles also appeared necrotic and similarly sometimes retained the shape of collapsed necrotic host cells. Chloroplasts (plate 2.1) were invariably associated with necrotic host cytoplasm suggesting they arose from necrotic mesophyll cells.

The structure of pre-necrotic complexes ranged between the healthy and necrotic conditions. Typically the haustorial cytoplasm resembled that of healthy haustoria, retaining membrane integrity. However, in some members of this class the cytoplasm was slightly disorganised. It contained irregularly shaped electron dense deposits which were usually attached to the plasma membrane (plates 2.4a; 2.5b; 2.7a) and only occasionally found in healthy haustoria. The deposits may be formed at breaks in the plasma membrane and have a function similar to the plug in the septal pore. Indeed the

appearance of the deposits at both sites was similar; an osmiophilic material was arranged in a hemisphere around a less dense component directly adjacent to the plasma membrane or septal pore respectively (plate 2.3). Convolutions of the extrahaustorial membrane were absent or less distinct than in the healthy class (plate 2.5b). Sometimes it showed the beaded appearance, and small pieces of adhering host cytoplasm (plate 2.4a), both characteristic of necrotic haustorial complexes. The beading shown by extrahaustorial membranes of pre-necrotic and necrotic haustorial complexes sometimes seemed to be symmetrical about the membrane (plate2.5b) but in many instances (plates 2.5c; 2.6c) the opaque globules lay near or attached to the matrical surface. The detailed shape (plate 2.5c), positions of the globules and absence of membrane convolutions indicated that they had arisen by condensation of invaginations of the extrahaustorial membrane. The extrahaustorial matrix of pre-necrotic complexes contained denser areas than usually found in healthy complexes (plate 2.5b).

2.2.Infected leaves.

Haustorial complexes of the three types were also recognised in infected epidermes. Healthy haustoria were common and necrotic parts of epidermis showed haustoria in different phases of necrosis.

Epidermal cells at the centre of necrotic flecks contained fully necrotic complexes and had walls which were highly folded in a manner suggesting that turgor had been completely lost (plates 2.6a; 2.8b).

Their membranes, including the extrahaustorial membrane, organelles and cytoplasms were so densely stained that they were often indistinguishable from one another (plates 2.6b; 2.8b). Other inclusions were less dense and may represent condensed contents of vacuoles. The walls of cells containing less necrotic complexes (plates 2.6c; 2.7a) were folded to a lesser degree. Their cytoplasm was disrupted and shrunken but remained as a distinct layer around haustoria and cell walls and was less densely stained than in the extreme necrotic condition (plate 2.6b). Membranes and organelles could be recognised and the associated extrahaustorial membrane resembled that of isolated pre-necrotic complexes with the loss of convolutions and areas of increased electron density described before. The vacuoles contained floccular deposits (plates 2.6c; 2.7a) which were also present in epidermal cells with normal cytoplasm at the edges of the necrotic regions (plate 2.8a). In addition these last cells sometimes showed an extra layer between the cytoplasm and cell wall and usually at the wall shared with necrotic cells (plate 2.8a). The electron lucent matrix of the deposit showed dense regions and contained fragments of membrane and its ultrastructure resembled that of collars (plates 2.10a; 3.11a; 3.13) around haustorial necks at the point of penetration of the epidermal wall.

Most mesophyll cells had a normal cytoplasm but a few showed changes that were characteristic of necrosis including increased electron density of cytoplasm and

organelles, osmiophilic globules associated with membranes and folded cell walls (plate 2.7b). An additional layer (approx. 0.25 μm thick) was always associated with the region of the cell wall proximal to necrotic epidermal cells (plates 2.7b; 2.9a,b). The plasma membrane formed a convoluted boundary with this apposition which was non-fibrillar and differed in appearance from those in epidermal cells. Granules (approx. 36 nm diameter) were arranged as irregular patches within a less dense matrix (plates 2.7b; 2.9a,b) and were often associated with fragments of membrane (plate 2.9a). Their appearance did not alter when the cell became necrotic (plate 2.7b). Vesicles in the cytoplasm were similar in size and electron density to the granules whilst others had less dense contents (plate 2.9a). The latter appeared to be associated with golgi dictyosomes which were particularly frequent in the cytoplasm adjacent to the wall apposition.

Fixation with caffeine altered neither the distribution of the contents of necrotic cells nor the appearance of the associated wall deposits.

Necrosis of the haustorial cytoplasm did not immediately lead to necrosis of the cytoplasm in the appressorium and surface hyphae. This is probably because the necks of necrotic haustoria became occluded (plate 2.10a) by a material resembling the irregular deposits associated with the plasma membrane of pre-necrotic haustoria and the plug in the pore in the neck septum (Gil and Gay,1977). This contrasts with necrosis in rust haustoria where there is no neck septum and the

mother cell is also affected (Abu-Zinada et al,1975; Heath,1972).

2.3.Isotope distribution in the isolated fraction.

The distribution of silver grains followed closely the classes of constituents recognised in the fraction (table 1.1). Eighty-six percent of the isotope in the constituents was found associated with haustorial complexes and 77.5% was with healthy complexes. Pre-necrotic and healthy haustorial complexes showed twice and six times respectively the concentration of isotope found over host cell contaminants (wall and cytoplasmic fragments).

Correction for positive chemography and background showed that necrotic complexes and the crystals did not contain the isotope. The apparent absence of labelling of necrotic complexes and crystals was not due to negative chemography because controls (plate 2.11b) showed the even distribution of characteristic filamentous silver grains over sections of labelled and unlabelled fractions and over all constituents of the fraction. Further, silver grains were observed occasionally over necrotic complexes (plate 2.11d).

2.4.Isotope distribution among the classes of haustorial complexes.

The statistical significance of the distribution of silver grains in the three classes of haustorial complex was analysed by determining the grain densities for randomly selected profiles of haustorial complexes in each class and correcting them for positive chemography

and background. The mean density per profile and the standard deviation from the mean for each of the three classes are given in table 2.2 which shows that the grain densities of profiles varied considerably within each class (figure 2.1).

However despite the variation that the standard deviations show, there are clear differences in the accumulation of isotope by complexes of the three classes (table 2.2).

The profiles of haustorial complexes were also classified by their grain densities (table 2.3). This indicates three major classes; i) profiles with grain densities below the level of host contaminants (<1.22 grains $\mu m^{-2} \times 10^{-2}$); ii) profiles with grain densities between the level of host contaminants and 12grains $\mu m^{-2} \times 10^{-2}$ (this includes the majority of the pre-necrotic class); iii) profiles with grain densities greater than 12 grains $\mu m^{-2} \times 10^{-2}$. Only 18% of the complexes accumulated significantly more than the pre-necrotic class.

2.5.Isotope distribution among components of healthy haustorial complexes.

The distribution of silver grains among components of healthy haustorial complexes is shown in plate 2.11a and in table 2.6 which takes account of grains situated over the extensive boundaries between individual components. The shared grains counted were reallocated as described in the methods section, using data in tables 2.4 and 2.5.

The distribution of grains can be considered by

comparing either the proportion of grains over each component or the respective grain densities and several aspects are worthy of special consideration.

The body contains approximately the same quantity of isotope as the lobes but as it occupies twice the volume it has only a half the concentration. The strictly fungal components (body, lobes and haustorial wall) contain 70% of the grains in the whole complex and thus considerably more label than the extrahaustorial matrix and membrane. The extrahaustorial membrane, whose volume amounts to about 5% of the volume of the average complex, contains a concentration of isotope similar to that in the body and lobes. This may be an over estimate of its concentration since the majority of grains designated exclusive to the membrane also overlay the surrounding embedding medium. The density calculated for the matrix is lower, but since Gil and Gay (1977) showed that its volume varied considerably with osmotic environment it cannot be exactly compared with that of other components.

Few sections of haustorial necks were encountered but none showed silver grains (plate 2.11c).

2.6.Light microscopy and staining with SITS and aniline blue.

Isolated haustorial complexes from pea were recognised by their characteristic pear shape and appearance as described by Gil and Gay (1977). The necrotic complexes described above from electron microscopy could not be distinguished by light microscopy with or without SITS and UV from contaminants, and thus the

structures recognised as haustorial complexes included only the healthy and pre-necrotic classes of electron microscopy. Within these, two types could be distinguished by light microscopy. Most appeared translucent with visible light and their extrahaustorial membrane fluoresced strongly in SITS, whilst a small number corresponding to pre-necrotic complexes appeared a yellow-brown and showed no fluorescence with SITS (plate 2.11e,f). Yellow-brown haustoria intermediate in colour between healthy haustoria and necrotic-infected cells could be detected in epidermes. All haustorial complexes had lost their ability to stain with SITS when stored for several days at $4^{o}C$, and haustoria of E. graminis in barley epidermis did not fluoresce under any conditions (plate 2.11g,h).

Haustorial complexes from pea showed no fluorescence with aniline blue. Fluorescence was restricted to papillae and infrequently the anticlinal walls associated with necrotic regions (plate 2.10b,c). No fluorescence was seen in necrotic cells or mesophyll cell walls in epidermal strips or sections of leaves cut with the freezing microtome.

3.Discussion.

The autoradiography confirms the results of Manners and Gay (1980) that only small quantities of radioisotope are present in particles contaminating haustorial complex fractions and thus analyses of the fraction provide reliable indications of the composition and function of the parasitic interface. The autoradiographic analysis has also enabled particular components

of this interface to be examined with a precision not previously achieved and by correlating these observations with those of detailed structures it has been possible to gain evidence of mechanisms which lead to the breakdown of the delicate balance necessary for the continued function of haustoria.

3.1.Assimilate distribution in the compatible interaction.

Manners (1979) showed that in similar haustorial complex fractions prepared without fixation the majority (60-70%) of the fraction label was in ethanol insoluble form and that 80-90% of this was associated with haustorial complexes. The present results show a similar proportion (86%) of ^{14}C photosynthate associated with haustorial complexes which was insoluble in the electron microscope preparative solutions (glutaraldehyde, acetone and Spurr's embedding medium). Most of this resided in haustorial complexes described here and previously (Gil and Gay, 1977) as healthy indicating that this major class was indeed assimilating host metabolites. The insoluble compounds are likely to be present as the result of growth processes in the haustorial cytoplasm and deposition in walls and other structures. In addition, a proportion of free amino acids present will have been rendered insoluble by glutaraldehyde (Peters and Ashley, 1967) and therefore their distribution also has been recorded by the autoradiography. Such amino acids may have been in transit and would have been included in the soluble fraction in analyses by Manners (1979).

The isotope concentration in the lobes was

double that found in the body. This may have been due to high rates of uptake associated with the large surface area and abundant mitochondria. It is also likely that it is correlated with growth expressed as an increase in the number and length of the haustorial lobes which occurs as haustoria age (Gil and Gay,1977). The extrahaustorial membrane is also heavily labelled indicating its continuing extension and probably its synthesis of matrical material as suggested by Gil (1976), Bushnell and Gay (1978) and Manners (1979). The matrix is also labelled but as indicated above, the concentration there is uncertain because the volume of this component is extremely variable, being dependent on the osmotic environment. The evidence discussed by Bushnell and Gay (1978) indicates that the matrix is not extensive in the living condition, distended matrices being the results of damage to the host cell by fixation or mechanical means. Thus the matrical concentration of insoluble isotope in living infected cells is probably comparatively high. (If in the current experiments it is seen as double its normal volume, its true concentration would equal that of the highest concentration found in the complexes). This is the first occasion on which significant matrical labelling has been shown, and the level attained suggests the matrix is derived directly from the host. Microauto-radiographic studies of rust fungi carried out either by labelling uredospores (Ehrlich and Ehrlich,1970; Mendgen and Heitefuss,1975) or the host (Manocha,1975; Mendgen, 1977) failed to detect isotope in the equivalent component. Only very low levels have been detected in the

structure around haustoria of downy mildews in hosts exposed to isotope (Takakashi et al,1977).

Thus extrahaustorial (interfacial) structures are the site of considerable deposition (30%) of host derived material which is insoluble and probably corresponds to cell wall components as suggested by Gil and Gay (1977) and Manners (1979). This does not preclude the possibility that these insoluble compounds may be later mobilised and translocated into the fungus but the author is not aware of evidence to support this notion.

3.2.Structure of the extrahaustorial membrane and ^{14}C accumulation.

This study has also confirmed the heterogeneity of photosynthate incorporation by haustoria and the interfacial structures, large variations being correlated with recognisable structural differences. The ultra-structural differences between healthy and necrotic complexes are such that these classes are quite distinct but light microscopy distinguishes the necrotic type only in infected tissue.

The first symptom of incipient necrosis is seen by electron microscopy as an alteration of the extra-haustorial membrane, in complexes of the pre-necrotic class which has not been described before. Identification of pre-necrotic complexes of electron microscopy with the yellow-brown, non-SITS staining haustorial complexes indicates that the quality of haustorial complex fractions can be evaluated by light microscopy and is based on the following observations:-

i) the proportions of each in fractions of isolated haustorial complexes were similar;

ii) by light microscopy their colour resembled that of haustoria in epidermal cells which were intermediate in colour between healthy and necrotic infected cells;

iii) the degree of leaf necrosis was approximately correlated with the proportion of SITS-negative haustorial complexes in the isolated fraction;

iv) SITS could be seen staining the extrahaustorial membrane of healthy complexes in a manner consistent with the mechanism described by Maddy (1964) who claimed that it binds to lipoproteins at the membrane surface. Absence of staining by complexes which, in visible light appeared yellow-brown, suggests that the surface groups of their extrahaustorial membranes were masked by adherent material or that structural alteration of the lipoprotein had occurred.

The reduced folding in the extrahaustorial membrane and the position of the osmiophilic sites on the extrahaustorial and host cell membranes associated with pre-necrotic and some necrotic complexes clearly indicates a change in the membrane rather than deposition of material on it. These sites are similar to those found on membranes of leaf cells of various plant species damaged by freezing or osmotic effects (Nir et al,1969; Pearce and McDonald,1977; Singh,1979) where it has been claimed they are a direct result of dehydration of cell membraneous elements. The dehydration is thought to

change the membrane phospholipid from a bilayer to a micellar conformation (Simon,1974) and to cause aggregation of lipoproteins (Pearce and McDonald, 1977), producing osmiophilic sites which are ultrastructurally distinguishable.

The leaf surface is a desiccative environment, and powdery mildews have become specifically adapted to it (Boughey,1949; Schnathorst,1965). However, premature desiccation is a common symptom of E. pisi infection (Ayres,1976), and the evidence presented above suggests that the osmiophilic sites on extrahaustorial membranes are lipoprotein and/or phospholipid formed on dehydration during death of the infected host cell. Reduction in the convolution of this membrane may be the effect of this rearrangement of membrane components and the loss of phospholipid which occurs in senescing cells (Ferguson and Simon,1973). A decrease in membrane area would itself reduce the passage of translocates and the disorganisation of the host cytoplasm may also contribute to the decreased isotope incorporation of pre-necrotic complexes. However, it seems very likely that an exact molecular arrangement in the extrahaustorial membrane is essential for metabolite passage and indeed Manners (1979) has put forward evidence that the transport is an active or facilitated process (see also Chapter 3).

3.3.Mechanism of haustorial necrosis.

It is clear in the interaction between E. pisi and P. sativum that necrosis of the host cytoplasm precedes that in the haustorium. Similarly Edwards (1975)

and Stavely et al (1969) with powdery mildews and other workers with rust fungi (Abu-Zinada et al,1975; Heath, 1972) and downy mildews (MacLean et al,1974) suggested that because haustorial death follows host cell necrosis, it might be attributable to the exclusion of host translocates. The present study shows that reduced transfer of host metabolites does indeed follow host cell necrosis. This sequence, however, is not universal; for example necrosis of the Rhizobium bacteroid occurs before host cell death in leguminous plants (Kijne,1975), and in some instances necrotic haustoria of rusts (eg. Harder et al,1979) and downy mildews (plate 3.18) are found in host cells with normal cytoplasm.

Present evidence suggests the following mechanisms in the breakdown of the function of haustoria. An intact host cytoplasm is essential for hyphal growth and its disturbance causes effects which are attributed to depleted transport (Sullivan et al,1974). This is supported by the virtual absence of sugar uptake by isolated haustorial complexes (Dekhuijzen,1966; Manners, 1979) and the transport rates characteristic of the functional extrahaustorial membrane (Manners,1979). It has been shown here that transport of photosynthates into haustoria was inhibited at necrosis of host cytoplasm and that it further depends on the particular structure of the host membrane around the haustorium. However, although haustorial necrosis follows depleted transport the two may not be causally related. Indeed it seems unlikely that reduced transport alone causes haustorial

necrosis because haustorial complexes suspended in buffer for 44 hours showed an unchanged rate of O_2 uptake (Manners,1979) and normal ultrastructure. However this does not preclude the possibility that prolonged exclusion of assimilates by encasements around haustoria of rust and powdery mildew fungi (see Perera and Gay,1976) results in their necrosis.

Necrosis was not limited to infected cells, adjacent uninfected epidermal cells and occasionally mesophyll cells also showing these changes. Similar effects have also been described for powdery mildewed barley (Edwards,1975), but in contrast Stavely et al (1969), in a resistant reaction in clover described hypersensitive necrosis limited to cells containing haustoria.

Since all the primary effects are exhibited by the host cell, other initiating causes should also be sought there. Pisatin accumulates in the susceptible reaction with E. pisi but the fungus is highly tolerant of this phytoalexin (Shiraishi et al,1977). Since this is limited to the infected epidermis, localised host necrosis may result from a pisatin concentration toxic to the epidermal cell itself (Bailey,1970; Shiraishi et al,1975). This phytoalexin is lipophilic and possibly produces its effect by binding to membranes and causing increased permeability (Ayres,1978). In addition, membrane permeability would be increased if the activity of lipoxygenase, which catalyses the oxidation of fatty acids, was elevated as has been reported for mildewed

tobacco (Lupu et al,1980). Further, it is likely that the permeability of the cuticle will be increased by the removal of epicuticular waxes (Schonherr,1976) under appressoria (Day and Scott,1973; Kunoh et al,1977; Sargent and Gay,1977). In mildewed barley excessive evapotranspiration is limited by haloes containing lipid and silica (Sargent and Gay,1977) and although there is no evidence for a similar process in pea, increased water loss would occur if maintenance of these barriers was disrupted. It is now suggested that a combination of these events leads to water loss from the host cytoplasm and the observed desiccative effects which in turn lead to reduced transport. Subsequent exposure of haustoria to a desiccative environment results in loss of water from them and their eventual necrosis.

It should be noted that breakdown in the function of this mechanism in E. pisi contrasts with the findings from the examination of rust haustoria. In resistant cultivars, haustoria were established but never incorporated isotope fed to the host, to the same extent as in the compatible interaction (Manocha,1975; Mendgen, 1977). In addition, reduced incorporation was correlated with a definite ultrastructural modification in the extrahaustorial matrix (Manocha,1975), indicating that resistance to the rust and termination of the susceptible reaction in Erysiphe are distinct mechanisms.

3.4.Necrosis of infected cells and the nature of wall appositions in mesophyll cells.

Necrotic flecking of leaves and stems in E. pisi infections is accompanied by restricted growth of the

mycelium and production of conidia. This effect is particularly frequent at high temperatures which suggests that expression of susceptibility is temperature dependent. Similar effects are reported for infections by other biotrophic fungi (see Harder et al,1979; Toyoda et al,1979) and more detailed investigations with controlled growth conditions are required to determine the mechanisms involved. However the present work shows that changes in the ultrastructure of epidermal cells associated with necrosis can be interpreted as events which occur in chronological order. Cells adjacent to necrotic regions (and probably those initiating necrotic flecks too) have a normal cytoplasm but the vacuoles contain deposits which become progressively more frequent. Subsequently the cytoplasm becomes electron dense and osmiophilic globules are associated with the membranes. Loss of turgor results in the collapse of anticlinal cell walls and is followed by dehydration of the cell contents.

These events are paralleled by the deposition of an additional wall layer in mesophyll cells. Similar thickenings are common in response to infection by rust fungi in immune combinations (Heath,1972, 1974 and 1982; Leath and Rowell,1969) and are characterised by electron opaque deposits on and within affected plant walls. Silica is a major component of these in french bean and from comparative evidence Heath (1979) suggests this may represent a non-specific response common to a wide variety of plants. Deposits of silica also occur in haloes of mildewed wheat and barley (Kunoh and Ishizaki,

1976; Sargent and Gay,1977) in response to localised increases in evapotranspiration and are thought to restrict the flow of water through the cell wall (Sargent and Gay,1977). Similarly, the thickenings in rust-infected leaves may reduce the movement of solutions through affected walls in response to the increased permeability of plasma membranes (Thatcher,1942) and leakage of solutes (Hoppe and Heitfuss,1974; Wheeler and Hanchey,1968) which occurs in infected tissues.

In the present study the appositions of mesophyll walls were probably formed in response to similar stimuli but the composition of the layer was not determined. Its structure indicates the presence of at least two components and more than one process may be involved in its deposition. The lack of fluorescence with aniline blue suggests that it probably does not contain callose (Fulcher et al,1976; Smith and McCully, 1978b) and the possibility that silica is a component should be investigated by X-ray microanalysis. Undulation of the adjacent plasma membrane suggests secretory activity by the cytoplasm and the increased golgi activity may indicate synthesis of polysaccharide (Northcote and Pickett-Heaps,1966).

The granular component is similar to the contents of vesicles in the adjacent cytoplasm and thus may be derived from them. The association of membrane with granules in the wall layer suggests the membranes of the vesicles are tightly bound to their contents and become sequestered in the apposition as additional material is layed down. Vesicles usually discharge their contents

by fusion with the plasma membrane and variance from this normal event suggests that the structure of the membrane is modified. Indeed, in mesophyll cells that are necrotic the sequestered membranes do not show the changes characteristic of the plasma membrane and membranes of organelles.

These observations are consistent with the suggestion of Sargent and Gay (1977) that lipidic material provides focal sites for deposition of silica, although in barley the granules are not associated with membrane. Similarly, formation of granules in vesicles corroborates evidence that an intact cytoplasm is necessary for silica deposition in barley (Sargent and Gay,1977) and that metabolic activity of some kind is involved in silica deposition in french bean (Heath, 1979).

Table 2.1. Microautoradiographic distribution of silver grains in haustorial complex fractions which were isolated from P. sativum infected with E. pisi and exposed to $^{14}CO_2$ for 2h.

	Constituent	No. of grains	Constituent area (μm^2)	Grain density (grains $\mu m^{-2} \times 10^{-2}$)[1] Uncorrected	Corrected for: Background	Corrected for: Background and Chemography	Corrected no. of grains[2]	% total corrected no. of grains
Labelled fraction	Healthy haustorial complexes	224	2802.35	7.99	7.22	7	196.17	77.5
	Pre-necrotic haustorial complexes	30	929.5	3.23	2.46	2.46	22.87	9
	Necrotic haustorial complexes	2	397.57	0.5	+	+	+	+
	Host contaminants	65	2799.44	2.32	1.55	1.22	34.15	13.5
	Crystalline inclusions	5	734.49	0.68	+	+	+	+
	Background	140	18061	0.77				

1. Sampling error (%); 4.75 for labelled fraction.
2. The product of grain density (corrected for background and positive chemography) and constituent area.

+. Grain density less than background.

Table 2.1. Microautoradiographic distribution of silver grains in haustorial complex fractions which were isolated from P. sativum infected with E. pisi and exposed to $^{14}CO_2$ for 2h. (Continued).

	Constituent	No. of grains	Constituent area (μm^2)	Grain density (grains $\mu m^{-2} \times 10^{-2}$)[1] Uncorrected	Corrected for: Background	Corrected for: Background and Chemography	Corrected no. of grains[2]	% total corrected no. of grains
Unlabelled fraction (Positive chemography control)	Healthy HC	7	1955.33	0.36	0.22			
	Pre-necrotic HC	0	35.65	0	+			
	Necrotic HC	0	57.59	0	+			
	Host contaminants	4	844.66	0.47	0.33			
	Crystalline inclusions	0	38.39	0	+			
	Background	13	9474.99	0.14				

1. Sampling error (%); 20.47 for unlabelled fraction.

2. The product of grain density (corrected for background and positive chemography) and constituent area.

+. Grain density less than background.

Table 2.2. Microautoradiographic distribution of silver grains in classes of haustorial complexes which were isolated from P. sativum infected with E. pisi and exposed to $^{14}CO_2$ for 2 hours.

Class of haustorial complex	Number of profiles	Number of grains	Mean grain density[1]	Standard deviation
Healthy	52	232	7.06	8.43
Pre-necrotic	20	26	3.6	4.52
Necrotic	16	2	0.26	0.73

1 Mean grain density corrected for background and positive chemography (grains μm^{-2} $profile^{-1}$ x 10^{-2}). Significant differences between means as follows: healthy / necrotic $P<0.01$; healthy / pre-necrotic $P<0.1$; necrotic / pre-necrotic $P<0.01$. Sampling error 6.78%.

Table 2.3. Microautoradiographic distribution of silver grains in haustorial complexes which were isolated from P. sativum infected with E. pisi and exposed to $^{14}CO_2$ for 2 hours. Profiles of haustorial complexes are classified by grain density (grains μm^{-2} $profile^{-1}$ x 10^{-2}) as follows: class (i), less than 1.22; (ii) between 1.22 and 12; (iii) greater than 12.

Class of haustorial complex	Number of profiles	Number of grains	Mean grain density[1]	Standard deviation
(i)	24	4	0.13	0.32
(ii)	35	112	5.13	2.59
(iii)	13	141	19.11	7.43

1 Mean grain density corrected for background and positive chemography (grains μm^{-2} $profile^{-1}$ x 10^{-2}). Significant difference between means: $P<0.001$. Sampling error 6.87%.

Table 2.4. Microautoradiographic distribution of silver grains in components of healthy haustorial complexes in fractions which were isolated from P. sativum infected with E. pisi and exposed to $^{14}CO_2$.

Exclusive grains	
Body	72
Lobes	43
Extrahaustorial matrix	26
Extrahaustorial membrane[1]	14
Total	155
Shared grains	
Body + extrahaustorial matrix	9
Lobe + extrahaustorial matrix	30
Lobe + extrahaustorial matrix + extrahaustorial membrane	9
Extrahaustorial matrix + extrahaustorial membrane	6
Total	54
Grand total	209

1. Only one grain was entirely exclusive, the rest overlying the extrahaustorial membrane and the embedding medium.

Table 2.5. Correction indices for component diffuseness of healthy haustorial complexes in fractions isolated from P. sativum infected with E. pisi determined with a grid of equidistant points and random silver grains.

Haustorial complex component	% Area		Correction index $({}_nV_p)/({}_nV_o)$
	Equidistant points $({}_nV_p)$	Random grains $({}_nV_o)$	
Body	42.05	32.17	1.307
Lobes	21.9	21.17	1.035
Matrix	30.48	31.88	0.9561
Extra-haustorial membrane	5.57	14.78	0.3769

Table 2.6. Microautoradiographic distribution of silver grains (exclusive + shared) allocated to components of healthy haustorial complexes which were isolated from P. sativum infected with E.pisi and exposed to $^{14}CO_2$. (Based on data in tables 2.4 & 2.5).

Haustorial complex component	Silver grains	% total grains	Area of component (μm^{-1})	Grain density[1] (grains $\mu m^{-2} \times 10^{-2}$)
Body	79	38	975.08	7.11
Lobes	67	32	507.84	12.2
Matrix	49	23	706.9	5.94
Extrahaustorial membrane	14	7	129.29	9.84
Total	209	100	2319.11	-

1. Corrected for background and chemography, assuming an equal concentration over all components. Sampling error 7.05%.

Figure 2.1. Microautoradiographic distribution of silver grains in classes of haustorial complexes isolated from P. sativum infected with E. pisi and exposed to $^{14}CO_2$ for 2 hours. Results are presented to show that the grain densities of profiles varied considerably within each class.

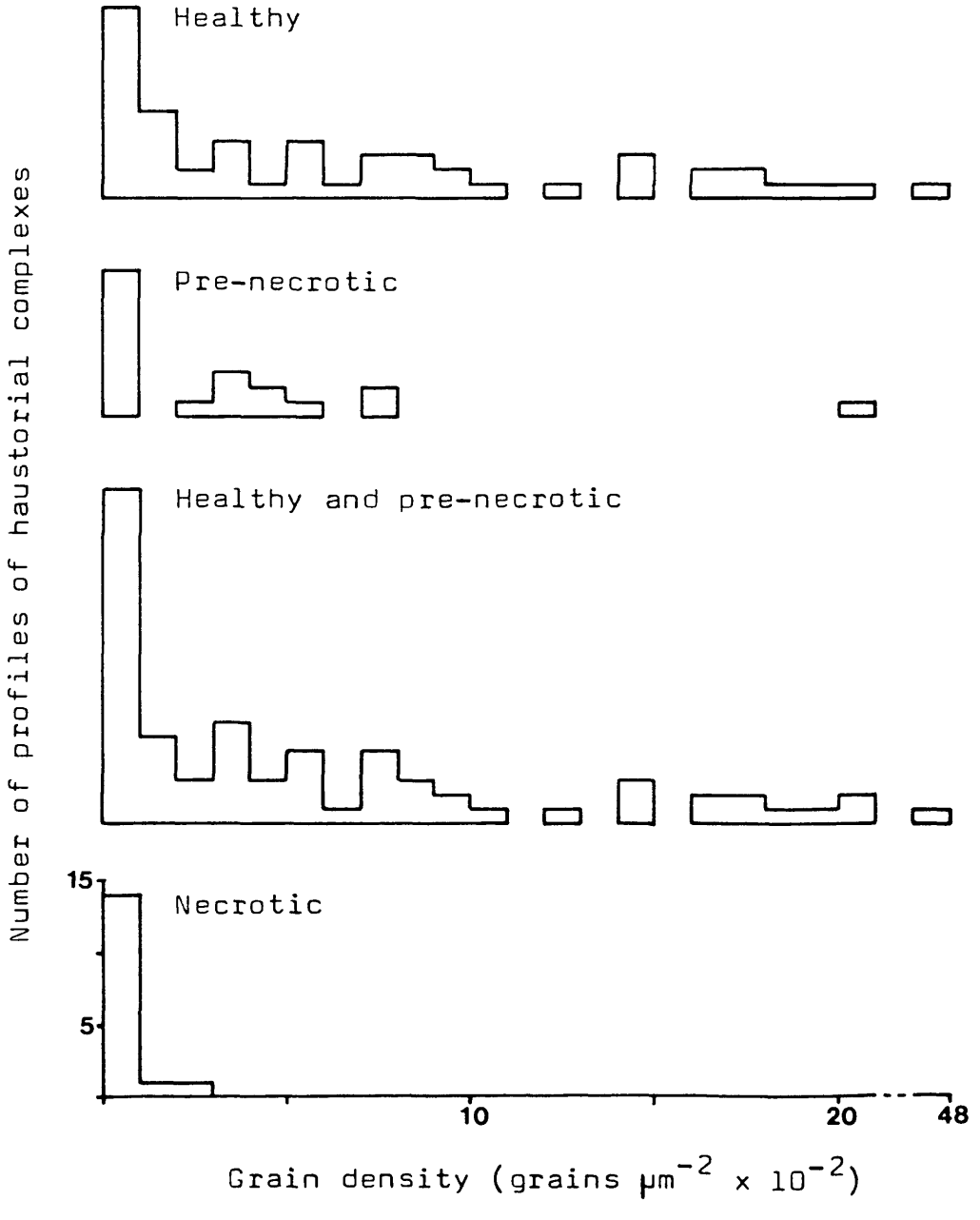


Plate 2.1.

An illustrative field of a section through a pelleted haustorial complex fraction. Haustorial complexes (hc) are the major constituent. Other constituents include trapezoid crystals (asterisk) and contaminant host cytoplasm (Cy) with recognizable nucleus (n) and chloroplasts (Cl). Part of a necrotic haustorial complex is sectioned longitudinally through the neck region (hn). Neg. no. 3602, x 4,700.

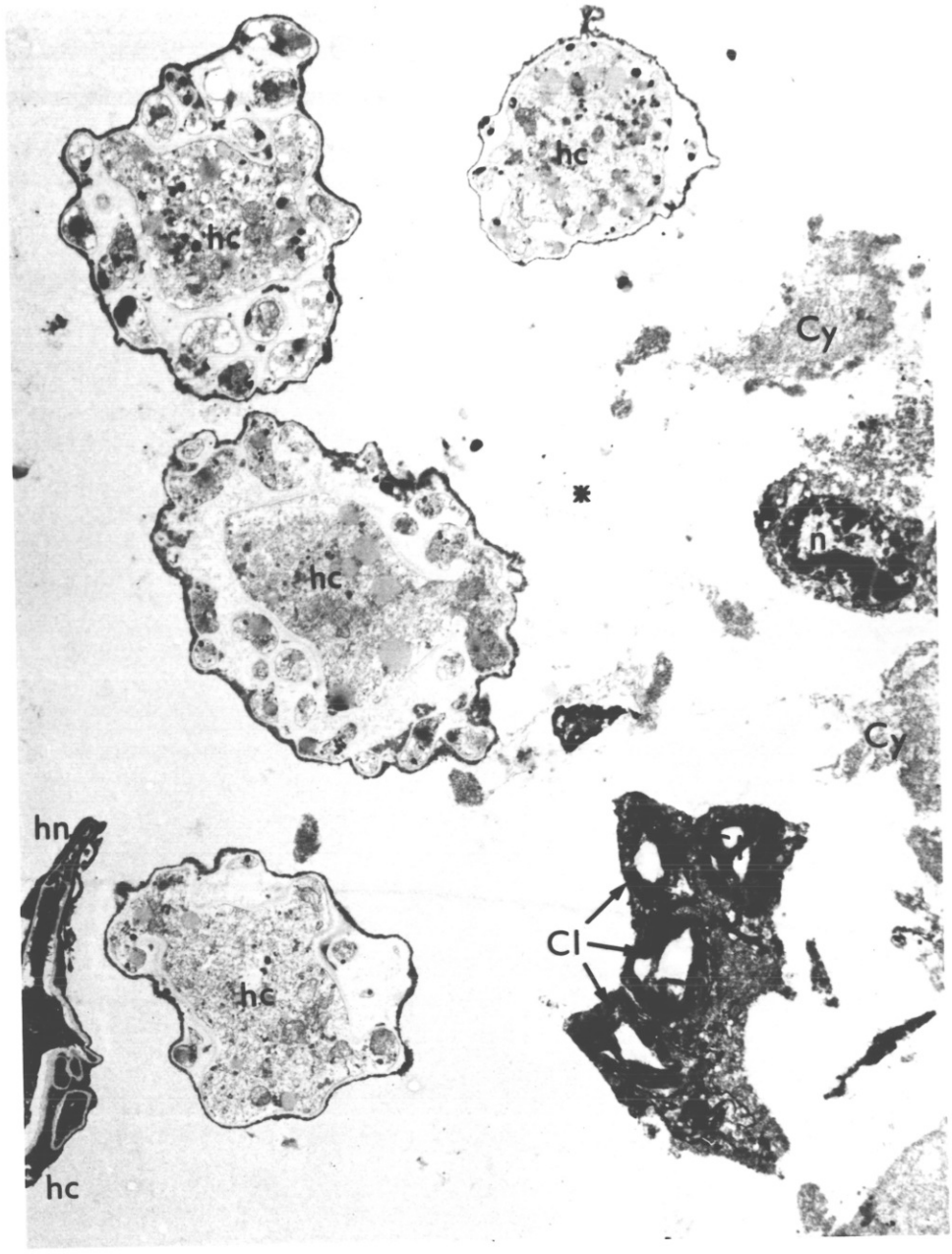

hc
hc
Cy
hc
n
Cy
hn
hc
Cl
hc

Plate 2.2.

Longitudinal section through a healthy haustorial complex. The cytoplasm in body (hb) and lobes (hl) is retained by a plug (arrow) in the pore of the neck septum. The extrahaustorial matrix (Ma) separates the haustorium from the host derived extrahaustorial membrane (Em). hn = haustorial neck. Neg. no. 3758, x 12,800.


hn
hl
Em
hb
Ma
hl

Plate 2.3.

Longitudinal sections of neck regions of healthy haustorial complexes; x 37,600.

a. Magnified portion of plate 2.2. The neck (hn) is devoid of cytoplasm except for osmiophilic deposits associated with the haustorial plasma membrane. The extrahaustorial membrane (Em) is closely adpressed to the neck at the A and B bands, but appears unattached to the interconnecting portion of neck wall (arrows). Haustorial cytoplasm (hcy) is retained at the septum (s) by a plug in the pore. The plug comprises a central zone directly adjacent to the pore surrounded by a more electron dense outer region (see also b). Ma = extrahaustorial matrix. Neg. no. 3757.

b. Section of neck atypically containing fibrils (asterisk) which in this complex alone were shown by serial sectioning to completely fill the lumen. Neg. no. 6336.

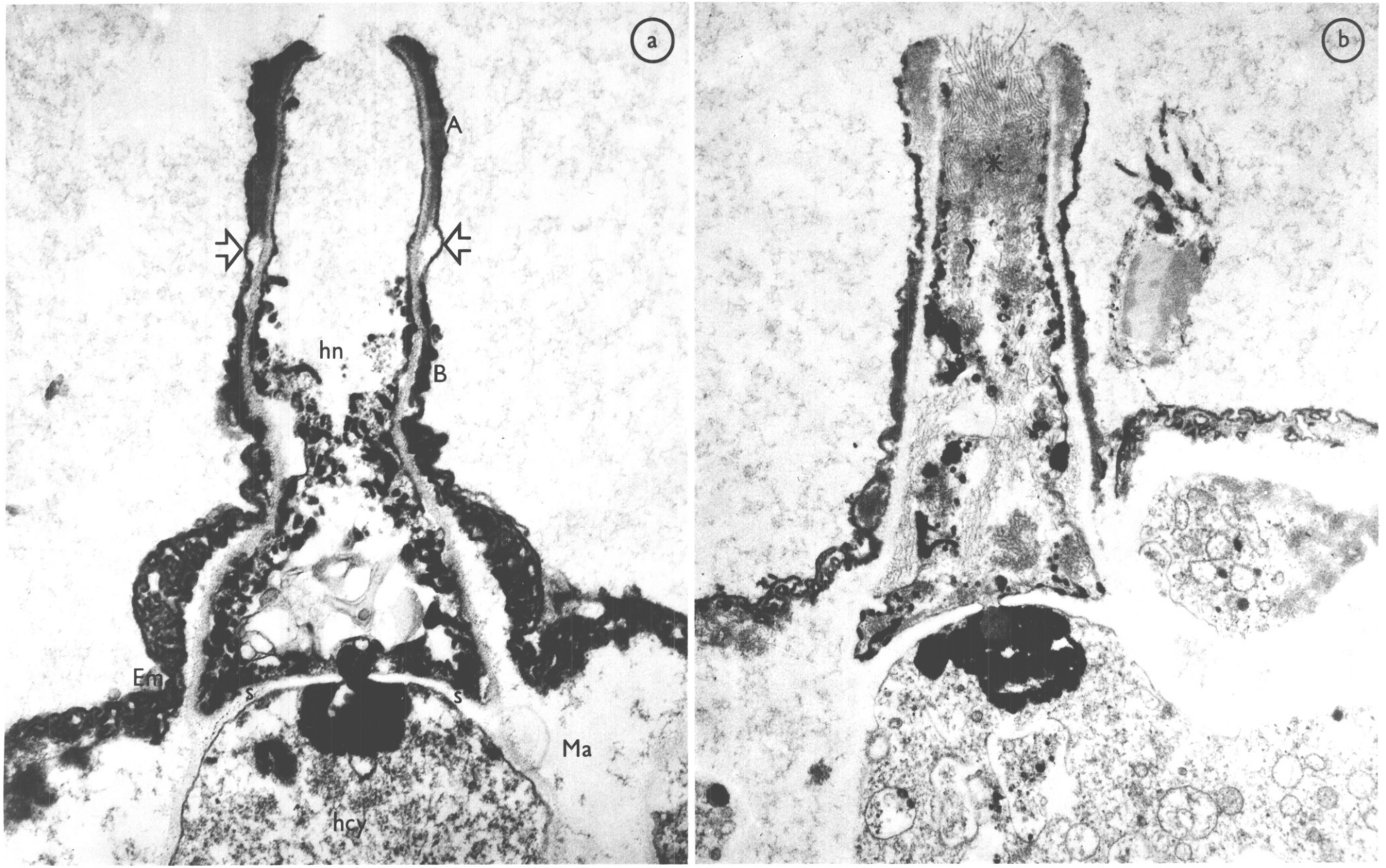

a
A
hn
B
Em
s
s
Ma
hcy
b

Plate 2.4.

a. Representatives of the three classes of isolated haustorial complexes. The healthy complex (Hhc) shows a central haustorial body (hb) and peripheral lobes (hl) containing cytoplasm of normal appearance, surrounded by the extrahaustorial matrix (Ma) and enclosed within the extrahaustorial membrane (Em). The necrotic complex (Nhc) has disorganised and electron dense haustorial cytoplasm, a dense granular extrahaustorial matrix (Ma) and a prominent covering of necrotic host cytoplasm (Cy) adhering to the extrahaustorial membrane. The pre-necrotic complex (Phc) has healthy haustorial cytoplasm with the osmiophilic inclusions (arrows) also observed in necrotic haustoria, and a varying amount of host cytoplasm (Cy) attached to the extrahaustorial membrane. Neg. no. 3752, x 5,550.

b. Haustorial complex in extreme state of necrosis with adherent host cytoplasm (Cy) retaining the shape of a collapsed epidermal cell. The whole complex has a compressed appearance and the dense extrahaustorial metrix (Ma) is much reduced in volume and is barely discernable between the lobes. Neg. no. 3336, x 7,450.

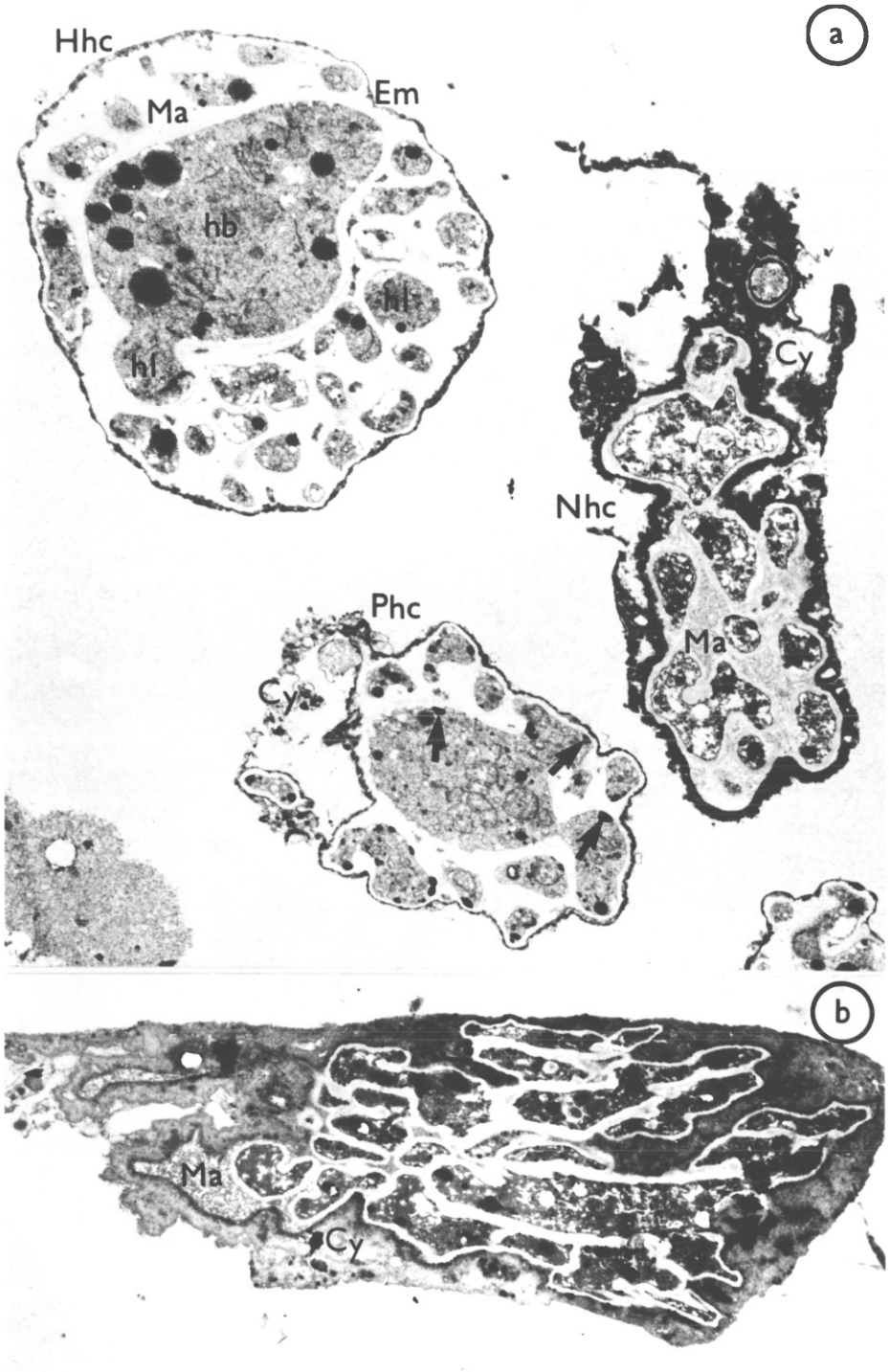

a
Hhc
Em
Ma
hb
hl
hl
Cy
Nhc
Ma
Phc
Cy
b
Ma
Cy

Plate 2.5.

Comparison of extrahaustorial membranes of the three classes of haustorial complex:

a. Healthy complex showing the convolutions of the extrahaustorial membrane (Em). The characteristic thickness of the extrahaustorial membrane can be seen by comparison with the fungal plasma membrane (arrow). Ma = extrahaustorial matrix. Neg. no. 6275, x 41,000.

b. Pre-necrotic haustorial complex. The extrahaustorial membrane (Em) has lost many of the convolutions seen in the healthy condition and has distinct osmiophilic globules, which give a beaded appearance similar to that seen in necrotic complexes. Note the plasma membrane-associated osmiophilic inclusion in the haustorial cytoplasm (arrow). Neg. no. 6265, x 41,000.

c. Necrotic complex showing an unconvoluted extrahaustorial membrane (Em) with distinct osmiophilic globules giving an assymetrical beaded appearance to the membrane. A layer of adhering necrotic host cytoplasm (Cy) is closely associated with the extrahaustorial membrane. The clarity of the haustorial plasma membrane (arrows) and other cytoplasmic membranes is often lost and the haustorial cytoplasm (hcy) disorganised. Ma = extrahaustorial matrix. Neg. no. 3747, x 43,300.

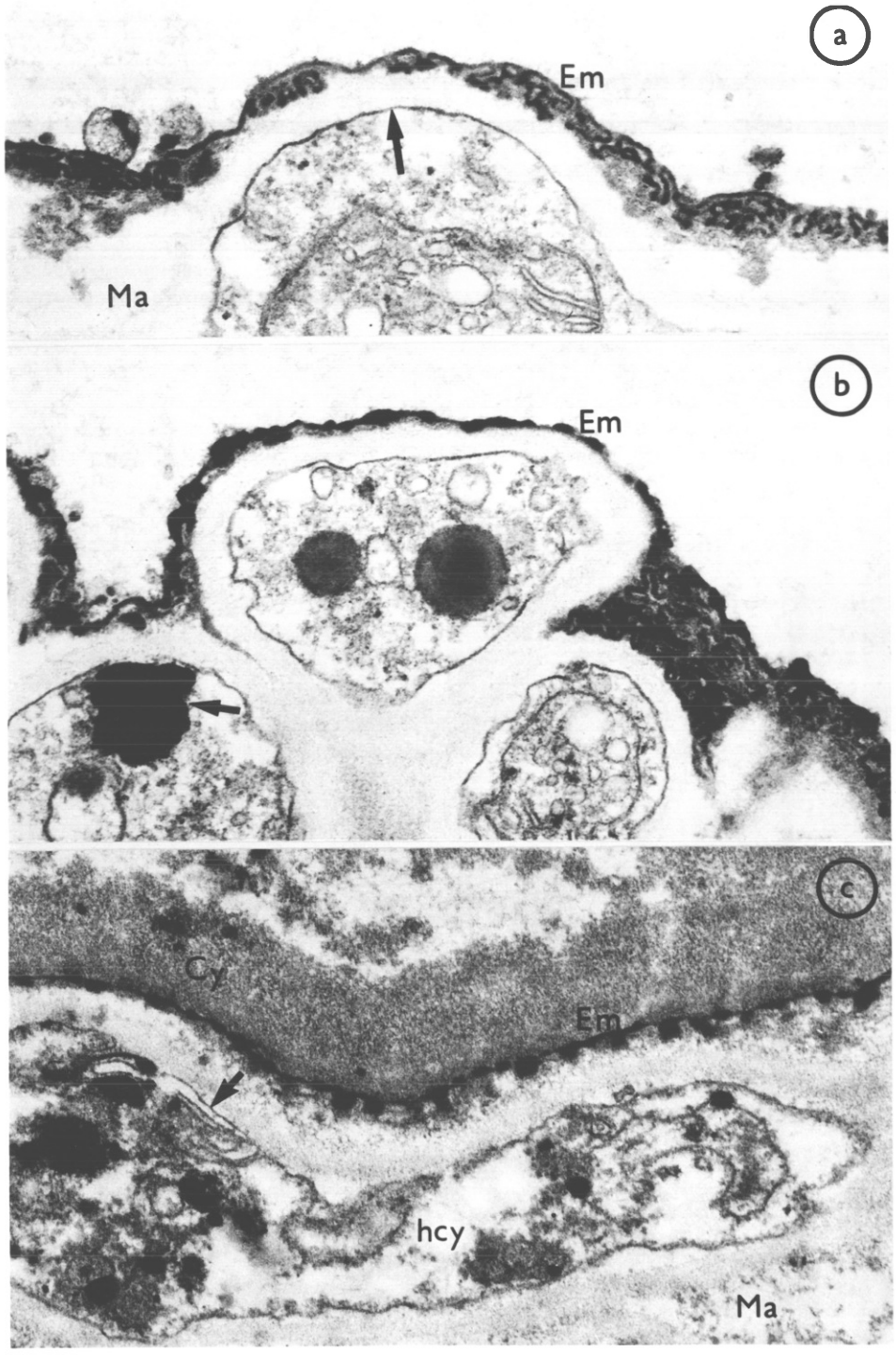

a
Em
Ma
b
Em
c
Cy
Em
hcy
Ma

Plate 2.6.

Sections of necrotic epidermal regions of infected leaves.

a. Necrotic haustorial complex (Nhc) in a cell with necrotic cytoplasm (Cy) and collapsed walls (arrowed, see also plate 2.8.b). The haustorial and epidermal cytoplasms are considerably more electron dense than in the overlying fungal hyphae (hy) and underlying mesophyll cells. Neg. no. 4018, x 2,950.

b. Detail of the haustorial complex in a (adjacent section) showing disorganised cytoplasms (Cy and hcy). The extrahaustorial membrane is virtually indistinguishable and its position is indicated (arrows). Osmiophilic granules lie near its matrical face. W = epidermal cell wall. Neg. no. 4010, x 15,600.

c. Haustorial complex in a less necrotic condition than in b. Membranes in the haustorial cytoplasm (hcy) are still visible. The extrahaustorial membrane (Em) is becoming beaded on its matrical face and the beads are replacing the convolutions. Host cell membranes also have characteristic osmiophilic regions (arrows). t = tonoplast; v = vacuole. Neg. no. 4095, x 25,100.

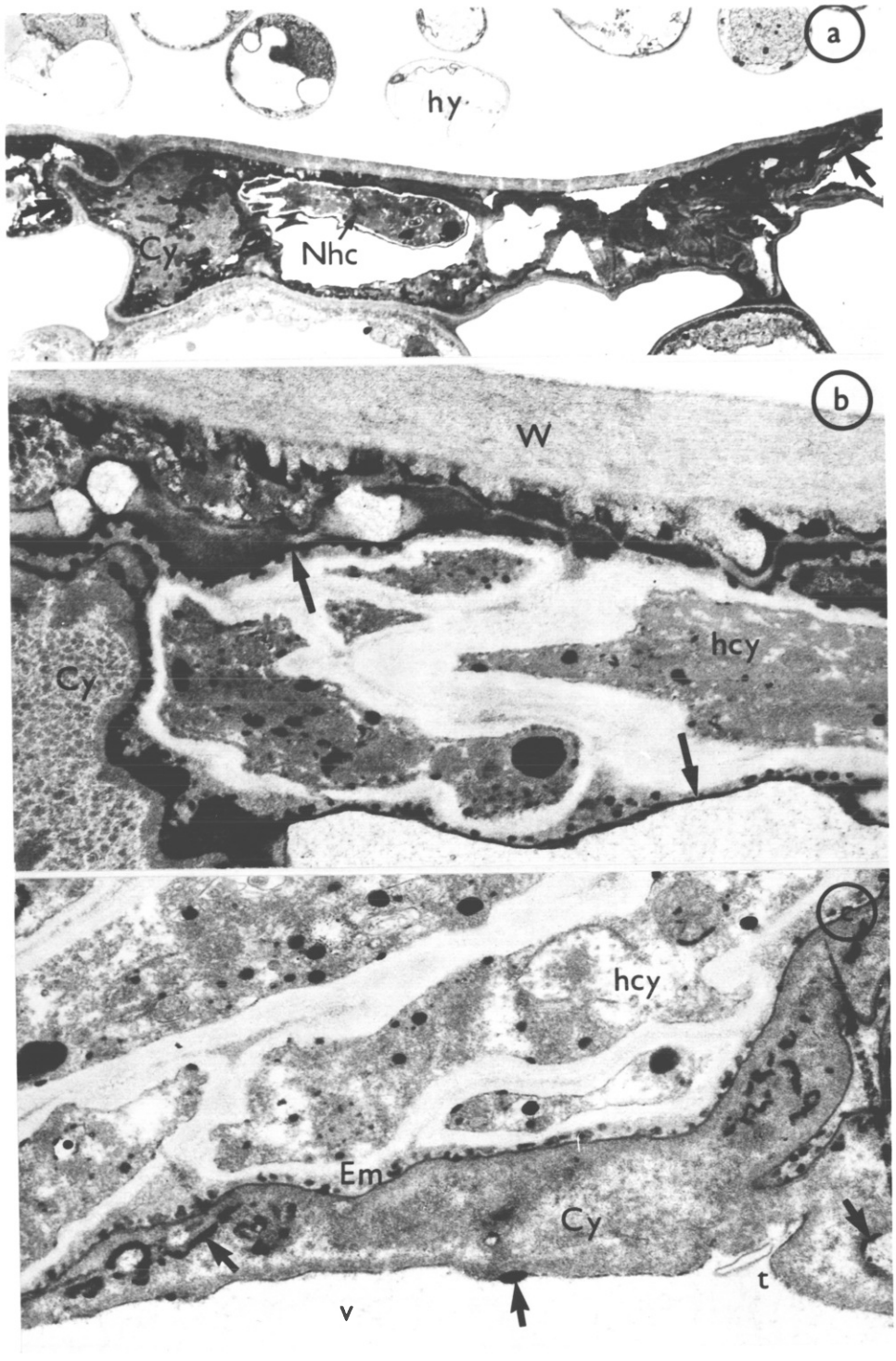

a
hy
Cy
Nhc
b
W
hcy
Cy
hcy
Em
Cy
t
v

Plate 2.7.

Sections of epidermal regions of necrotic leaves.

a. The cytoplasm of the epidermal cell (Cy) is more disorganised and osmiophilic than in the haustorial body (hb) and lobes (hl). Note the floccular deposits in the vacuole (v). The osmiophilic inclusions (arrows) associated with the haustorial plasma membrane are also seen in isolated haustorial complexes of the pre-necrotic and necrotic classes. hy = hyphae; Ma = extrahaustorial matrix; W = epidermal cell wall. Neg. no. 11363, x 11,500.

b. Epidermal cell (with vacuolar deposits, v) and two mesophyll cells. All have osmiophilic deposits in their cytoplasms (Cy) and the mesophyll cells an additional layer (asterisked and absent in the uninfected condition) on the protoplasmic aspect of their cell walls (W). Neg. no. 4245, x 20,100.


a
hy
W
Cy
hl
hb
Ma
v
b
v
*
*
Cy
W

Plate 2.8.

a. Epidermal cells at the edge of a necrotic lesion. Cytoplasm (Cy) of the necrotic cell is disrupted and osmiophilic. The vacuole (v) of the cell with normal cytoplasm contains floccular precipitates characteristic of cells containing pre-necrotic haustoria. An extra layer (asterisk) is present between the cytoplasm and wall adjacent to the necrotic cell. Neg. no. 11371, x 12,300.

b. Part of necrotic epidermal cell in plate 2.6.a. The anticlinal cell wall (W) has collapsed. v = vacuole. Neg. no. 4022, x 27,900.

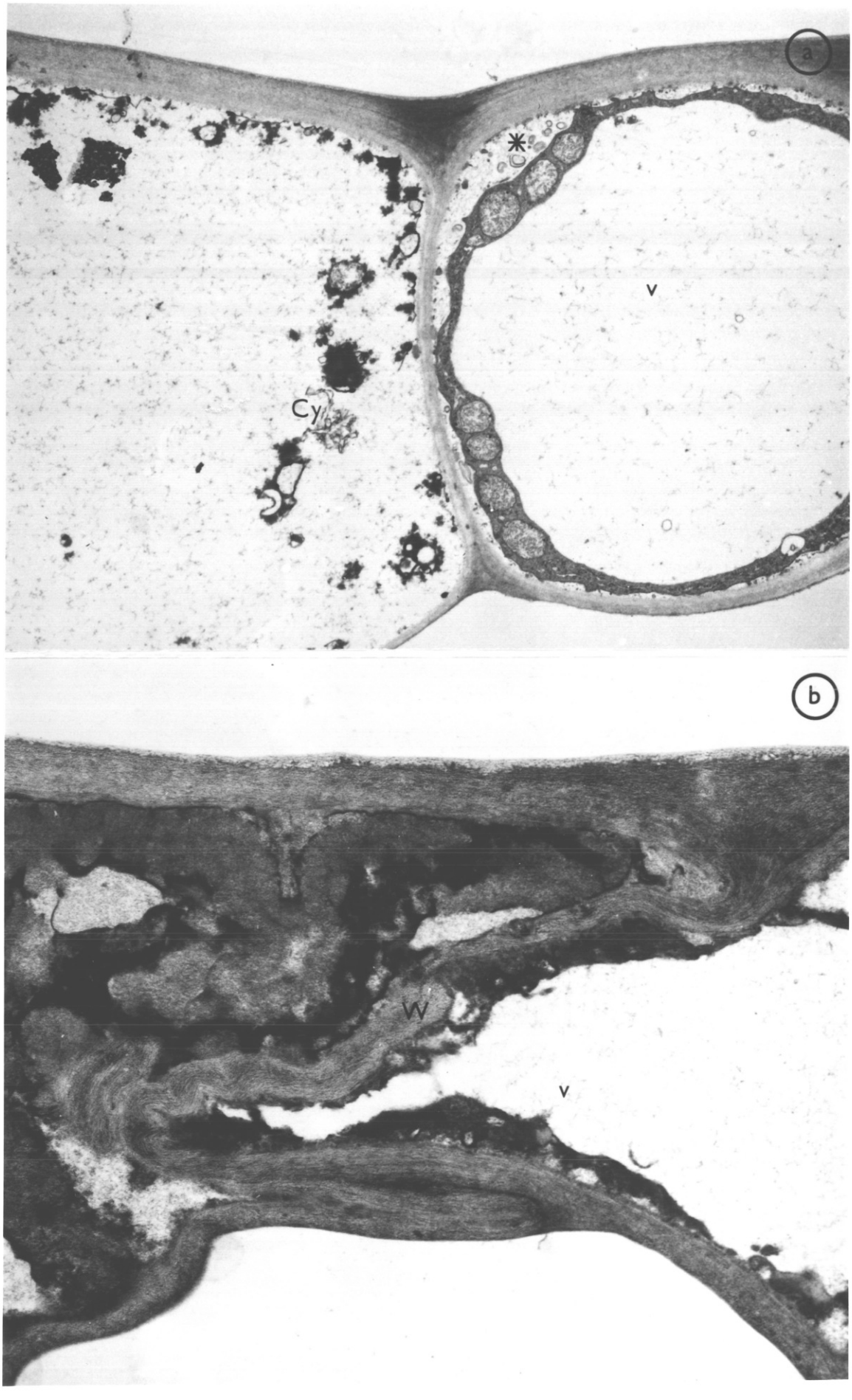

a
Cy
v
b
W
v

Plate 2.9.

Sections of cell walls (W) between mesophyll and necrotic epidermal cells (cytoplasm, Cy in b.). The mesophyll plasma membrane (Pm) forms a convoluted boundary with the wall apposition (asterisked) which appears to be formed from granular vesicles (arrows, in a.) sequestered in a translucent matrix. Note granules also in cytoplasm. Larger vesicles with less dense contents are also frequent and often associated with golgi dictyosomes (d). a, neg. no. 4012, x 74,500. b, neg. no. 4246, x 37,600.

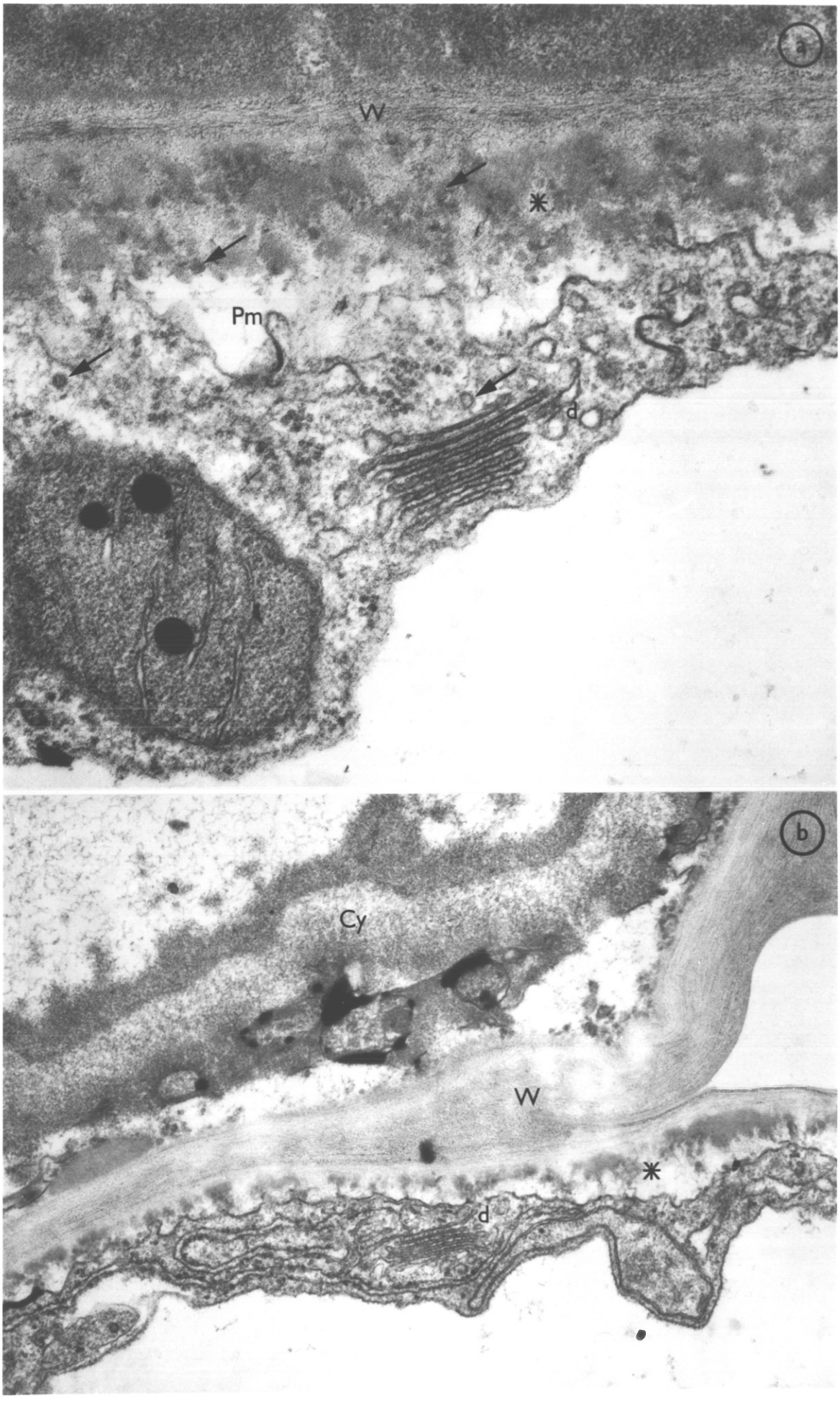

a
W
Pm
d
b
Cy
W
d

Plate 2.10.

a. Point of penetration of the epidermal wall (W). The haustorium was fully developed but lay out of the plane of section shown. The host (Cy) and haustorial (hcy) cytoplasms are necrotic but the cytoplasm of the appressium (ap) appears normal. The small collar (C) is characteristic of *E. pisi* infections of pea (c.v. Onward). hn = haustorial neck. Neg. no. 4126, x 15,600.

b,c. Peels of epidermis of *P. sativum* infected with *E. pisi*; mounted in aniline blue and observed with U.V. light. Fluorescence is only associated with papillae around necks of haustoria (h) and in c, anticlinal walls of epidermal cells in necrotic regions. b, neg. no. 41.8, x 1,600. c, neg. no. 41.14, x 1,600.

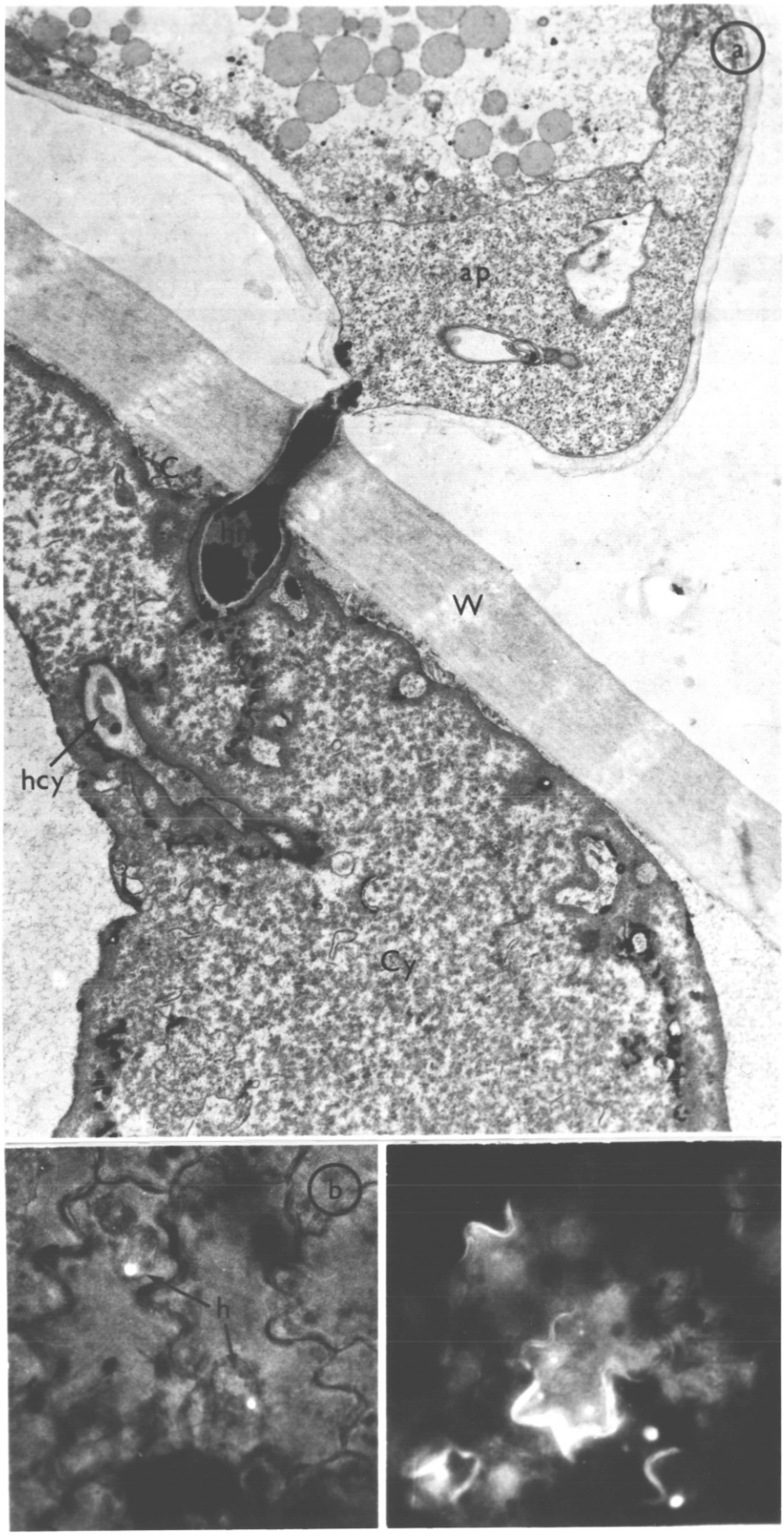

a
ap
W
hcy
Cy
b
h

Plate 2.11.

a. Autoradiogram of healthy haustorial complex. Silver grains (circled) lie over the body (hb), lobes (hl) and extrahaustorial matrix (Ma). Em = extrahaustorial membrane. Neg. no. 5461, x 8,600.

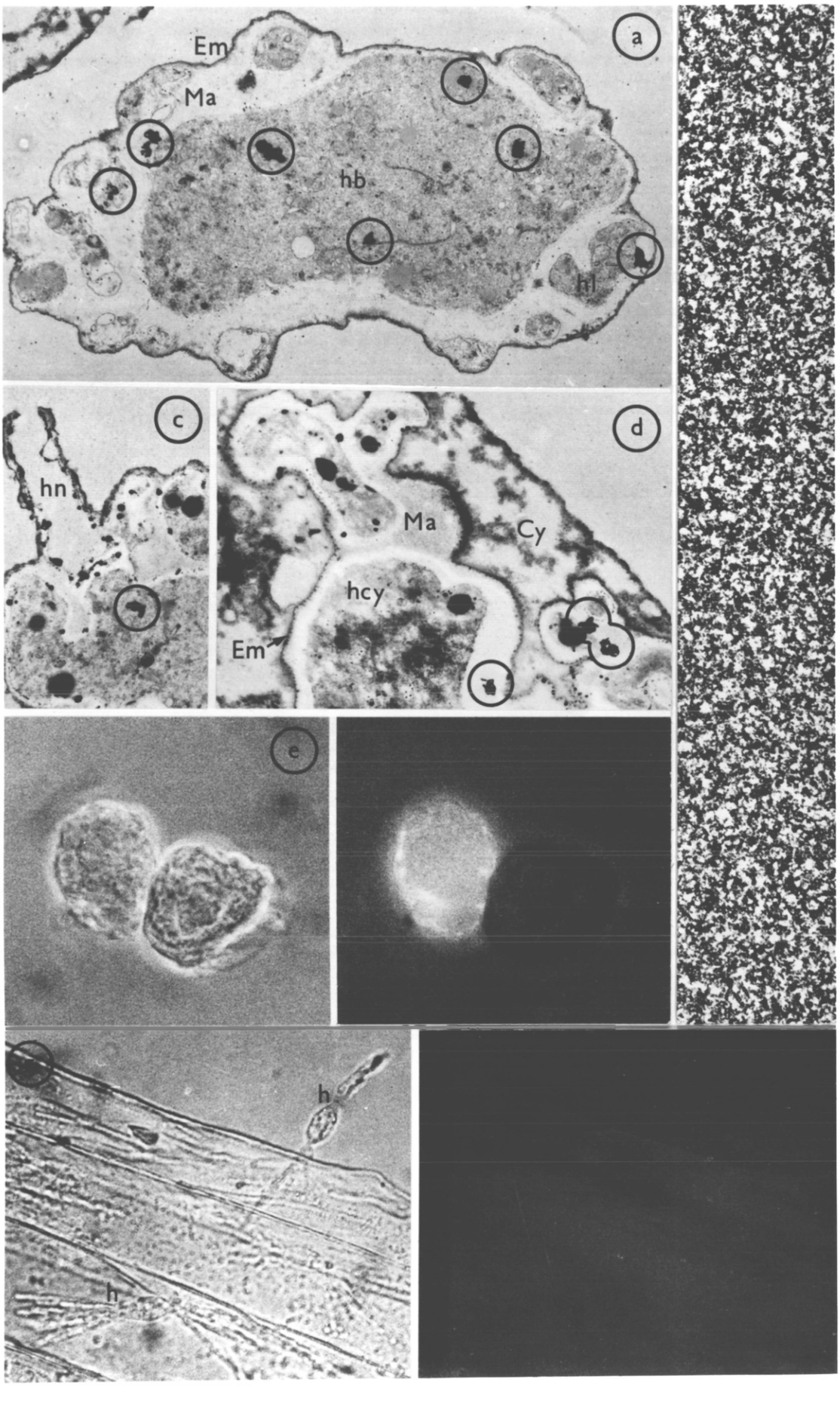
b. Negative chemography control showing an even distribution of silver grains over section of haustorial complex fraction. Neg. no. 4540, x 2,250.

c. Autoradiogram of a longitudinal section of the neck of a healthy haustorial complex (silver grain circled). Few autoradiograms included the neck region and no label accumulation was apparent at this site. Neg. no. 5687, x 10,000.

d. Autoradiogram of part of necrotic haustorial complex. Silver grains (circled) are atypically frequent in this example. Cy = necrotic host cytoplasm; Em = extrahaustorial membrane; hcy = haustorial cytoplasm; Ma = extrahaustorial matrix. Neg. no. 5683, x 10,500.

e,f. Light micrographs of isolated healthy and pre-necrotic haustorial complexes mounted in SITS and viewed with visible (e) and u.v. (f) light. In visible light, the right hand (pre-necrotic) complex (e) appeared browner than its neighbour but it is easily distinguished by absence of fluorescence in u.v. (f). Strong fluorescence is especially associated with the extrahaustorial membrane of the healthy complex. x 2,100.

g,h. Light micrographs of peels of epidermis from barley leaves infected with Erysiphe graminis; mounted in SITS and viewed with visible (g) and u.v. (h) light. No fluorescence was observed. h = haustorium. x 1,100.


a
Em
Ma
hb
hl
c
hn
d
Ma
Cy
hcy
Em
e
h
h

CHAPTER 3.

Phosphatase activity in tissues infected by rust, powdery and downy mildew fungi.

1.Introduction.

Infections by rust and powdery mildew fungi alter the patterns of translocation and accumulation of metabolites in host tissues (Bushnell and Gay,1978; Cooke, 1977) to the extent that leaves with established colonies of powdery mildew become net importers of photosynthates (Gay and Manners,1981). This implies that the direction of translocation in the vascular tissues is reversed by infection and translocates are unloaded from the phloem of minor veins in infected leaves. Transfer cells are thought to mediate exchange of solutes between phloem sieve elements and the surrounding tissues (Pate and Gunning, 1972) and are therefore likely to play an essential role in redirecting photoassimilates in these tissues. Indeed there is evidence that transfer cells specifically develop in situations which require active uptake of solutes for short-distance translocation (Jones and Gunning,1976; Kramer,1980) and revert to an undifferentiated condition when the requirement has been fulfilled (Schnepf and Pross,1976).

Haustoria of Erysiphe pisi also mediate rapid transport of photoassimilates over short distances (Gay and Manners,1981; Manners and Gay,1982) and haustoria of other biotrophic plant pathogens probably have a similar function (see Chapter 2, section 1). Neckbands of rust and powdery mildew haustoria impose a barrier to the movement of

solutes from the apoplast of infected tissues to the extrahaustorial matrix and prescribe a pathway across the extrahaustorial and haustorial plasma membranes (Gay and Manners,1984; Gil and Gay,1977; Heath,1976). Manners (1979) has calculated that the flux of photosynthates across these membranes in E. pisi infections is at least an order of magnitude greater than effluxes of similar metabolites which result from diffusion down large concentration gradients. This suggests that transport through infected cells is an active process requiring energy and therefore special mechanisms probably operate at the parasitic interface.

Similar arguments may apply to infections of downy mildew fungi. The osmiophilic material between the haustorial neck and host cell wall in these infections (eg. Hickey and Coffey,1977) may perform a similar function to the neckbands of powdery mildews and rusts, but there is no evidence that apoplastic pathways to downy mildew haustoria are restricted. Additionally there have been very few investigations concerning the accumulation of metabolites around sites of infection (Ingram,1981) and no specific mechanisms are implicated.

Phosphatases are especially associated with cells and tissues involved in secretion and absorption (Schnepf, 1974) and as infected cells effectively secrete metabolites at the parasitic interface and haustoria probably function as absorptive structures, both are expected to show characteristic levels of phosphatase activity. More specifically, present evidence suggests that phosphatases couple cellular energy to transport of solutes via electrogenic pumps which establish ionic

gradients across membranes (Raven and Smith,1980).

In higher plants and fungi the most important electrogenic system appears to be an H^+-efflux pump operating at the plasma membrane (Poole,1978; Raven and Smith,1980) which is energised by membrane-bound ATPases. An important function of this pump is the regulation of cytoplasmic pH (Smith and Raven,1979) but additionally the chemiosmotic theory (Mitchell,1967) predicts that movement of solutes could be mediated by substrate-specific carriers either via a uniport mechanism dependent upon the electrical potentials generated or via symport/ antiport with ionic components of the pH gradient.

Slayman (1974) subsequently proposed a model for proton-dependent co-transport of uncharged substrates which has been supported by much evidence for sugars and amino acids in fungi (eg. Brocklehurst et al,1977; Slayman and Slayman,1975) and higher plants (see Baker,1978). However most of the evidence for higher plants is circumstantial and includes demonstration of transient alkalinisation of bathing media in the presence of sugars (Colombo et al,1978; Delrot,1981), depolarisation of membrane potential during transport of sugars (Franz and Tattar,1981; Novacky et al,1978) and amino acids (Etherton and Rubinstein,1978; Franz and Tattar,1981) and increased or decreased transport in the presence of stimulators or inhibitors respectively of proton extrusion (Colombo et al, 1978).

Thus although the general conclusion that electrogenic pumps are ATP dependent is probably correct (Spanswick,1981) there is no unequivocal proof that ATPases

directly energise co-transport in plants. However the kinetic and inhibitor similarities of membrane transport and ATPases are consistent with the notion that the two are closely linked (Poole,1978; Raven and Smith,1980; West,1980), and as several plasma membranes may be traversed by photosynthates *en route* to haustoria it is essential to determine their phosphatase activities in order to elucidate the mechanisms involved.

Despite the significance of phosphatases in this respect there have been suprisingly few investigations of their role in plant tissues infected by fungi. Acid phosphatases and other hydrolases have been implicated in hypersensitve death in several infections by necrotrophic fungi (Hänssler *et al*,1978; Mansfield and Sexton,1974; Pitt and Galpin,1972) whilst studies of infections by biotrophic fungi have been restricted mainly to acid phosphatases in tissues infected by *Erysiphe graminis* (Atkinson and Shaw,1955; Fric,1975) and *Uromyces phaseoli* (Staples,1965; Staples and Stahman,1964; Williams and Staples,1964).

In the present study, investigations of phosphatase activity in infections by rust, powdery and downy mildew fungi are reported. The distribution of activity in infected tissues has been determined by electron microscopy and cytochemistry whilst the effect of infection on total and specific ATPase activities has been estimated in fractions prepared from plants of *Pisum sativum* infected by downy and powdery mildews. Although the results are interpreted with special regard to the processes involved in transfer of assimilates across the pathogenic

interface, movement of translocates within infected tissues and the role of transfer cells are also considered.

2.Experimental procedures.

The success of recent investigations of phosphatases in fungi and higher plants has depended largely on improved methodology for subcellular fractionation (Quail,1979). However the value of these techniques remains limited by difficulties associated with the heterogenous nature of most fractions. At best their properties represent an average for a population of similar components but frequently contaminant particles are also present (cf. "haustorial complex" fraction) and their contribution is often difficult to determine. Characterisation is further complicated by the lack of specific cytochemical and biochemical markers for most subcellular components (Bowles et al,1979; Quail,1979).

In the present study crude fractions were prepared by differential centrifugation and no attempt was made to establish their composition.

Cytochemical procedures provide a valuable complementary approach for localising enzymes. They avoid many of the problems associated with fractionation techniques as they are applied to intact tissues and cells whose components are readily identified by microscopy. However the methods usually employed for phosphatase cytochemistry are primarily qualitative and particularly subject to artefactual localisations. The main arguments concerning their validity are summarised by Essner (1973) and those pertaining to the choice of experimental

procedure employed in the current study are considered below.

The most widely used procedures are based on the method developed for light microscopy by Gomori (1939) and later adapted for electron microscopy (Sheldon *et al*, 1955). The medium commonly used for localising acid phosphatases was devised by Barka and Anderson (1962) whereas ATPases are localised by various adaptations of the method described by Wachstein and Meisel (1957). These procedures rely on precipitation by lead ions of inorganic phosphate at the site of substrate hydrolysis.

Tissues must be chemically fixed to preserve fine structure and immobilise enzymes at their *in vivo* sites. Fixation also improves permeation of the specimen by the several solutes employed in the localisation procedure, although the extent to which permeability barriers are altered is contentious. Washitani and Sato (1976) showed that intracellular phosphate leaked out of tobacco cells to equilibrium in 30min. during fixation in glutaraldehyde and concluded that *in vivo* barriers to permeability were totally eliminated. However experiments monitoring the slow leakage of betacyanin from fixed beetroot slices were interpreted as showing the barriers remained partially intact, complete release of betacyanin being effected only by freezing (Sexton and Hall,1978). However as betacyanin is largely confined to the vacuole these data probably relate more to diffusion rates of large molecules through gelled cytoplasm and ultrastructurally intact tonoplasts and plasma membranes and indicate that penetration of incubation media will be

slow too.

In the present study various procedures have been employed to improve permeation of the tissues. In particular, as haustoria of Erysiphe pisi are mostly confined to epidermal cells of pea (Gil,1976) the possibility of using the epidermis alone in cytochemical studies of the parasitic interface was examined. Epidermes were prepared enzymically from the upper surface of leaves and mechanically from infected stems and uninfected leaves and stems. Epidermal peels from stems were floated on distilled water and infected with conidia brushed from infected leaves held above them.

The condition of the epidermal peels was monitored with the vital dyes neutral red and Evans blue. Neutral red is actively transported through the cytoplasm and accumulated against a concentration gradient in the vacuole where its presence is confirmed by plasmolysis which concentrates the stain. The ability of cells to absorb neutral red can therefore be used to assess viability (Tribe,1955) and has also been used to estimate rates of solute transport (Itai and Meidner,1978). Conversely Evans blue only enters the cytoplasms of cells with damaged plasma membranes (Gaff and Okong'o-Ogla,1971) and has a distinct advantage to neutral red as it can be washed from cells required for further experimentation.

In addition to its beneficial effects, fixation also inhibits phosphatase activity; mitochondrial ATPases are particularly sensitive and for this reason are not readily localised (Essner,1973). Glutaraldehyde is particularly inhibitory due to the cross-linking effect

of the dialdehyde groups which alters the tertiary structures of proteins and also to the various impurities which inhibit enzyme activities. Thus the choice of fixative, its concentration and duration of treatment must combine sufficient preservation of ultrastructure with minimum loss of activity. The effects of various fixatives and the purity of the glutaraldehyde solutions were investigated in the present study.

After fixation specimens must be washed with buffer to remove free fixative and adjust pH to the value required for subsequent treatments. Tris-maleate is especially suitable at this stage as it revives activity lost during fixation (Arborgh et al,1971) and stabilises lead ions in solution (Barka and Anderson, 1962). It also buffers efficiently over a wide pH range and for these reasons was selected for the current comparison of ATPase (pH 7.2) and acid phosphatase (pH 5.5) activities.

Phosphatase activities are inhibited by lead ions as well as by fixatives (Sexton and Hall,1978; Washitani and Sato,1976). Most ATPase-dependent transport systems in animal cells are completely inhibited by lead ions at the concentrations used in cytochemical studies and it has been suggested that membrane transport ATPases are not localised by these methods (Essner,1973; Firth and Stranks,1981). For this reason the concentration of lead in incubation media used in the present study was minimised and used equimolar with substrate to optimise trapping of all phosphate released at the site of substrate hydrolysis (Winter-Sluiter et al,1977). Higher

proportions of lead have frequently been used (eg. Hall and Flowers,1976; Robards and Kidwai,1969), but even in these conditions trapping is never complete (Washitani and Sato,1976).

3.Results.

3.1.Phosphatase cytochemistry.

3.1.1.Distribution of precipitates in pea and bean leaves.

Fine granular and flocculent precipitates were seen in sections of Pisum sativum and Phaseolus vulgaris. The fine granular particles occurred over components of the cytoplasms, nuclei and cell walls even in the absence of substrate (plates 3.11a; 3.14a) and their precise distribution is shown in table 3.1. They were particularly associated with mitochondrial cristae (plates 3.2b; 3.9c; 3.14c), chloroplast thylakoids (plates 3.2b; 3.3d; 3.8a) and heterochromatin (plates 3.4a; 3.10b) but most consistent in golgi dictyosomes (plates 3.2b; 3.7b) although the density of precipitation sometimes varied between cisternae (plate 3.3a, b). The cuticle/cell wall interface in pea leaves infected with powdery mildew also showed granular precipitates especially around sites of penetration and where hyphae were in close proximity with the cell wall (plate 3.12b). Granular precipitates were not associated with plasma membranes, tonoplasts, vacuoles, chloroplast stroma, mitochondrial matrices and intercellular spaces.

Flocculent precipitates were only formed where

substrate had been employed and were present at similar locations in pea and bean (table 3.1) except for the peripheral reticulum and envelope of chloroplasts which in bean occasionally showed precipitates with ATP as substrate (plate 3.3d, e). Most sites with granular precipitates in the absence of substrate also showed flocculent deposits which were especially conspicuous in nuclei (plate 3.15b) and mitochondria (plate 3.8b) but usually absent from golgi cisternae, chloroplast thylakoids, nuclear envelopes and the cell wall/cuticle interface in all treatments. However granular precipitation was often enhanced without becoming flocculent by media containing substrates. This was presumably due to trapping of phosphate and phosphate-lead complexes which had diffused from elsewhere.

Flocculent precipitates alone were associated with intercellular spaces (plates 3.3d; 3.4a), vacuoles (plates 3.3e; 3.10b), tonoplasts (plates 3.4a; 3.6), plasmodesmata (plate 3.4b) and plasma membranes, but only in the last were their frequencies significantly reduced by sodium fluoride (compare plates 3.6 with 3.8a, b and 3.9a with 3.9b in pea; 3.1a with 3.1b in bean). In pea fixation with impure glutaraldehyde (see appendix) reduced all flocculent precipitates to insignificant levels but did not affect the granular precipitation.

Frequencies of precipitates typically associated with plasma membranes in bean and pea are summarised in tables 3.2 and 3.3 respectively. Although the ultra-structures of cell types in epidermal and mesophyll tissues of both species were comparable, an important

difference was noted in vascular bundles in minor veins. In pea some of the parenchyma associated with phloem sieve elements had elaborate wall ingrowths and dense cytoplasms which were characteristic of transfer cells (plates 3.5; 3.6). Similar differentiation had not occurred in bean where phloem companion cells and parenchyma were not easily distinguished (plate 3.1a, b). Thus with the exception of the bundle sheath, xylem vessels and phloem sieve elements all cells in vascular bundles in bean leaves were collectively termed companion parenchyma.

With ATP as substrate, deposits were especially abundant at the epidermal plasma membranes in both species (plates 3.4b; 3.9b) and their frequencies were only equalled in phloem transfer cells in pea (plates 3.8a, b; 3.10b, c) and occasionally companion parenchyma cells in bean (plates 3.1a; 3.2a). Deposits were less frequent at mesophyll plasma membranes (plates 3.9b; 3.3d). With β-GP at pH 7.2 a high level of activity was shown by bean epidermal plasma membranes but it was less in the plasma membranes of pea epidermis (plate 3.12) and virtually absent from those of pea and bean mesophyll. In pea, phloem transfer cells alone showed activity with β-GP at pH 7.2 (plate 3.7a), but at pH 5.5, activity was negligible at all plasma membranes of the leaf (plates 3.5; 3.7b; 3.9c; 3.10a). In both species precipitates were associated with plasmodesmata with ATP (plates 3.2a; 3.4b; 3.10c) and β-GP (plate 3.7a) at pH 7.2 but not in pea with β-GP at pH 5.5 (plate 3.7b). The frequency of precipitation usually reflected the activities of adjoining plasma membranes and was accordingly reduced by sodium fluoride

(plate 3.2b) with a few exceptions (plate 3.3c).

The results reported above represent the activities typically associated with plasma membranes in each tissue but precipitates showed a wide range of frequencies in both species. These variations were evident both between and within tissues and were not due to localised regions of high or low activity nor to gradual changes over a series of adjoining cells. Indeed the activities of plasma membranes of cells connected by plasmodesmata were often distinctly different (plate 3.4b).

Although in pea most cells of the upper epidermis, palisade mesophyll and vascular tissue were well preserved, the spongy mesophyll was severely disrupted by removal of the lower epidermis prior to fixation. Thus the results for phosphatase activities for these tissues and stomatal guard cells, which are mostly in the lower epidermis, are not available. However the frequencies of precipitates at plasma membranes of bean leaves were assessed for each tissue to illustrate the variation between cells (figs. 3.1, 2, 3). The data were compiled by examining the plasma membranes in sections from two leaf pieces for each treatment. In total 505 cells were examined; of these 35 were excluded because they were necrotic or disrupted with flocculent precipitates throughout their cytoplasms and specific sites of activity could not be distinguished.

The range of frequencies were similar at plasma membranes of the upper and lower epidermes (fig. 3.1) with ATP as substrate. β-GP also gave similar levels of activity in both epidermes but a smaller proportion of plasma membranes showed precipitates at the most frequent density.

Plasma membranes of stomatal guard cells had lower activities with both substrates.

Deposits at mesophyll plasma membranes (fig. 3.2) were consistently less frequent than in epidermal cells especially with β-GP as substrate. With ATP, activity was noticably higher in the spongy mesophyll; however this may reflect slower permeation of the closely packed palisade cells by substrate and/or lead ions and not different specific or total activities of their ATPases.

The range of frequencies shown by plasma membranes in minor veins (fig. 3.3) reflected the various structures and functions of the cells present (plate 3.1a, b). No minor veins were sectioned in leaf pieces treated with β-GP alone and so useful information was restricted to activity with ATP. Flocculent precipitates were frequently associated with plasma membranes of companion parenchyma and bundle sheath cells and sodium fluoride reduced their activities to similar levels as its effect in epidermal and mesophyll cells. Plasma membranes of phloem sieve elements showed low activities in all treatments. Deposits were also infrequently associated with the lumen and cell wall boundary in xylem vessels which did not have plasma membranes when fully differentiated.

3.1.2.Effect of infection on the distribution of precipitates.

Infection of pea by Erysiphe pisi and bean by Uromyces appendiculatus caused modification only in cells containing haustoria. The wall-lining region of the plasma membranes retained the levels of activity characteristic of

the uninfected condition (see figs. 3.1, 2, 3 for detailed analysis in bean) but the region invaginated around each haustorium was devoid of precipitates with either substrate (plates 3.12b; 3.13; 3.14c; 3.15a; 3.16a, b). The transition was abrupt and, in the powdery mildew infection, occurred precisely where the invagination began (plate 3.13); in the rust infection it was part way along the surface of the haustorial neck (plate 3.16b). In each infection the transition co-incided with the neck bands where the plasma membrane follows closely the contour of the neck of the haustorium (Gil and Gay,1977; Hardwick et al,1971). There are two neck bands in E. pisi (plate 2.3) whilst in U. appendiculatus a single band occurs part way along the neck (plates 3.14b; 3.16a, b).

The plasma membranes of haustoria of E. pisi showed high activity with both substrates at pH 7.2 (plate 3.12a, b) and β-GP at pH 5.5 (plate 3.10a) which was reduced by NaF, but not to the same extent as the activity of epidermal plasma membranes (plate 3.11b). The characteristic flocculent deposits were absent from the plasma membranes and elsewhere in the surface hyphae, appressorium and the adjoining region of the haustorial neck (plates 3.12b; 3.13). The transition to activity occurred between the A and B neck bands (plate 3.13). In U. appendiculatus there was no evidence for activity with either substrate at pH 7.2 associated with the plasma membranes of haustoria (plates 3.14c; 3.15a), haustorial mother cells (plate 3.16a) or intercellular hyphae. Indeed flocculent precipitates were only present at the outer

surface of cell walls of the intercellular mycelium (plate 3.16a).

In both fungi fine granular deposits were conspicuous in some profiles of the endoplasmic reticulum (plates 3.11a; 3.12a; 3.15b) after all incubations with lead in the medium. Similar deposits were inconsistently associated with nuclear envelopes, heterochromatin and cristae of mitochondria.

The effect of infection by Peronospora pisi on phosphatase activities in pea was inconsistent. Plasma membranes of both organisms sometimes showed electron dense precipitates which often had jagged outlines (plates 3.17a; 3.18a, b) giving a crystalline appearance instead of the flocculent precipitation typically associated with enzyme activity. Furthermore, deposits were sometimes more frequent in sodium fluoride controls (plate 3.17a) than with substrate alone (plate 3.17b). However in all treatments precipitation was less abundant at mesophyll plasma membranes in infected regions than elsewhere.

Interpretation was additionally complicated by the effects of unfavourable growth conditions and poor development of the infection. Intercellular mycelium was not extensive and sporangiophores infrequent. There were few haustoria and many were necrotic and encased by callose-like deposits (plate 3.18a, b). Infected and uninfected plants, grown in similar conditions, were etiolated and weak compared with those of the same age in a normal greenhouse environment.

Localisation of phosphatase activity in epidermis of barley was also unsuccessful although strong infections

of Erysiphe graminis were established. Epidermal cells were not fixed satisfactorily by the procedure employed and their tonoplasts and plasma membranes were fragmented (plate 3.20a). However the cytoplasms of mesophyll cells (plate 3.20a) and haustoria (plate 3.19a, b) were well preserved. Specific sites of phosphatase activity could not be distinguished in epidermal cells as precipitates were present throughout the cytoplasm in all treatments with ATP (plate 3.19a, b). A similar effect occurred in disrupted cytoplasms in pea and bean. The plasma membranes of haustoria, appressoria and surface mycelium of E. graminis showed no activity with ATP at pH 7.2.

3.1.3.Isolation of epidermis from Pisum sativum; phosphatase localisation and infection with Erysiphe pisi.

Digestion of leaf pieces with cellulase and macerozyme resulted in hydroysis of cell walls of the epidermis as well as the underlying mesophyll and examination by electron microscopy showed the cuticle alone remained floating on the surface of the enzyme solution (plate 3.20b, c).

Epidermes were easily peeled from lower surfaces of leaves but only the stomatal guard cells accumulated neutral red (plate 3.21a) as the cytoplasms of other cells were disrupted. Peels of epidermis from leaves crumpled immediately after stripping but stem epidermis was more rigid and consequently less susceptible to damage during further manipulation. Most cells of the epidermis from uninfected stems excluded Evans blue (plate 3.21d) and

retained neutral red (plate 3.21b) although the plasma membranes of infected cells and their uninfected neighbours were usually disrupted by stripping (plates 3.19c; 3.21c). In consequence, specific sites of phosphatase activity in infected peels could not be assessed by cytochemical procedures as flocculent precipitates occurred throughout their cytoplasms after incubation with ATP (plate 3.19c). Precipitates were similarly dispersed in mesophyll cells which were ruptured during preparation of the epidermal peel and remained attatched throughout further manipulations (plate 3.19c).

Infected cells occasionally accumulated neutral red (plate 3.21b). Most of their protoplasts plasmolysed partially for a brief period before disrupting and releasing the dye to the bathing solution. Infrequently protoplasts plasmolysed completely as in the uninfected condition. In a single instance a protoplast separated from the haustorium during plasmolysis (plate 3.21f) but the two usually remained in close association (plate 3.21b).

Infections of E. pisi were established on peels of epidermis and mesophyll floating on distilled water. Colonies developed to produce conidiophores and conidia (plate 3.21e). Haustoria were not observed and were certainly not present in epidermal cells from which the mesophyll was completely removed despite formation of appressoria (table 3.6). Additionally, the protoplasts of these epidermal cells retained the ability to exclude Evans blue and accumulate neutral red throughout the

period of ten days they were monitored. These and the infected epidermal and mesophyll peels were not examined by electron microscopy or cytochemically for phosphatases.

Although peels of infected epidermal cells free from mesophyll were not routinely obtained by these procedures, present results provide a basis for further investigations. In particular the potential use of epidermal peels from stems as a model system for elucidating early events during infection, with especial regard to the factors influencing initiation of haustoria, is clearly indicated. Once infection has been established the physiological interactions between haustoria and the cytoplasms of infected cells, without the confusing effects of other tissues, are equally open to investigation.

3.2. Assays of phosphatase activities.

3.2.1. Infections of *Erysiphe pisi*.

a. Activities of ATPase in crude extracts from leaves, epidermes and haustorial complexes.

Table 3.7 shows specific activities of ATPase in crude extracts of epidermis from the upper surface of leaves of *Pisum sativum* and of whole leaves (midveins excluded) that were uninfected or infected with *Erysiphe pisi*. The activity of Mg^{2+}-activated ATPase was calculated as the difference between the activity in the presence of $Mg(NO_3)_2$ and the activity in its absence. Activities of ATPases were inhibited by Mg^{2+} in both tissues and hence Mg^{2+}-ATPase activities have negative values.

Extracts from upper epidermis and whole leaf had similar activities but extracts from infected leaves showed higher activities in all incubations although the resulting Mg^{2+}-ATPase activity was slightly lower than in similar preparations from uninfected leaves. These results indicate that infection may alter ATPase activities but it is not clear whether the observed changes occur throughout the leaf or are restricted to specific locations.

Activities of ATPases in extracts from stem epidermes (table 3.8) were also inhibited by Mg^{2+}. In contrast to the data for whole leaves, activities of extracts from epidermes with infections of Erysiphe pisi were lower in all incubations than the activities of similar fractions from uninfected epidermes. However, the specific activity of Mg^{2+}-ATPase was increased by infection (i.e. was less negative). The differences between infected and uninfected extracts, shown as relative activities in table 3.8, were similar whether they were expressed with respect to protein or surface area of the epidermis from which they were prepared.

The contribution of ATPases from haustoria to the activity of infected epidermis was estimated by assay of homogenates of haustorial complexes isolated from leaves with infections of Erysiphe pisi (table 3.9). The specific activity of Mg^{2+}-ATPase in these homogenates was nearly three times higher than the activity in control incubations without Mg^{2+} ; 74% of the activity was Mg^{2+} activated. Thus the ATPase activity of haustorial complexes is quite distinct from the Mg^{2+}-inhibited activities of extracts from leaves and epidermes. Furthermore, the specific

activities of homogenates of haustorial complexes were over twice the comparable values for extracts from tissues of P. sativum when Mg^{2+} was included in the incubation medium. The results (table 3.9) indicate that haustorial complexes contribute less than 3% of the ATPase activities of infected epidermis (in incubations with Mg^{2+}). The activity contributed by haustorial complexes was calculated as the product of activity/haustorial complex and their frequency in epidermis from infected stems. The last was estimated as 237.5 mm^{-2} from a count of 741 haustoria in peels of epidermis from stems with infections similar to those used for the experiments recorded in table 3.8. However, direct comparison of specific activities must be interpreted with caution as homogenates of haustorial complexes were prepared by mortar and pestle whilst leaves and epidermis were disintegrated by Potter homogenisation. Examination by light microscopy showed the last method disrupted only a small proportion of haustorial complexes. No haustoria were intact after homogenisation by mortar and pestle which also released $1\frac{1}{2}$ times more protein than Potter homogenisation of an identical sample. Storage of isolated haustorial complexes at $4^{o}C$ overnight before homogenisation may also have affected their ATPase activities.

Expression of ATPase activities as proportions of control activities in incubations without Mg^{2+} (tables 3.10, 3.13) effectively removes differences between preparative procedures and permits more accurate comparison of the various samples. With a single exception ATPase activities of crude extracts (table 3.10) from

leaves and epidermis were inhibited by Mg^{2+}. The slight stimulation shown by the mean activity of extracts from infected stem epidermis was not significantly different from the uninfected condition ($0.1<P<0.2$).

b. Activities of Mg^{2+}-ATPase in fractions from stem epidermis.

The specific and total activities of Mg^{2+}-activated ATPase in the crude extracts and various sub-cellular fractions from stem epidermis are illustrated in table 3.11 which gives results from a typical experiment. The specific and total activities of Mg^{2+}-activated ATPase were highest in the 10,000 xg precipitates after fractionation of crude extracts. Activities in 10,000 xg supernatants only were inhibited by Mg^{2+} and thus there are probably two kinds of ATPases in crude extracts which differ in their response to Mg^{2+}. Similar results have been reported for extracts from lower epidermis of tobacco leaves (Kasamo, 1979).

Infection with E. pisi did not significantly alter the distribution of Mg^{2+}-ATPase between fractions (table 3.12) whilst specific activities in all fractions were increased by infection; this was independent of whether activities were calculated with respect to protein or area of epidermis. However, analysis of the data by the student's t-test indicated that the increase was only significant in the 1,500 xg precipitate when activities were calculated with respect to area ($P<0.01$). Similarly, although the proportion of activity stimulated by $Mg^{2+}$was higher in the 1,500 and 10,000 xg precipitates

from infected epidermis (table 3.13), the increased activities were also not significantly different from the uninfected condition ($0.1<P<0.2$).

Conversely, treatment of the data for the 1,500 and 10,000 x g precipitates by analysis of variance showed the Mg^{2+}-ATPase activities of these fractions (table 3.12) were clearly increased by infection (activity expressed as $\mu g\ Pi\ h^{-1}\ mg^{-1}$ protein, $P<0.05$; $\mu g\ Pi\ mm^{-2}$ epidermis, $P<0.01$). This last statistical method increases the degrees of freedom for residual error from 2 to 7 and allows the conclusion that infection with E. pisi significantly increases Mg^{2+}-ATPase activities in the 1,500 and 10,000 x g precipitates prepared from homogenates of epidermis peeled from stems of P. sativum.

c. Inhibition of Mg^{2+}-ATPase by NaF.

Sodium fluoride inhibited ATPase activity more than Mg^{2+} ($P<0.001$, data in table 3.10) in all preparations (tables 3.10, 3.14) and reduced the activity of Mg^{2+}-inhibited ATPase by about 50% (table 3.10). In crude extracts from epidermes and haustorial complexes Mg^{2+}-ATPase activities were reduced to 65 - 70% of the activities in controls without NaF whereas activities of similar preparations from whole leaves were inhibited to a slightly higher degree (approximately 50%; table 3.14). In all fractions of epidermis from uninfected stems ATPase activities were inhibited by similar amounts (approximately 40% inhibition) but the enzymes in fractions from infected epidermis were markedly more susceptible to inhibition by sodium fluoride. The activities of the 1,500 and 10,000 x g precipitates were especially reduced with their

activities in incubations with NaF at half the level of similar preparations from uninfected epidermis.

3.2.2. Infections of Peronospora pisi.

The Mg^{2+}-activated ATPases in fractions from leaves of plants grown under successive conditions necessary for infection and sporulation of Peronospora pisi had distinctly different activities from the enzymes of similar fractions from plants grown under normal greenhouse conditions. Activities in crude extracts from plants used for experiments with P. pisi (table 3.15) were not inhibited by Mg^{2+} but greatly stimulated instead (compare with Mg^{2+}-ATPase activities in tables 3.7 and 3.11). Fractionation showed that this was probably due to relatively low inhibition by Mg^{2+} of the activity in the 10,000 xg supernatant fraction. The highest ATPase activity in fractions from the uninfected plants was located in the 10,000 xg precipitate which was also characteristic of similar fractions of stem epidermis from plants used for the powdery mildew investigation (table 3.11).

Infection by P. pisi resulted in slightly reduced activities of Mg^{2+}-ATPase in crude extracts from leaves, which was complemented by increased inhibition by Mg^{2+} of ATPase activity in the 10,000 xg supernatant. More significantly, activity of the 10,000 xg precipitate was reduced by infection to a level slightly lower than the activity of the 1,500 xg precipitate, which itself showed higher activity than the equivalent fraction from uninfected leaves.

Increased inhibition by Mg^{2+} of activity in the

10,000 xg supernatant and reduction of Mg^{2+}-ATPase in crude extracts from leaves with infections of P. pisi are both completely opposite to the results obtained from powdery mildew infection of the epidermis of stems.

4. Discussion.

4.1. Interpretation of precipitates in phosphatase cytochemistry of pea and bean leaves.

Before commenting on the distribution of phosphatase activities it is necessary to consider the validity of the cytochemical approach. The problems associated with maintaining sufficient enzyme activity whilst optimising ultrastructural preservation, tissue permeability and precipitation of phosphate were discussed in relation to the choice of methodology (this chapter, section 2). Furthermore, extreme caution is also necessary when interpreting the significance of electron dense precipitates in sections prepared for microscopy as it is likely that some are artefactual.

The present study has identified several lead binding sites in leaf cells of pea and bean (see table 3.1) which show granular precipitates after incubation in media without ATP or β-GP. Incubation with the substrates results in flocculent precipitation at many of these sites which is not reduced by sodium fluoride and therefore probably does not represent in situ activity. In particular the nucleus, cell wall, tonoplast and cisternae of nuclear envelopes, endoplasmic reticula and golgi dictyosomes are recognised currently and widely in the literature (Jones and Bowen, 1980; Washitani and Sato, 1976)

as non-specific sites of precipitation. Despite the high insolubility of lead-phosphate complexes these and free phosphate formed by non-enzymic hydrolysis of substrates and enzyme activity will probably diffuse from remote sites because crystal clusters of a particular size are necessary before precipitation takes place. Additionally, precipitation requires conditions of supersaturation which can be catalysed by particles other than lead phosphates (Cornelisse and Van Duijn , 1973). The situation is further complicated as lead at high concentrations complexes with phosphate esters removing them from solution and accelerating their non-enzymic hydrolysis. However although mostly a problem with ATP (Rosenthal et al, 1966) rather than substrates such as β-GP (Washitani and Sato, 1976) this effect is not considered to cause significant artefacts in plant tissues (Hall, 1969) for which the lead capture method of phosphatase cytochemistry is established as a valid technique (Hall et al, 1980).

Although the current study is mainly concerned with phosphatase activities of plasma membranes the precipitates in bean leaves associated with chloroplast envelopes are briefly considered in relation to the reliability of the techniques employed. Deposits here in tendrils of pea have previously been interpreted as indicating that ATPase activity is associated with chloroplast envelopes (Sabnis et al, 1970). However precipitates were not present in the chloroplast envelopes of the pea leaves currently investigated. Furthermore most demonstrations of ATPase at this site

are cytochemical whilst investigations with isolated envelopes have only detected very low levels of activity (Heber and Heldt, 1981). Indeed chloroplast envelopes isolated from Phaseolus vulgaris showed no activity (Preistly and Woolhouse, 1980). Thus it is likely that the precipitates recorded for this species presently were artefactual and their incidence provides additional evidence that flocculent precipitates at locations which show granular precipitation after incubation in media without substrates are typically non-specific.

In contrast the precipitates at plasma membranes most probably resulted from the activity of ATPases associated with them. Plasma membranes did not show granular precipitation and the flocculent deposits were significantly reduced by sodium fluoride.

4.2. Phosphatase activities and translocation in powdery mildew and rust infected tissues.

The distribution of activities currently described for plasma membranes in the vascular tissues of pea and bean corroborates previous evidence for these two species (Bentwood and Cronshaw, 1978; Cronshaw, 1980). There was no evidence from the cytochemistry that infection altered the distribution of activities, except in cells containing haustoria (see section 4.3). Thus phloem loading and unloading probably require similar distributions of ATPase activity because the direction of translocation in the phloem is probably reversed in leaves with heavy infections which become net importers of photosynthates. A similar interpretation was drawn

from the results of a cytochemical study of phosphatase activities in phloem tissues of Ricinus communis where precipitates showed the same distribution at plasma membranes in source (leaf) and sink (root) tissues (Browning et al, 1980). However these studies do not provide quantitative data for the specific and total activities which may differ at the various locations.

Specific activities of Mg^{2+}-ATPase were consistently increased by infection with E. pisi in all fractions prepared from stem epidermis of P. sativum despite large variations between duplicate experiments. Although the fractions were not characterised, comparison with similar preparations (e.g. Kasamo, 1979) indicates that the 1,500 x g precipitate contains intact cells and large subcellular components including cell wall fragments, nuclei and chloroplasts. Centrifugation at 10,000 x g sediments large fragments of membrane from the endoplasmic reticulum, tonoplast and plasma membrane as well as small organelles such as golgi dictyosomes and mitochondria. Smaller particles including ribosomes and microsomal vesicles (e.g. of plasma membrane) remain in the 10,000 x g supernatant. Cytochemistry showed that ATPase activity was mostly located at plasma membranes and the high specific and total activities of the 10,000 x g precipitates indicates that this fraction is particularly enriched with these membranes (Bowles et al, 1979). The increased Mg^{2+}-ATPase activity (manifest as reduced inhibition by Mg^{2+}) of whole homogenates of stem epidermis probably reflects changes at the wall lining regions of plasma membranes especially as infection

increased the ATPase activity of the 10,000 xg precipitate considerably more than other fractions (table 3.13) in incubations with Mg^{2+}. However the possibility that increased activity is due to other subcellular components cannot be discounted. In particular the contribution from mitochondria, also mainly sedimenting at 10,000 xg, may be higher as respiration increases in infected tissues of pea (Manners, 1979). Furthermore the ATPase activities of fractions prepared from infected epidermis were particularly sensitive to inhibition by NaF and although the significance is not certain it may indicate increased activity of non-specific phosphatases which are usually more sensitive to inhibition by fluoride than ATPases (Hollander, 1971). Indeed, in a comprehensive characterisation of soluble extracts from leaves of barley Fric (1975) showed the activity of acid phosphatase increased after infection with Erysiphe graminis in susceptible varieties.

In contrast to the results with epidermis, infection slightly reduced Mg^{2+}-ATPase activity in homogenates of leaves. This suggests that higher activities in the epidermis are contrasted by reduced activities at other sites such as plasma membranes of mesophyll and transfer cells. These arguments assume that infection has similar effects on ATPase activities in epidermis from leaves and stems. The comparison is probably valid as both tissues are non-photosynthetic and perform similar functions with regard to mechanical protection and regulation of gaseous exchange and transpiration. Additionally Mg^{2+} and NaF had similar

effects on ATPase activities in uninfected samples of both.

Critical examination of micrographs of transfer cells in pea leaves indicates that the distribution of wall ingrowths may also be altered by infection. Bentwood and Cronshaw (1978) reported that "transfer cells had well developed, irregular wall ingrowths except in areas of wall adjacent to seive elements". However in several instances they were also present in these areas in infected tissues (e.g. plate 3.5). Clearly a comprehensive survey of a large sample is necessary to provide more conclusive evidence. Polarity of solute transport through transfer cells is probably determined by the unequal distribution of wall ingrowths as the plasma membranes do not show distinct domains of ATPase activity. Any deviation from the polarisation would impair efficiency of phloem loading (and unloading) and together with reduced ATPase activities contribute to the altered concentrations of solutes in the apoplast of infected tissues (see Bushnell and Gay, 1978). An abundant supply of photosynthates in the apoplast resulting from reduced translocation from infected leaves would facilitate transport to haustoria via the epidermis. Clearly, haustoria of powdery mildew and rust fungi are able to accumulate sufficient assimilates without infected cells developing the wall ingrowths characteristic of transfer cells as evidence from other species indicates that cells of both the epidermis (Barnabas et al., 1982; Kramer, 1983) and mesophyll (Jones and Gunning, 1976) are capable of such differentiation.

4.3. Domains of ATPase in plasma membranes and transport in powdery mildew and rust infected cells.

The distribution of ATPase activity of the plasma membranes of infected cells of P. sativum and P. vulgaris corresponds to the structural domains recognized in pea mildew (Gil and Gay,1977) and flax rust (Littlefield and Bracker, 1972) infections. Phosphatase activity, where present, showed the same polarized distribution. In infections by E. pisi and U. appendiculatus the transition in the enzymic activities of the wall-lining and invaginated regions of the host plasma membrane occurred at neckbands which have been shown to prevent the passage of various molecules along the walls of the haustorial necks (Gay and Manners, 1984; Gil and Gay, 1977; Heath, 1976). The present evidence confirms the conclusion by Gil and Gay (1977) that the neckbands also prevent the interchange of membrane components so that distinct domains of the plasma membrane are maintained. Enzymic activity in the plasma membrane of E. pisi is also segregated within the same region of the haustorial neck and it should be noted that this is not at the septum which separates the neck from the haustorial body. This membrane also is closely adherent to the neck wall (plate 2.3) and like the invaginated region of the host plasma membrane, still remains attached in the absence of cytoplasm (Gil and Gay, 1977). The spatial association of wall-membrane attachment, impermeability and domain delimitation in plant and fungal membranes suggests that a common factor is responsible for these properties.

Uptake of assimilates by haustoria of E. pisi has been demonstrated conclusively (Manners and Gay, 1978, 1980,

1982; Spencer-Phillips and Gay, 1980a) and the distribution of ATPase activity is likely to be a key factor in their transport. About one fifth of the total product of photosynthesis in an infected pea leaf enters the mycelium of the pathogen (Manners and Gay, 1982). Since powdery mildew infection is confined to epidermal cells and these possess only a few undeveloped chloroplasts, photoassimilates entering haustoria must first enter the epidermis. Furthermore, as already discussed above, the neckbands are seals which prescribe this pathway. In pea, plasmodesmata are rarely found connecting the mesophyll with the epidermis (Bushnell and Gay, 1978), and thus the high ATPase activity, equal to that in phloem transfer cells, of the wall-lining region of their plasma membrane suggests that epidermal cells scavenge the apoplast for photosynthates. These results also indicate that the plant cell is not able to utilise its ATP at the invaginated region of membrane at the parasitic interface to control solute efflux to the haustorium. Subsequently, uptake by the haustorium is likely to be by an active process through the haustorial plasma membrane which shows high activity with ATP. There is no evidence to support the suggestion (Gil and Gay,1977) that the contact areas of the haustorial lobes with the extrahaustorial membrane provide a special pathway into haustoria.

There is strong evidence that sucrose is a major translocate at the parasitic interface (Manners and Gay, 1982) and the rate of assimilate efflux for the invaginated portion of the host membrane has been estimated to be 2.4ng/100mm^2/sec (Manners, 1979). This is several orders of

magnitude higher than effluxes estimated for other plant cells (Edelman et al., 1971). Thus, by comparison with sucrose and glucose influxes calculated for higher plant (Humphreys, 1973, 1978) and fungal (Jennings, 1976) cells, both of which are thought to be ATPase coupled (Humphreys, 1973, 1978; Slayman and Slayman, 1975), Manners (1979) suggested that transport is by an active or facilitated process. Present evidence indicates that transport across the invaginated region is not directly ATPase coupled. However, the transport rate indicates that this domain does not impose an impedance of any significance in the series of three membranes which are traversed. This implies that there is a special relationship between the structure of the invaginated domain and the solutes transported. Furthermore, it is likely that efflux of solutes through the invaginated region is effected by forces originating outside it. The two membranes with ATPase activity have the same polarity with respect to both of their cytoplasms and the direction of photosynthate transport and thus their activities would be expected to result in a concentration gradient of sucrose across the invagination. Additionally, because on each side of the invaginated domain there exist sealed compartments (the epidermal cell and extrahaustorial matrix)(Gay and Manners, 1984; Gil and Gay, 1977) gradients of other species, for example ionic, resulting from the activity of electrogenic pumps in the two ATPase containing membranes may complement one another at the invagination to activate transport of photosynthates. These hypotheses are shown diagramatically in figure 3.4.

More specifically a role for anions as the

activating species can be postulated. Studies with red blood cells have shown that SITS and related compounds bind specifically to the anion transporting proteins in their plasma membranes (reviewed by Cabantchik et al., 1978). The presence of a similar protein in the extrahaustorial membrane is indicated by the strong fluorescence when healthy haustorial complexes are treated with SITS (Chapter 2, section 2.6). Masking or denaturation of an anion transporting protein which energises photosynthate transport across the extrahaustorial membrane would lead to decreased incorporation shown by the pre-necrotic complexes which did not fluoresce with SITS.

It is widely assumed that ATPases energise an H^+-efflux pump operating at plasma membranes of higher plants and fungi (see this chapter, section 1) and direct evidence for its electrogenic properties was first established for the ascomycete Neurospora crassa (Scarborough, 1976) and subsequently for several higher plant species (e.g. Churchill and Sze, 1983; Sze and Churchill, 1981) including Pisum sativum (Rasi-Caldogno et al., 1981). If the ATPases of the plasma membranes in E. pisi infected cells are functioning as proton efflux pumps then their activities will result in a gradient of protons across the extrahaustorial membrane with the higher concentration at the matrical face. This may result in movement of protons down the concentration gradient and into the cytoplasm of the infected cell but this would not be in the correct direction to energise co-transport of assimilates to the matrix as current evidence favours a symport mechanism. However, the electrical potential created across the extrahaustorial membrane would favour movement of anions, such as OH^- and

HCO_3^-, in the opposite direction which could be coupled to transport of photosynthates. Suggesting such a role for anions is not entirely speculative as there have been several reports of anions as the primary transported species (see Spanswick, 1981; Lin, 1981) which may energise movements of uncharged metabolites. Furthermore there is no evidence to dispute the notion. Protons are implicated in co-transport largely because changes in $p[H]$ have been monitored (e.g. Delrot, 1981; Etherton and Rubinstein, 1978; Hutchings, 1978), but these can equally be interpreted as movements of OH^- or HCO_3^- (Smith and Raven, 1979).

Some of these arguments may apply to the rust infected cells. However, there is no published evidence of the function of rust haustoria beyond the dependance of colony development on their formation and incorporation into insoluble material of ^{3}H-leucine supplied to the host (Mendgen, 1977). It is conspicuous that in pea and french bean the ATPase activity of the plasma membranes is much less in mesophyll than epidermal cells. This is in agreement with the results of biochemical assays of ATPase activities in tobacco and other species (see Kasamo, 1979). The difference is also correlated with the presence of chloroplasts and thus it is likely that in the rust infection the infected mesophyll cells are the major source of photosynthates and not intermediaries as in epidermal infections. Furthermore, since enzymic activity has not been demonstrated at the haustorial plasma membrane of the rust fungus, there is no evidence to suggest that this membrane plays an active role in importing solutes. Indeed the narrow width of the extrahaustorial matrix in compatible

infections and reduced incorporation of amino-acids by haustoria with thickened matrices (Manocha, 1975; Mendgen, 1977) are consistent with a requirement for minimal distances for transport of metabolites by diffusion down concentration gradients.

Additionally, there is evidence that efflux of sugars across plasma membranes of mesophyll cells does not involve protons but is mediated by co-transport with potassium instead (Huber and Moreland, 1981). A proton extruding pump at the plasma membrane of rust haustoria would positvely charge the matrix and electrically impede effluxes of K^+ (and therefore co-transported photosynthates) across the extrahaustorial membrane. However translocates may not traverse this membrane at all since there is ultrastructural evidence for direct continuity with cisternae of endoplasmic reticulum in U. appendiculatus (plates 3.14c; 3.15a) and several other rust infections (see Littlefield and Heath,1979) which provides an alternative route for translocation to the extrahaustorial matrix not available in powdery mildew infected cells.

As in the rust haustoria, ATPase activity was not demonstrated at the haustorial plasma membrane of Erysiphe graminis. However the present results should be interpreted with caution as the enzymes may have been affected by the procedures employed during preparation of the specimens. Cytoplasms of epidermal cells of Hordeum vulgare were not preserved to a satisfactory degree and it was not possible to distinguish domains of ATPase activity in plasma membranes of infected cells as precipitates occurred throughout them. It is of interest to note that the

extrahaustorial membrane in this infection did not fluoresce with SITS (Chapter 2, section 2.6) and although the significance of these observations is uncertain they suggest transport of nutrients to haustoria of E. graminis and E. pisi may be by different mechanisms. Atkinson and Shaw (1955) showed acid phosphatase activity associated with haustoria of E. graminis by light microscopy and cytochemistry but the resolution was insufficient to establish the precise location of the precipitation and thus comparison with the current data cannot be made.

The present work does not distinguish between enzyme presence and activity. Freeze-fracture preparations of E. pisi and Melamspora lini (a rust fungus) infections have shown that the invaginated domain of the host plasma membrane lacks the 10nm particles characteristic of the equivalent face of the wall lining region (Gil, 1976; Gil, in Bushnell and Gay, 1978; Littlefield and Bracker, 1972). The authors have suggested that particle absence may be related to the absence of synthesis of normal wall components, but more significantly similar particles are only present in freeze-fracture preparations of reconstituted membranes of Neurospora crassa when ATPases are incorporated (Carolyn Slayman, verbal communication). Thus it may be that the particles seen contained ATPase and perhaps other components of a transport complex and the possibility that enzyme-deficient host plasma membrane is developed around haustoria should be borne in mind. Alternatively, Faull and Gay (1983) have recently suggested that ATPases in the extrahaustorial membrane may be inactiviated as a result of the action of phospholipases

produced by haustoria of E. pisi.

This author is not aware of any other systems in plants where major structurally and functionally distinct domains of individual plasma membranes have been described. Although the fluid mosaic model of Singer and Nicholson (1972) proposes that constituent molecules of a biological membrane are free to diffuse laterally throughout the structure many exceptions are reported for animal cell plasma membranes where particular domains have specific functions such as at cell and membrane junctions (Gilula, 1974, 1980) and where epithelial cells are concerned with transport (Evans, 1980; Kinne, 1976). The phenomenon is particularly well documented for absorptive epithelial cells of mammals where two domains of the plasma membrane are separated by intercellular junctional complexes. The transport ATPase is located on the unloading domain (Geck and Heinz, 1981) e.g. of proximal tubule epithelia of kidney (Kinne, 1976) and intestinal mucosa (Fujita et al., 1972) rather than the influx face as described above. However, in none of these systems is a sealed compartment interpolated between two cells transporting in series as occurs in the fungal infections which are now described. In these, the evidence indicates that the host co-operates in passing solutes to the fungus. The modifications which lead to this are confined to the region around the haustorium which indicates that it is the pathogen which controls efflux from the host.

In contrast, host cell plasma membranes in infections by Rhizobium bacteroids (Verma et al., 1978) and mycorrhizal fungi (Marx et al., 1982) show ATPase activity at similar

levels in all regions. However in these symbiotic associations metabolites are exchanged in both directions across the interface whilst current evidence for powdery mildew and rust infections suggests transport is in one direction alone, viz. from host to pathogen. Thus in these pathogenic associations the structural delimitation of the membrane domains is essential to the transport system because it organizes cellular function and is therefore an essential feature in the biotrophy of these fungi.

4.4. ATPase activities in leaves of *Pisum sativum* infected with *Peronospora pisi*.

The present ultrastructural evidence corroborates observations in the field (see Dixon, 1981) that the "Onward" cultivar of pea is not particularly susceptible to infection by *P. pisi*. This is probably because a large proportion of haustoria become necrotic and the mechanisms for transfer of assimilates from host to pathogen are consequently not established to a satisfactory degree. Similar conclusions were drawn by Beakes *et al* (1982) from their ultrastructural studies with other cultivars of pea and *P. viciae*.

Moreover, ATPase activities are depressed in infected tissues. The particularly low activity of Mg^{2+}-ATPase in the 10,000 xg precipitate from infected leaves and the infrequency of deposits in tissues prepared for cytochemistry indicate that the activities of plasma membranes are especially reduced by infection, which may directly limit fungal growth by reducing accumulation of assimilates and transport to haustoria. However it is not

clear if the reduced activity directly leads to necrosis of haustoria or is merely consequential to other events and does not directly contribute towards resistance. The depressed activities may be due to depletion of ATPase from the membranes or the action of inhibitors.

Toxins which affect ATPase activity are produced by several fungi that are plant pathogens and although some, for example fusicoccin (Beffagna et al., 1977; Marre, 1979) are stimulatory, others including Helmithosporium T toxin (Marre et al., 1980) and Cercospora beticola toxin (Macri and Vianello, 1979) are inhibitory. There is no evidence that downy mildew fungi produce toxins and furthermore there are no published records of previous investigations of phosphatase activities in infected tissues which can be directly compared with the present experiments.

Pisatin is produced by pea in response to various stimuli but there is no evidence that non-phenolic derivatives of pterocarpan phytoalexins inhibit ATPases. However resistance to infection by downy mildew fungi has been correlated with high levels of flavour volatiles including isothiocyanates (Greenhalgh and Mitchell, 1976) and it may be significant that the synthetic derivative acetamido-isothiocyanato-stilbene (SITS) inhibits plasma membrane ATPases of corn root protoplasts (Lin, 1981) and the yeasts Saccharomyces cerevisiae and Debaryomyces hansenii (Spencer-Phillips and Jennings, in preparation). Flavour isothiocyanates may therefore have a similar effect, although it must first be established conclusively that reduced ATPase activity is correlated with resistance before further investigations are initiated. In this

regard the present study should be viewed as preliminary and inconclusive particularly as interpretation of the results is complicated by the uncertain compatibility of the organisms and the effects of the unfavourable conditions in which the plants were grown.

Recent studies by Woods and Gay (1983) have shown that the distribution of ATPase activities at plasma membranes of cells of Cardamine hirsuta infected with the white blister fungus Albugo candida (Peronosporales) is similar to the results for rust and powdery mildew infections (this chapter, section 3.1.2.). Clearly, phosphatase activities in compatible interactions between pea and P. pisi should now be investigated.

Table 3.1. Locations of granular and flocculent precipitation in electron microscope sections of leaves of Pisum sativum and Phaseolus vulgaris incubated with ATP and β-GP at pH 7.2 after fixation in glutaraldehyde (0.5% $^{v}/_{v}$) and formaldehyde (4% $^{w}/_{v}$). The incubation medium comprised substrate, $Mg(NO_3)_2$ and $Pb(NO_3)_2$ all at 2mM. Results are recorded as precipitates present, + or absent, -.

Location		Precipitation Granular[1]	Flocculent
Plasma membranes		-	+
Plasmodesmata		-	+
Tonoplasts		-	+
Vacuoles		-	+
Endoplasmic reticulum		+	+
Golgi cisternae		+	-
Nuclear	envelopes	+	-
	heterochromatin	+	+
Mitochondrial	envelopes	+	+
	cristae	+	+
	matrices	-	-
Chloroplast	envelopes	+	-[2]
	thylakoids	+	-
	stroma	-	-
Cell walls		+	+
Interface of cuticle and cell wall		-[3]	-
Intercellular spaces		-	+

1. Granular precipitates were also present at these sites when substrates were not included in the incubation medium and in P. sativum with β-GP at pH 5.5.
2. Except in P. vulgaris where flocculent precipitates were occasionally located in chloroplast envelopes (plate 3.3d,e).
3. In P. sativum alone granular precipitates were especially frequent in E. pisi infections at the cell wall/cuticle interface of epidermal cells around penetration sites and where hyphae were closely associated with the cell wall.

Table 3.2. Phosphatase activities in electron microscope sections of plasma membranes of leaf cells of Phaseolus vulgaris incubated with ATP and β-GP at pH 7.2. Fixation and incubation media as for table 3.1. NaF was present at 10mM. Results are recorded as frequent deposits, ++; less frequent deposits, +; infrequent deposits, +-; deposits at level of no substrate control, -.

Cell type		Treatment			
		ATP	ATP+NaF	β-GP	β-GP+NaF
Epidermal	Upper	++	+-	++	+-
	Lower	++	+-	++	+-
Mesopyll	Palisade	+-	+-	+-	-
	Spongy	+	+-	+-	-
Vascular	Bundle sheath	+	+-	ND[1]	-
	Companion/ parenchyma	+	+-	ND	+-
	Sieve element	+-	+-	ND	-

1. ND= no data.

Table 3.3. Phosphatase activities in electron microscope sections of plasma membranes of leaf cells of Pisum sativum incubated with ATP and β-GP at pH 7.2 and 5.5. Fixation, incubation media and expression of results as for table 3.2.

Cell type	Treatment pH 7.2 ATP	ATP+NaF	β-GP	β-GP+NaF	pH 5.5 β-GP	β-GP+NaF
Upper epidermal	++	+-	+-	+-	+-	-
Palisade mesophyll	+	+-	+-	+-	+-	-
Vascular: Bundle sheath	+	+-	+-	+-	+-	-
Vascular: Parenchyma	+-	+-	+-	+-	+-	-
Vascular: Transfer	++	+-	+	+-	+-	-
Vascular: Sieve element	+-	+-	+-	+-	+-	-

Table 3.4. Phosphatase activities in electron microscope sections of plasma membranes of Uromyces appendiculatus and infected leaf cells of Phaseolus vulgaris incubated with ATP and β-GP at pH 7.2. Fixation, incubation media and expression of results as for table 3.2.

Cell type	Substrate	Wall lining	Plasma membrane		
			Extrahaustorial	Haustorial	Mycelial
Epidermal	ATP	++	-	-	-
	β-GP	++	-	-	-
Spongy mesophyll	ATP	+	-	-	-
	β-GP	+-	-	-	-
Palisade mesophyll	ATP	+-	-	-	-
	β-GP	+-	-	-	-
Bundle sheath	ATP	+	-	-	-

Table 3.5. Phosphatase activities in electron microscope sections of plasma membranes of Erysiphe pisi and infected leaf cells of Pisum sativum incubated with ATP and β-GP at pH 7.2 and 5.5. Fixation, incubation media and expression of results as for table 3.2.

Cell type	Substrate	pH	Wall lining	Plasma membrane		
				Extrahaustorial	Haustorial	Mycelial
Epidermal	ATP	7.2	++	-	++	-
	β-GP	7.2	+-	-	++	-
	β-GP	5.5	+-	-	++	-

Table 3.6. Germination of conidia of Erysiphe pisi and formation of appressoria after 67 h on distilled water and strips of epidermis from stems of Pisum sativum.

Surface	Number of conidia sampled	% Germinated conidia		% ungerminated conidia
		with germ tubes only	with germ tubes and appressoria	
Epidermis	207	25.1	45.4	29.5
Distilled water	474	68.1	0	31.9

Table 3.7. Activities of ATPase in crude extracts of homogenates of upper epidermis peeled from leaves of Pisum sativum and of whole leaves (midveins excluded) uninfected or infected with Erysiphe pisi. Mg^{2+}-ATPase activity was calculated as the difference between the activities with and without Mg^{2+} in the incubation medium. Homogenates were incubated at 37°C for 30 min. with 3mM ATP in 0.1M Tris-maleate buffer at pH 7.2. $Mg(NO_3)_2$ and NaF were used at 2mM and 10mM respectively.

Additions to medium	Specific activity (µg Pi (mg protein)$^{-1}$ h^{-1}) Uninfected		Infected	Relative activity (infected/
	Upper epidermis	Leaf	leaf	uninfected leaf)
None	77.46	83.66	111.34	1.33
Mg^{2+}	73.97	69.22	88.4	1.28
Mg^{2+} + NaF	50.71	35.61	45.31	1.27
Mg^{2+}-ATPase activity	-3.49	-14.44	-22.94	1.59

Table 3.8. Activities of ATPase in crude extracts of homogenates of epidermis peeled from stems of Pisum sativum that were uninfected or infected with Erysiphe pisi. Calculation of Mg^{2+}-ATPase activity and incubation media as for table 3.7. Specific activities are expressed as μg Pi $h^{-1}mg^{-1}$ protein and μg Pi h^{-1} mm^{-2} epidermis.

Additions to medium	Specific activity (μg Pi h^{-1}) Uninfected mg^{-1} protein	mm^{-2}	Infected mg^{-1} protein	mm^{-2}	Relative activity (infected/uninfected) Protein	Area
None	121.55	0.326	78.44	0.174	0.65	0.53
Mg^{2+}	100.3	0.269	75.98	0.169	0.76	0.63
Mg^{2+} + NaF	68.43	0.183	49.02	0.109	0.72	0.6
Mg^{2+}-ATPase activity	-21.25	-0.057	-2.46	-0.005	0.12	0.09

Table 3.9. Specific activities of ATPase in homogenates of haustorial complexes isolated from leaves of Pisum sativum infected with Erysiphe pisi. Calculation of Mg^{2+}-ATPase activity and incubation media as for table 3.7. Results are expressed as μg Pi (mg protein)$^{-1}$ h^{-1}, μg Pi (haustorial complex)$^{-1}$ h^{-1} and μg Pi (mm^2 epidermis)$^{-1}$ h^{-1}. The last was calculated as the product of activity/haustorial complex and the frequency of haustoria in epidermis from infected stems.

Additions to medium	ATPase activity (μg Pi h^{-1}) mg^{-1} protein	haustorial complex^{-1} ($X10^6$)	mm^{-2} infected epidermis ($X10^3$)
None	55.53	5.45	1.29
Mg^{2+}	210.05	20.61	4.9
Mg^{2+} + NaF	136.43	13.38	3.18
Mg^{2+}-ATPase activity	154.52	15.16	3.6

Table 3.10. Activities of ATPase with Mg^{2+} and Mg^{2+}+NaF in the incubation media expressed as a proportion of the activity in control incubations without Mg^{2+}. Crude extracts were prepared from homogenates of leaves and epidermis peeled from leaves and stems of Pisum sativum. Uninfected tissues are compared with tissues infected with Erysiphe pisi. Data derived from experiments recorded in tables 3.7, 3.8 and 3.12 ; the activity of control incubations without Mg^{2+} and NaF was designated unity.

Additions to medium	Leaf			Stem	
	Lamina		Epidermis	Epidermis[1]	
	Uninfected	Infected	Uninfected	Uninfected	Infected
Mg^{2+}	0.83	0.79	0.96	0.81($\pm$0.03)	1.07($\pm$0.14)
Mg^{2+}+ NaF	0.43	0.41	0.66	0.56	0.63

1. Activity in the presence of Mg^{2+} mean of two experiments ($\pm$ standard deviation).

Table 3.11. Distribution of Mg^{2+}-activated ATPase in fractions prepared from homogenate of epidermis peeled from stems of Pisum sativum. Incubation media as for table 3.7.

Fraction	Mg^{2+}-ATPase activity Specific[1]	Total[2]
Crude extract	-262.58	-814
1,500 xg precipitate	464.94	146.12
10,000 xg precipitate	1092.07	280.81
10,000 xg supernatant	-2991.15	-1300

1. μg Pi (mg protein)$^{-1}$ h^{-1}.
2. μg Pi (fraction)$^{-1}$ h^{-1}.

Table 3.12. Activities of Mg^{2+}-ATPase in fractions prepared from homogenates of epidermis peeled from stems of Pisum sativum in two experiments. Uninfected epidermis is compared with epidermis from stems infected wtih Erysiphe pisi. Incubation media and expression of results as for table 3.8.

Fraction	Experiment	Mg^{2+}-ATPase activity (μg Pi h^{-1})				Relative activities of infected/uninfected	
		Uninfected		Infected			
		mg^{-1} protein	mm^{-2}	mg^{-1} protein	mm^{-2}	Protein	Area
1,500 xg precipitate	1	235.38	12.7	309.89	31.4	1.32	2.47
	2	464.94	13.65	714	35.19	1.54	2.58
	Mean of 1 & 2	350.16	13.18	511.95	33.3	1.46	2.53
10,000 xg precipitate	1	911.25	30.1	998.57	51.97	1.1	1.73
	2	1092.07	26.24	1296.93	41.48	1.19	1.58
	Mean of 1 & 2	1001.66	28.17	1147.75	46.73	1.15	1.66
10,000 xg supernatant	1	-411.25	-129	-266.74	-98	0.65	0.76
	2	-2991.15	-83.91	-215	-26.68	0.07	0.32
	Mean of 1 & 2	-1701.2	-106.46	-240.87	-62.34	0.14	0.59

Table 3.13. Activities of ATPase in incubations with Mg^{2+} expressed as proportion of control activity (incubations without Mg^{2+}). Data from experiments recorded in table 3.12 ; standard deviations given in brackets.

Fraction	Uninfected	Infected
1,500 xg precipitate	1.37 (±0.01)	3.83 (±1.23)
10,000 xg precipitate	2.37 (±0.9)	15.87 (±6.7)
10,000 xg supernatant	0.72 (±0.04)	0.73 (±0.18)

Table 3.14. Inhibition by NaF (10mM) of ATPase activity in fractions incubated with Mg^{2+} and prepared from leaves and stems of Pisum sativum uninfected or infected with Erysiphe pisi. Compiled from data in tables 3.7, 3.8 and 3.9 with additional data from the experiments recorded in table 3.12.

		% inhibition	
		Uninfected	Infected
Crude extracts	Leaf	48.56	48.74
	Leaf upper epidermis	31.45	ND[1]
	Stem epidermis	31.78	35.5
	Haustorial complexes	35.05	
Fractions of stem epidermis	1,500 xg precipitate	41.81	83.1
	10,000 xg precipitate	37.33	77.73
	10,000 xg supernatant	39.9	50.68

1. ND = No data.

Table 3.15. Activity of Mg^{2+}-ATPase in fractions prepared from homogenates of leaves of Pisum sativum uninfected and infected with Peronospora pisi. Incubation media as for table 3.7.

Fraction	Mg^{2+}-ATPase activity (μg Pi (mg protein)$^{-1}$ h^{-1}) Uninfected	Infected	Relative activities of infected/uninfected
Crude extract	110.38	90.58	0.82
1,500 xg precipitate	264.5	415.67	1.57
10,000 xg precipitate	1196.25	409.69	0.34
10,000 xg supernatant	-76	-423.69	5.58

Figure 3.1. Distribution of frequencies of flocculent precipitates at plasma membranes of upper and lower epidermal cells in leaves of Phaseolus vulgaris infected with Uromyces appendiculatus. The data were compiled by examining electron microscope sections from two leaf pieces for each treatment. Fixation, incubation media and expression of results are as for table 3.2. Stomatal guard cells shown as stippled areas; infected cells are shaded, and the results refer to the wall-lining domain of each cell.

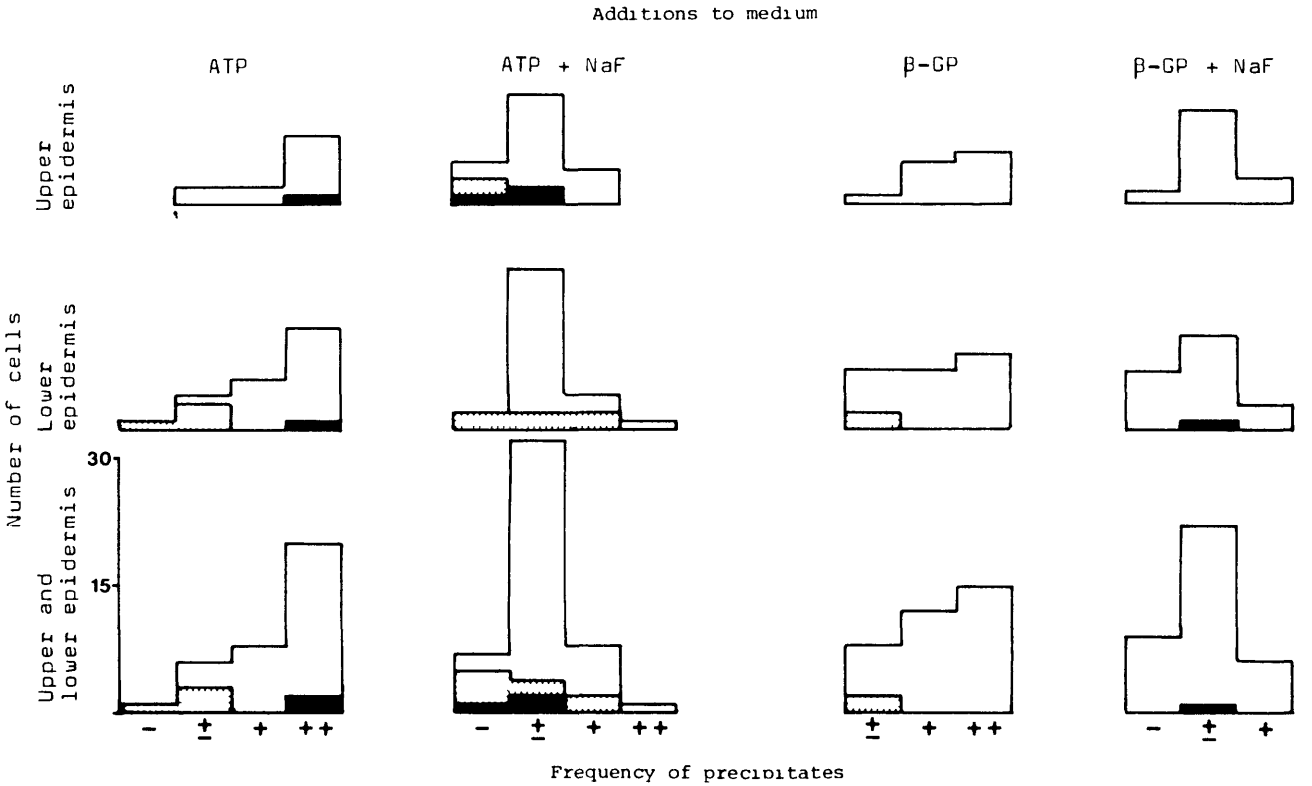


Figure 3.2. Distribution of frequencies of flocculent precipitates at plasma membranes of palisade and spongy mesophyll cells in leaves of Phaseolus vulgaris infected with Uromyces appendiculatus. Specimen preparation and expression of results as for fig. 3.1.

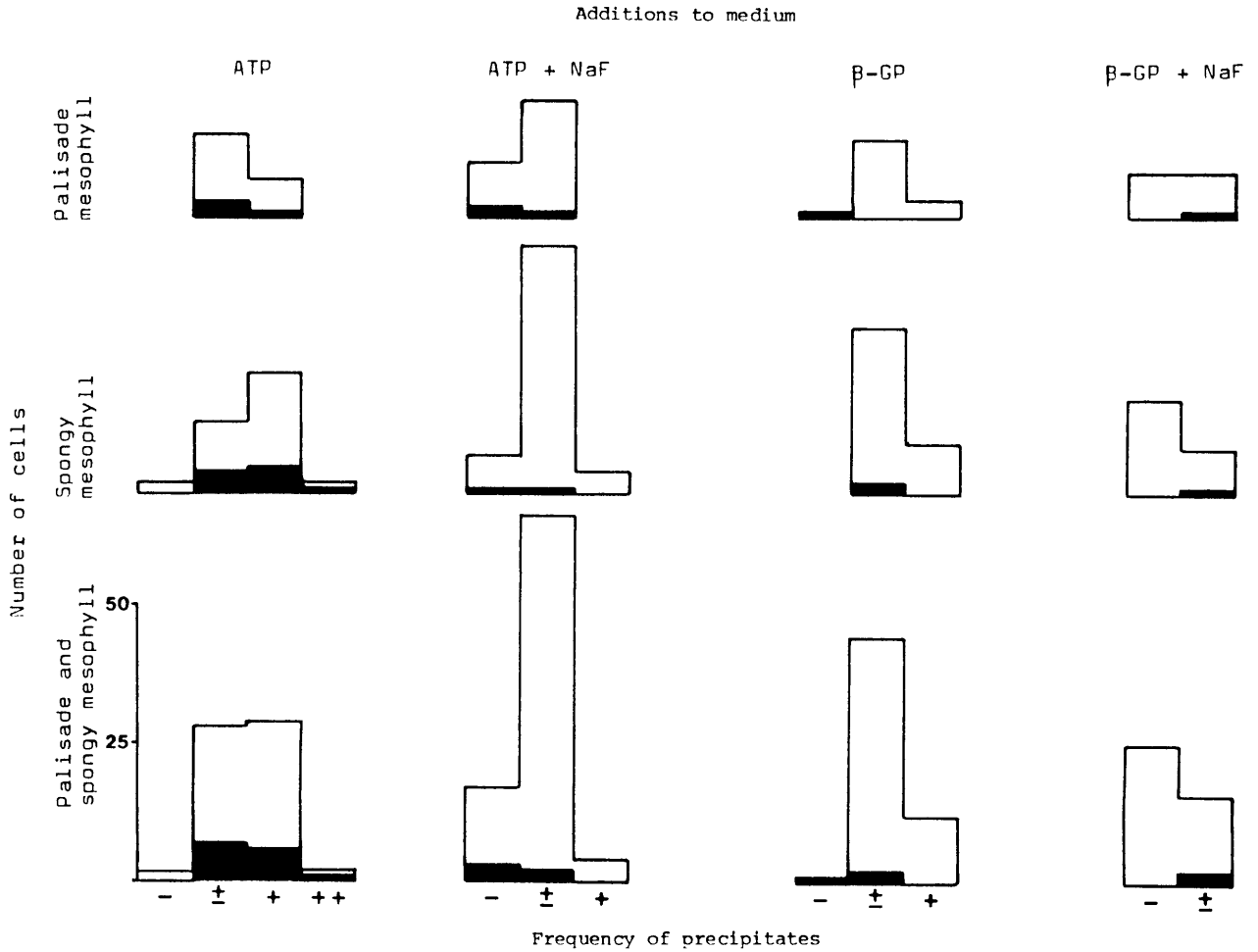


Figure 3.3. Distribution of frequencies of flocculent precipitates at plasma membranes in cells of minor veins in leaves of Phaseolus vulgaris infected with Uromyces appendiculatus . Specimen preparation and expression of results as for fig. 3.1. There are no data for β-GP as substrate in incubations without NaF.

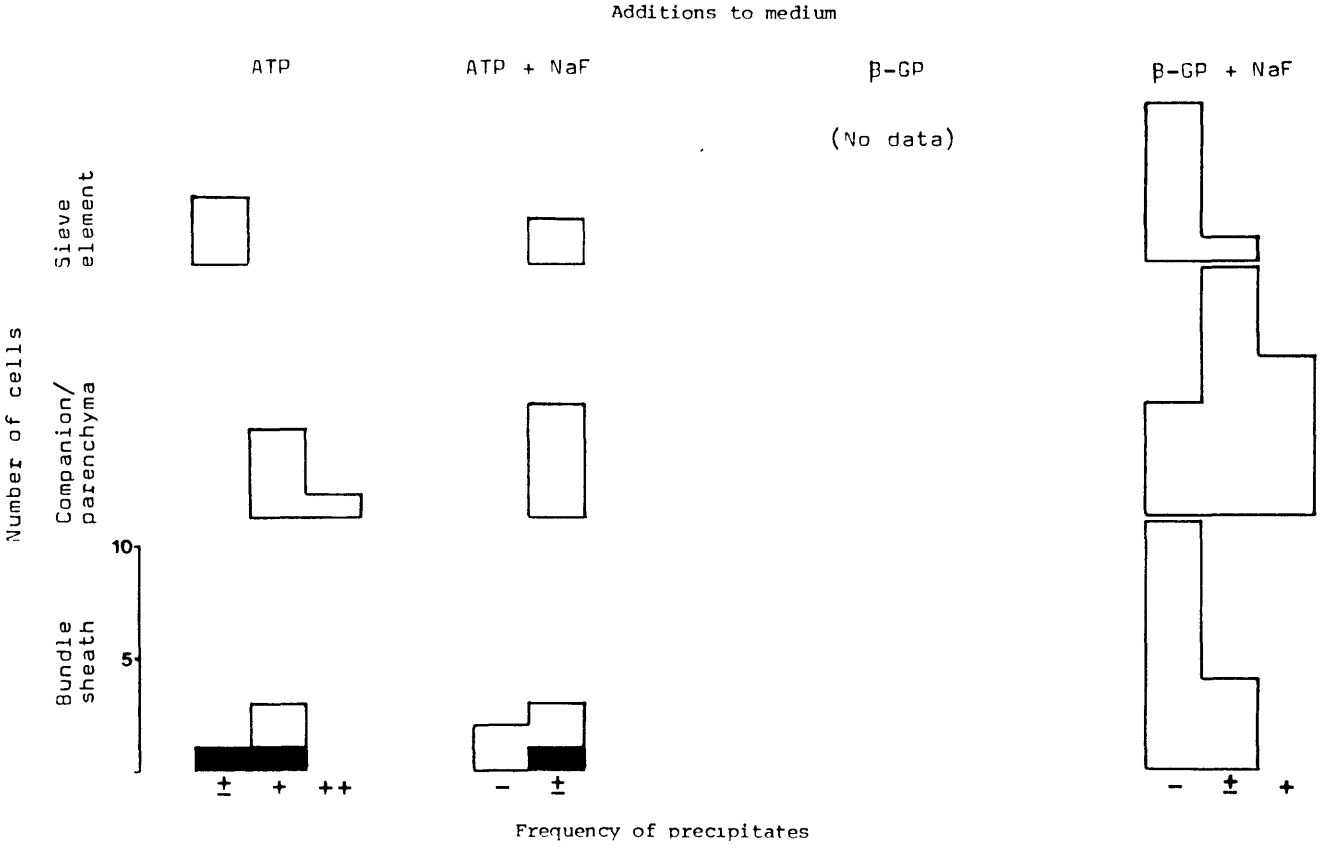


Figure 3.4. Diagram to show the proposed mechanisms of solute transport through the plasma membranes of pea epidermal cells and infecting haustoria of Erysiphe pisi. The arrows indicate ATPase activated influxes through the wall lining domain of the host and the haustorial plasma membranes. It is proposed that, because the matrix is maintained as a closed compartment by the seal between host and haustorial plasma membranes, efflux through the invaginated domain of the host plasma membrane (extra-haustorial membrane) is effected by either a high concentration difference of the transported species (left) or interaction of complementary ionic products of electrogenic pumps at the ATPase active membranes (right). The seal (neckbands) also maintains the segregation of the two domains of both the host and fungal plasma membranes.

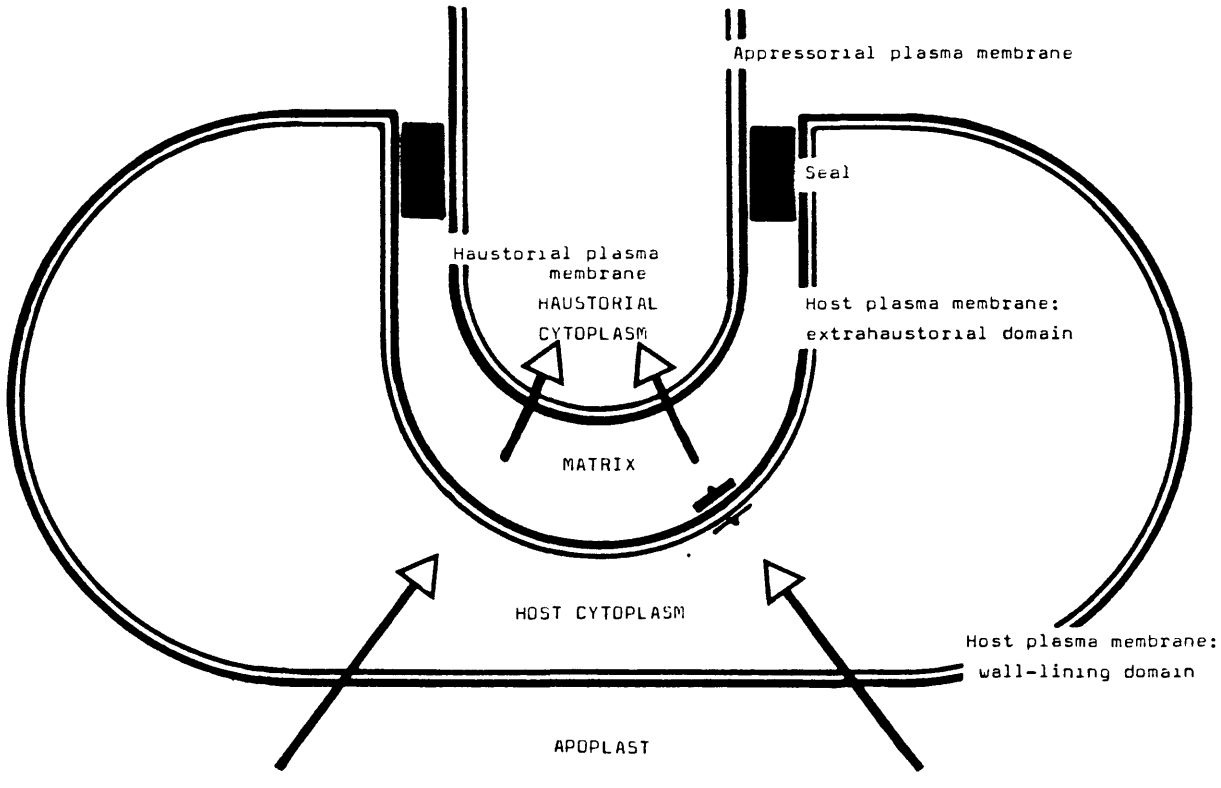


Plate 3.1.

a,b. Sections of minor veins in leaves of Phaseolus vulgaris stained with lead. Four cell types are distinguished. Cells of the bundle sheath (Bs) delimit the vascular tissue which comprises xylem vessels (Xy), phloem sieve elements (Se) and undifferentiated cells which are collectively referred to as companion parenchyma (P). None of the cells have wall ingrowths charateristic of transfer cells (cf. Pisum sativum, plate 3.5.).

a. Section prepared from material incubated with ATP and Mg^{2+} at pH 7.2. Dense precipitates are particularly frequent at plasma membranes of companion parenchyma (P) and bundle sheath (Bs) cells and throughout disrupted cytoplasms (*). Neg. no. 13118, x6,400.

b. Section prepared from material incubated with medium used for plate 3.1a but with addition of NaF (10mM). Precipitation at plasma membranes is slight. Neg. no. 9747, x 9,600.

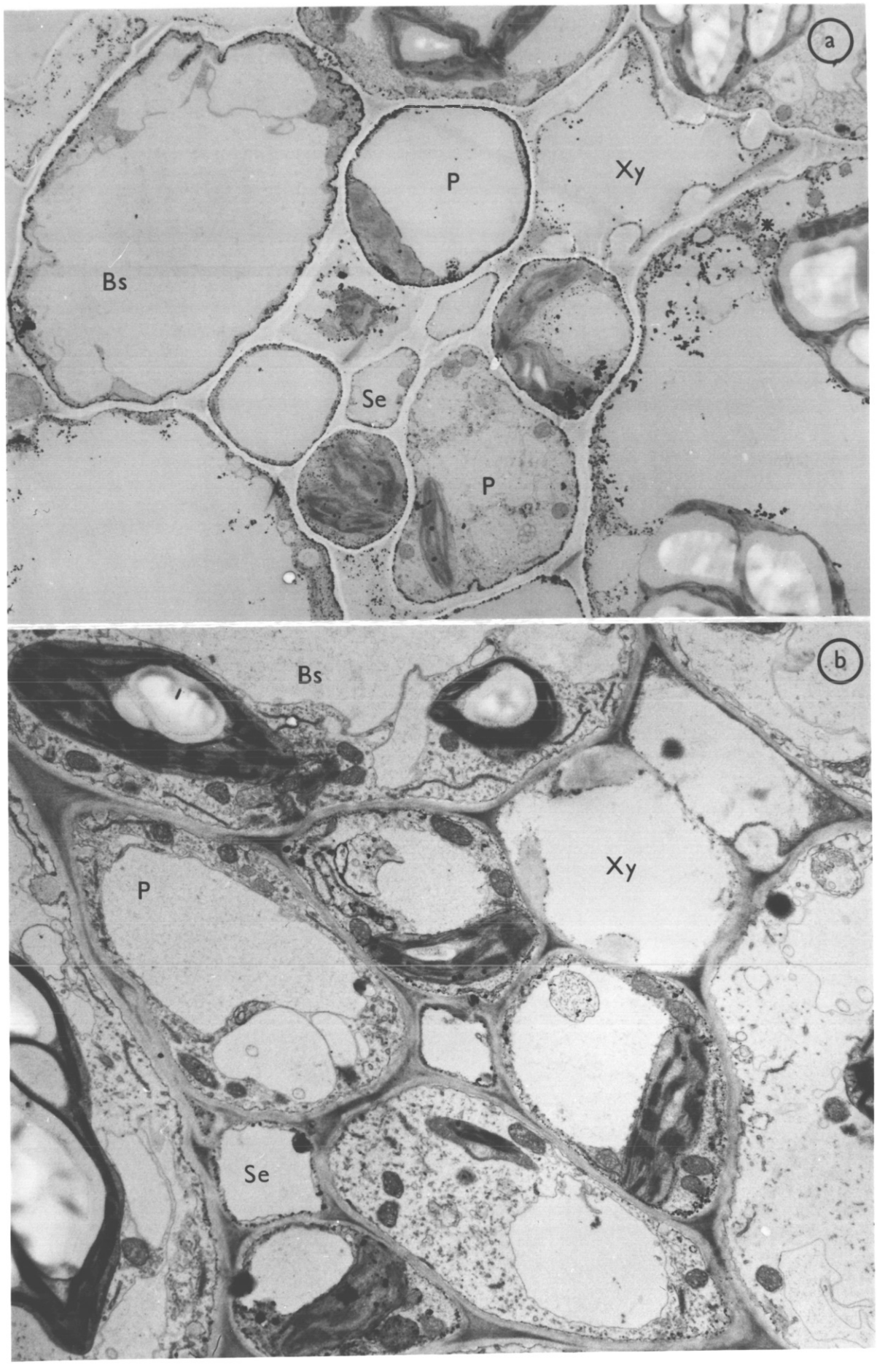

a
Bs
P
Xy
Se
P
b
Bs
P
Xy
Se

Plate 3.2.

a. Adjacent section to plate 3.1a, stained with lead. Detail of companion parenchyma cell (P) with high ATPase activity at the plasma membrane (Pm). Plasmodesmata (Pd) and cristae of mitochondria (m) also show precipitates. Bs = bundle sheath cell; Se = phloem sieve element. Neg. no. 13116, x 19,800.

b. Section of minor vein in leaf of P. vulgaris prepared from material incubated with β-GP and NaF at pH 7.2. Section stained with lead. Flocculent precipitates at plasma membrane (Pm) of companion cell indicate enzyme activity here alone. Thylakoids in chloroplasts (Cl), nuclear envelopes (n) and golgi dictyosomes (d) all show granular precipitates. Pd = plasmodesmata; Se = phloem sieve element. Neg. no. 13126, x 19,800.

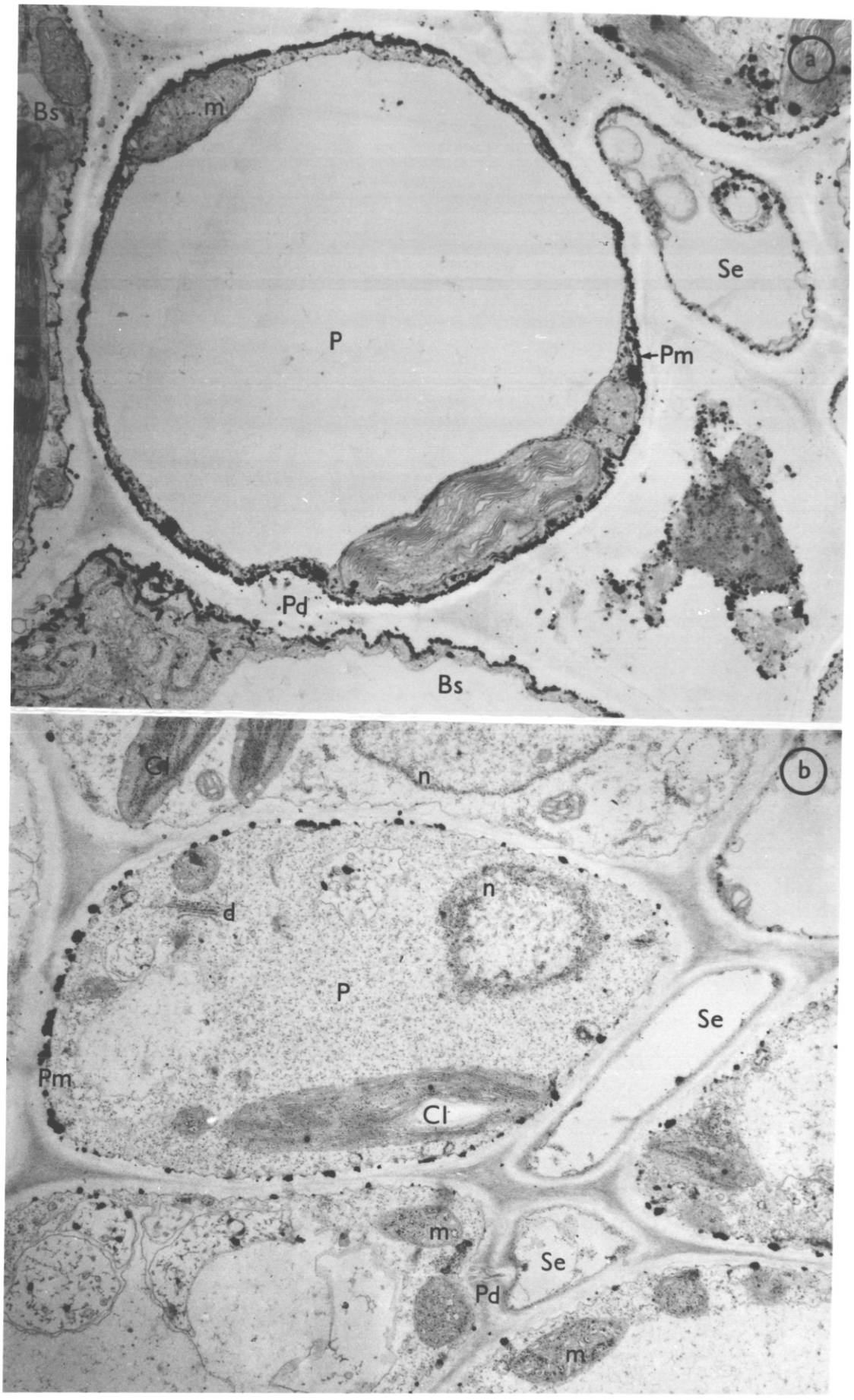

a
Bs
m
P
Pm
Se
Pd
Bs
b
Cl
n
n
d
P
Se
Pm
Cl
m
Se
Pd
m

Plate 3.3.

a,b,c. Sections of cells of the upper epidermis in leaves of P. vulgaris prepared from material incubated with medium used for plate 3.4 (ATP and Mg^{2+} at pH 7.2) but with addition of NaF (10 mM). Sections stained with lead, a and b; section stained with uranyl acetate and lead, c. Precipitates at plasma membranes (Pm) are infrequent (compare with plate 3.4b).

a, b. Granular precipitates are mostly confined to cisternae of golgi dictyosomes (d) but are not uniformly frequent in all cisternae (arrow). Precipitates are also associated with the outer portion of the cell wall (W). Ct = cuticle; v = vacuole. a, neg. no. 12003, x 37,600. b, neg. no. 12004, x 48,900.

c. Epidermal cell with large vacuole (v) connected to mesophyll by plasmodesmata (Pd) which show frequent precipitates despite low activities of plasma membranes (Pm). The plasmodesmata shown here are unusual in two respects; precipitates are normally absent after treatment with media containing NaF and additionally plasmodesmata between cells of epidermis and mesophyll are infrequent. Neg. no. 11787, x 27,900.

d, e. Sections of mesophyll cells in leaves of P. vulgaris prepared from material incubated with ATP and Mg^{2+} at pH 7.2. Sections stained with lead. Flocculent precipitates are associated with the plasma membrane (Pm), intercellular space (Is) and vacuole (v), and occasionally within chloroplast envelopes (Cl) and peripheral reticulum (arrowed). Thylakoids show fine granular precipitates (*). Neg. no. 11764 and 11765, x 60,900.

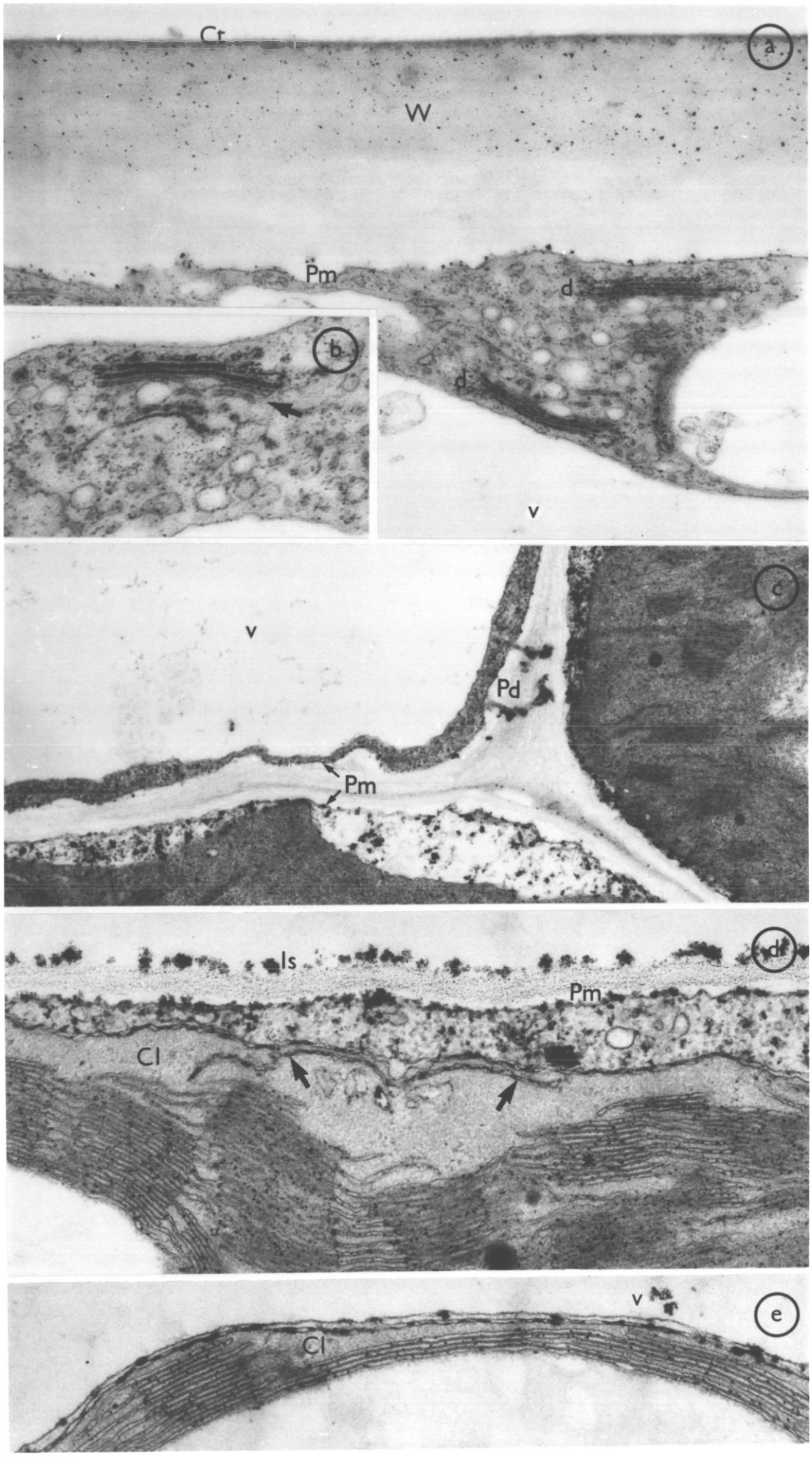

Cr
a
W
Pm
d
b
d
v
c
v
Pd
Pm
d
ls
Pm
Cl
e
v
Cl

Plate 3.4.

Sections of cells of the lower epidermis in leaves of P. vulgaris prepared from material incubated with ATP and Mg^{2+} at pH 7.2. Sections stained with uranyl acetate and lead.

a. Dense deposits indicate enzymic activity at the plasma membrane (Pm) and tonoplast (t) of subsidiary cell but activities of these membranes in guard cells are slight. Precipitates are also prominent in the substomatal cavity (Is) and the nucleus (n). v = vacuole. Neg. no. 11910, x 16,800.

b. Adjacent epidermal cells connected by plasmodesmata (Pd). The frequencies of precipitation indicate different enzymic activities of the plasma membranes (Pm) of the adjacent cells. Neg. no. 11908, x 45,950.


a
Pm
v
n
t
ls
b
Pm
Pd

Plate 3.5.

Section of minor vein in leaf of Pisum sativum prepared from material incubated with medium used for plate 3.7b (β-GP at pH 5.5) with the addition of NaF (10mM). Section stained with lead. Five cell types are distinguished as follows: Xylem vessels (Xy); transfer cells (T) with characteristic wall ingrowths are associated with phloem sieve elements (Se); parenchymatous cells (P) are undifferentiated and cells of the bundle sheath (Bs) delimit the vascular tissue. Flocculent precipitates are completely absent from all cells. Neg. no. 10997, x 9,700.

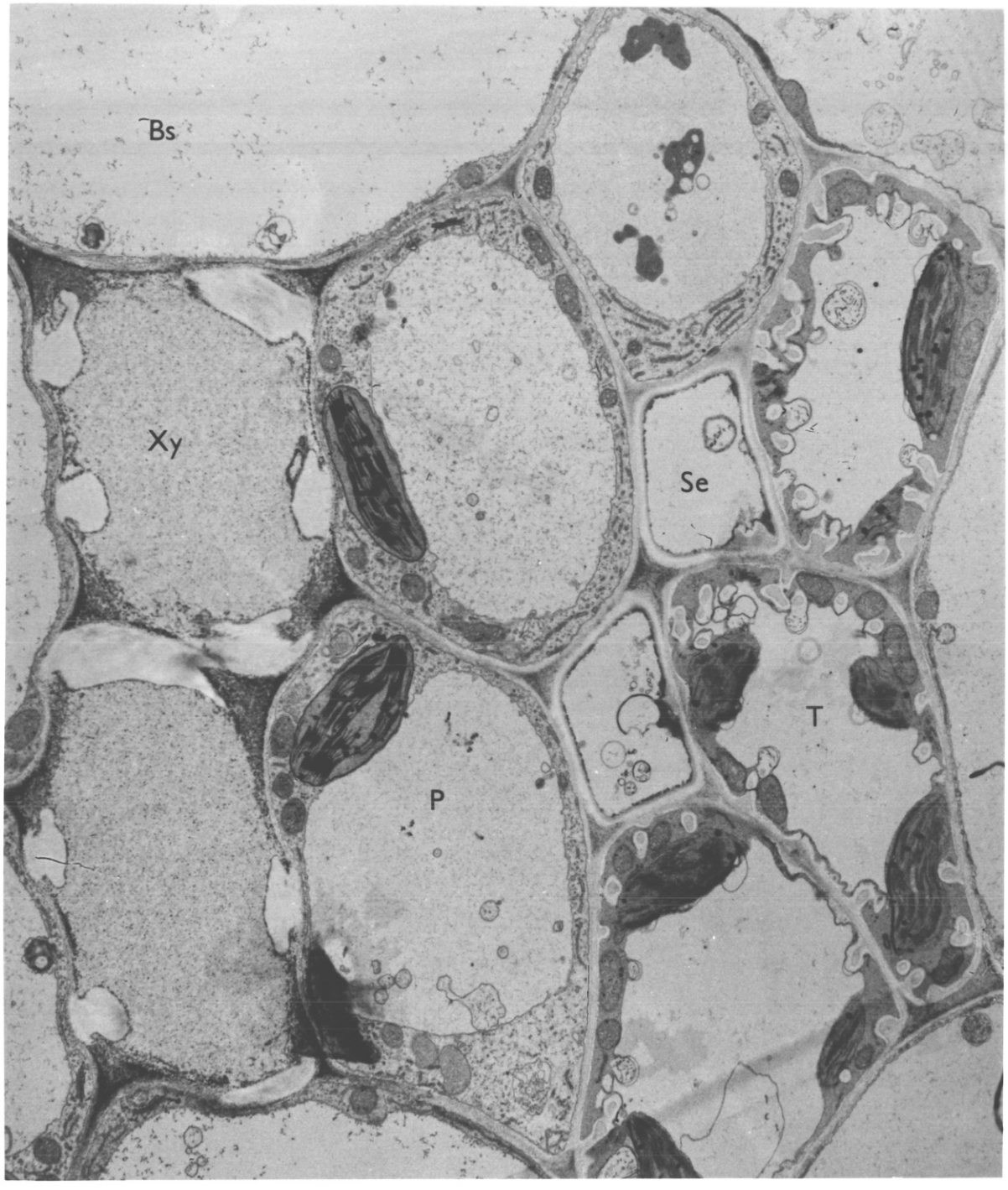

Bs
Xy
Se
T
P

Plate 3.6.

Section of minor vein in leaf of P. sativum prepared from material incubated with medium used for plate 3.8 (ATP and Mg^{2+} at pH 7.2) with the addition of NaF (10mM). Section stained with uranyl acetate and lead. Flocculent precipitates are most abundant at the tonoplast (t) in cells of the bundle sheath (Bs) and parenchyma (P). Slight precipitation at the plasma membranes of transfer cells (Pm) and other cells indicates low enzymic activity in the presence of NaF. Neg. no. 10668, x 16,400.

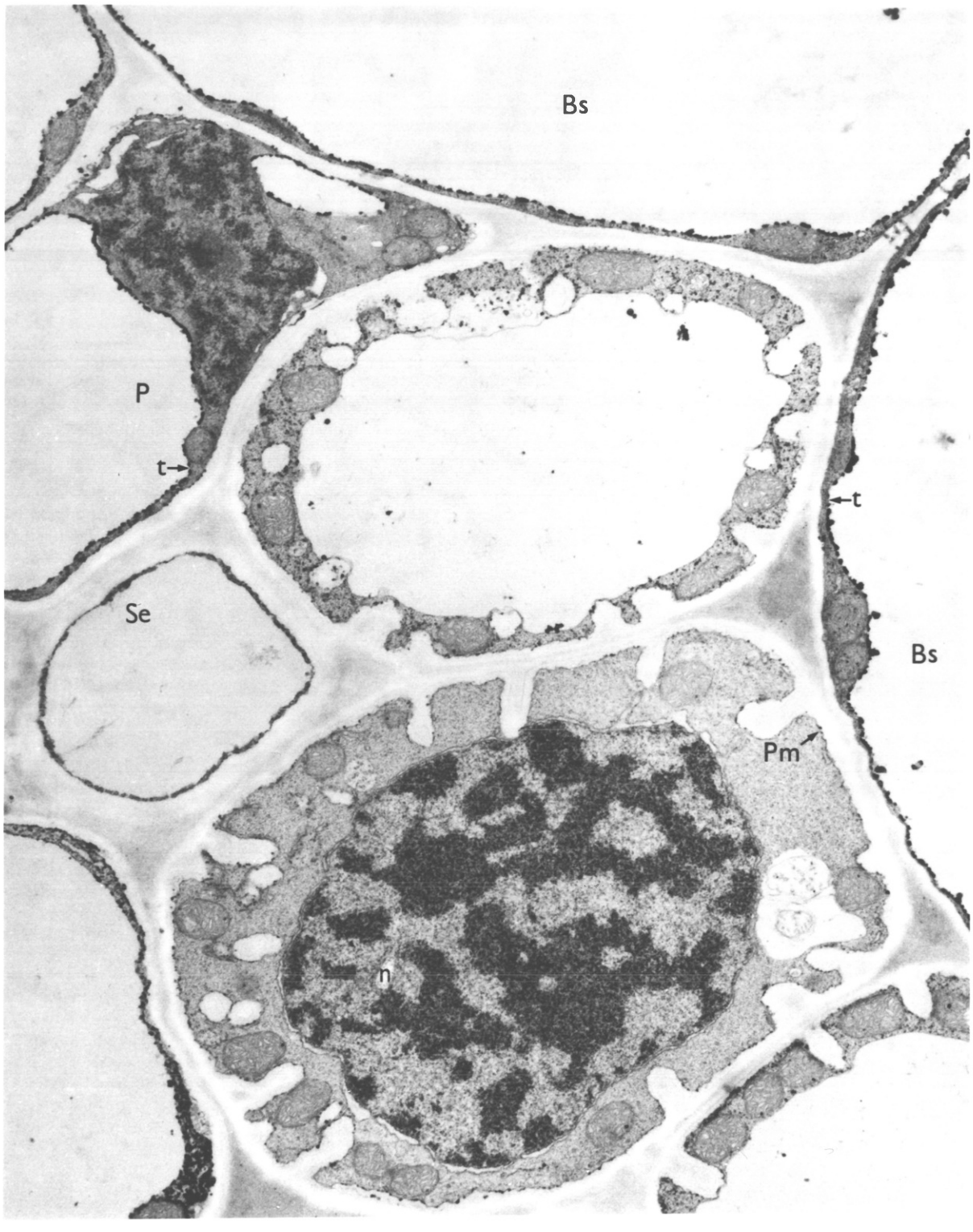
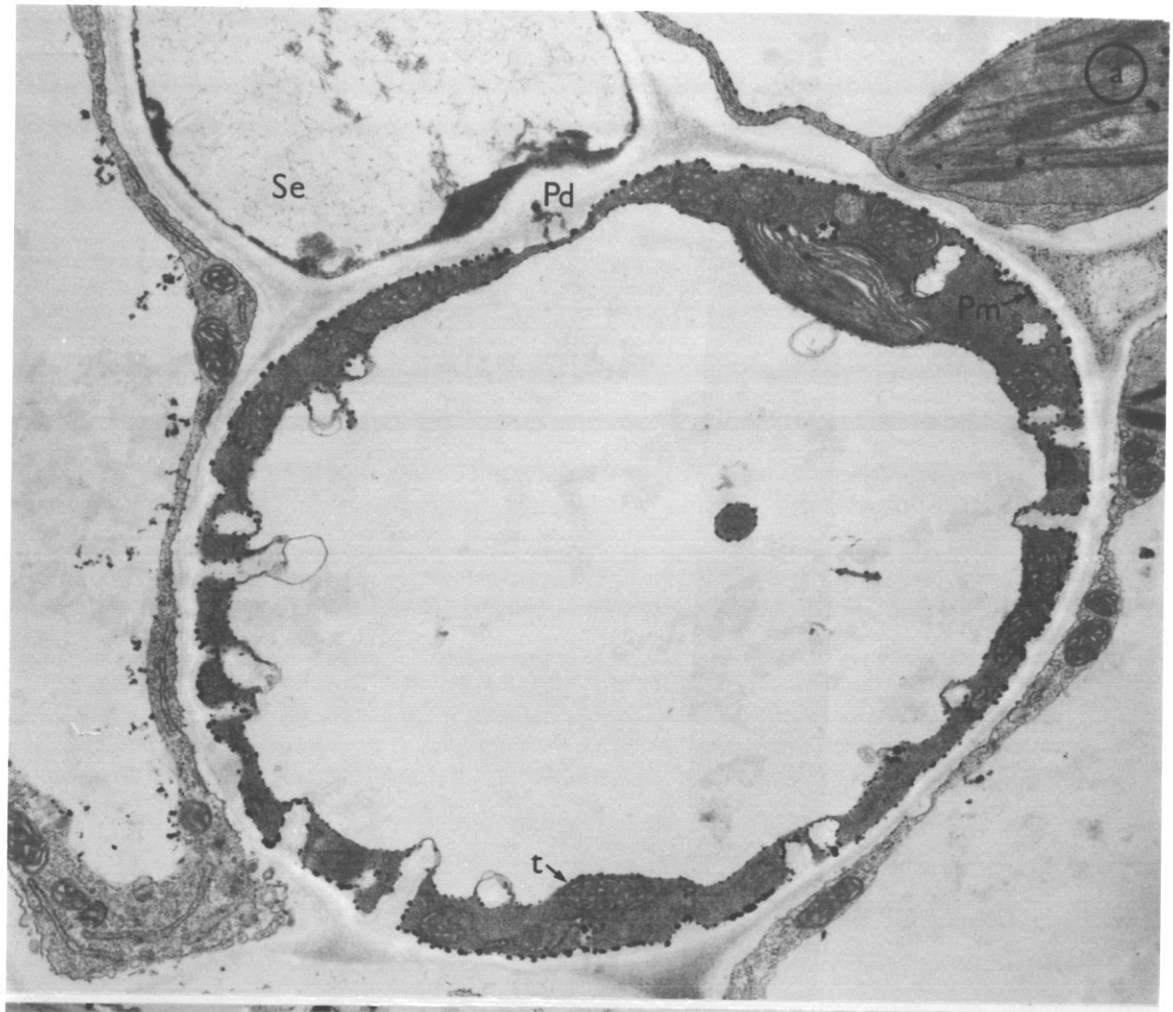

Bs
P
t
t
Se
Bs
Pm
n

Plate 3.7.

a. Section of transfer cell of minor vein in leaf of P. sativum prepared from material incubated with β-GP and Mg^{2+} at pH 7.2. The section was stained with uranyl acetate and lead. Flocculent precipitates indicate enzymic activity at the plasma membrane of the transfer cell (Pm); precipitation at the tonoplast (t) is slight. Plasma membranes of other cells in the minor vein are not active, but precipitates are associated with plasmodesmata (Pd) connecting the transfer cell and sieve element (Se). Neg. no. 11882, x 15,600.

b. Section of transfer cell of minor vein in leaf of P. sativum prepared from material incubated with medium used for plate 3.7a but at pH 5.5 and without Mg^{2+}. Section stained with lead. Precipitates are absent from the plasma membrane of the transfer cell (T) and associated plasmodesmata (Pd). Granular precipitates are particularly associated with the dictyosome (d).
Se = phloem sieve element. Neg no. 10922, x 27,900.


a
Se
Pd
Pm
t

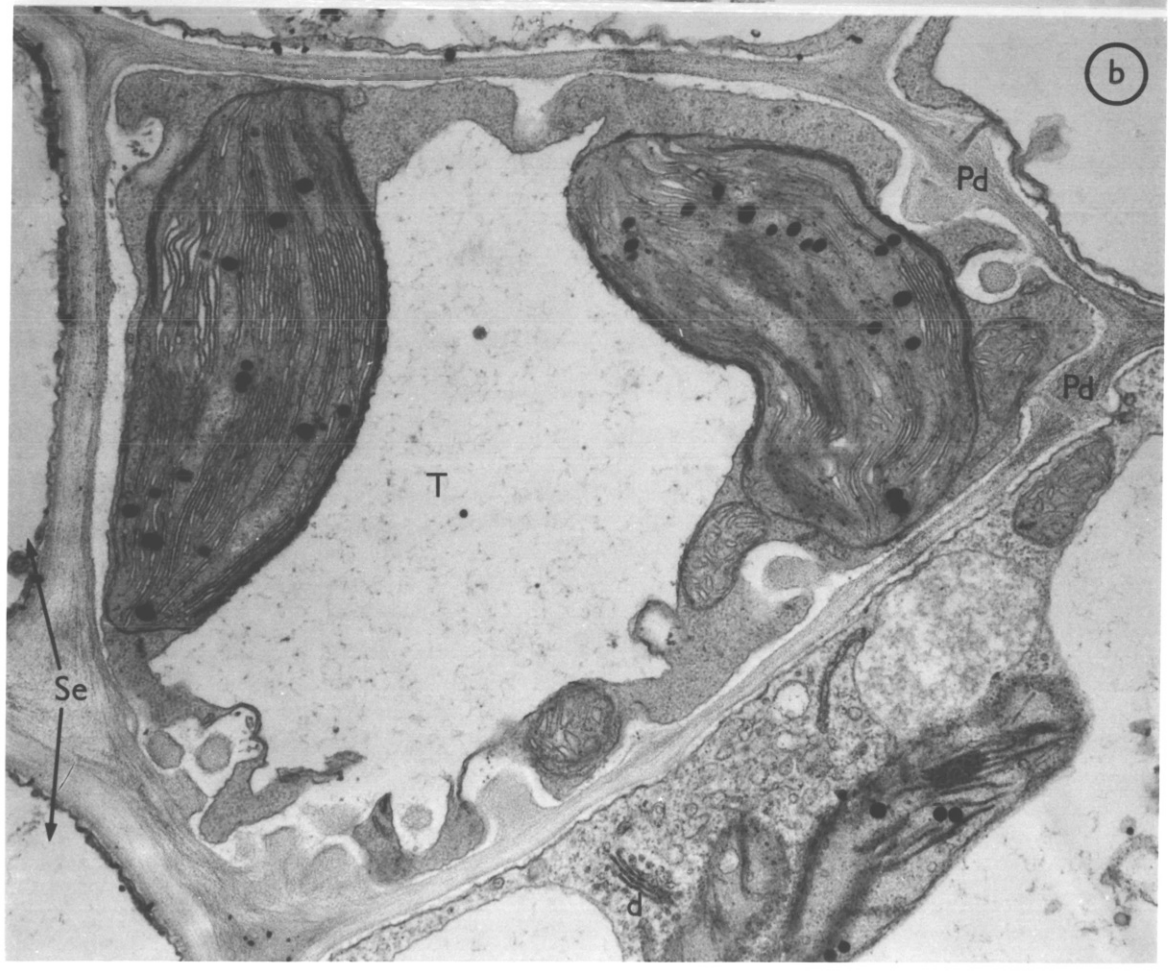

b
Pd
Pd
T
Se
d

Plate 3.8.

Adjacent sections of transfer cell (T) and sieve element (Se) of minor vein in leaf of P. sativum prepared from material incubated with ATP and Mg^{2+} at pH 7.2. a, section not post-stained; b, section stained with uranyl acetate and lead. Flocculent precipitates are especially abundant at the plasma membrane (Pm) of the transfer cell. Precipitates in the cytoplasm are mostly associated with endoplasmic reticulum (er) and cristae of some mitochondria (m). Fine granular precipitates over thylakoids of chloroplasts (Cl) are most easily seen in unstained sections. Neg. no. 11824 and 11570, x 15,600.

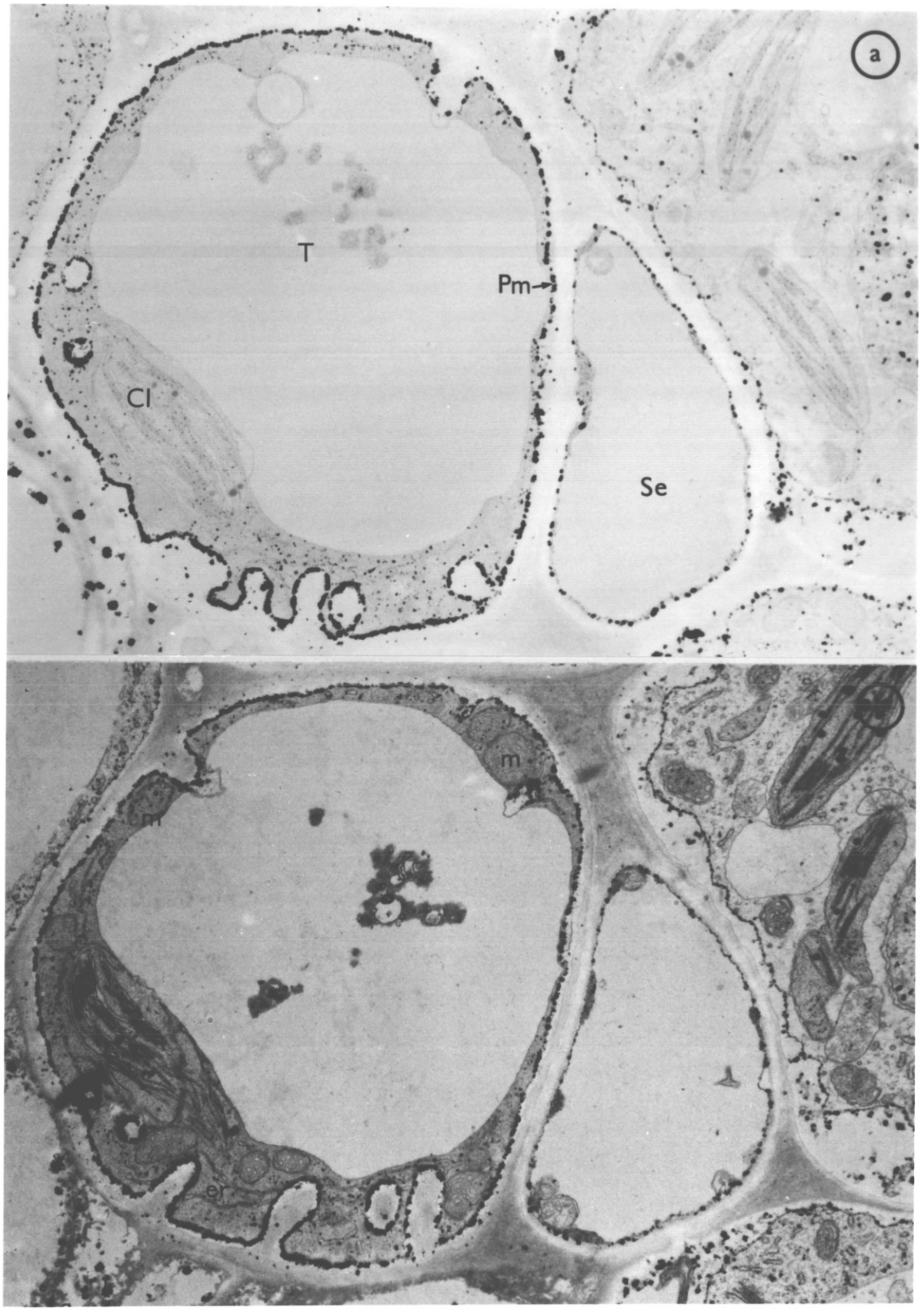

a
T
Pm
Cl
Se
m
m
er

Plate 3.9.

Sections of cells of the upper epidermis and, in b and c, palisade mesophyll in leaves of P. sativum.

a. Section stained with uranyl acetate and lead and prepared from material incubated with ATP and Mg^{2+} (as used for plate 3.9b) but with the addition of NaF (10mM). Flocculent precipitates are infrequent at the plasma membrane (Pm). Granular precipitation is particularly associated with heterochromatin in the nucleus (n) and the cuticle-cell wall (W) interface. v = vacuole. Neg. no. 10656, x 20,100.

b. Section prepared from material prepared as for plate 3.9a but without NaF and stained with lead. Epidermal cell characteristically has large vacuole (v) and thin layer of cytoplasm with small chloroplasts (Cl) adjacent to the cell wall (W). Flocculent precipitates indicate high ATPase activity at the epidermal plasma membrane (Pm); plasma membranes of the mesophyll show lower activities. Neg. no. 11569, x 12,300.

c. Section prepared from material incubated in medium with β-GP and NaF at pH 5.5 and stained with lead. Flocculent precipitates are associated with the vacuole (v) of the mesophyll cell and cristae of mitochondria (m) in the epidermal cells but not with their plasma membranes (Pm). Golgi dictyosomes and vesicles (d) show fine granular precipitates. Neg. no. 10987, x 20,100.

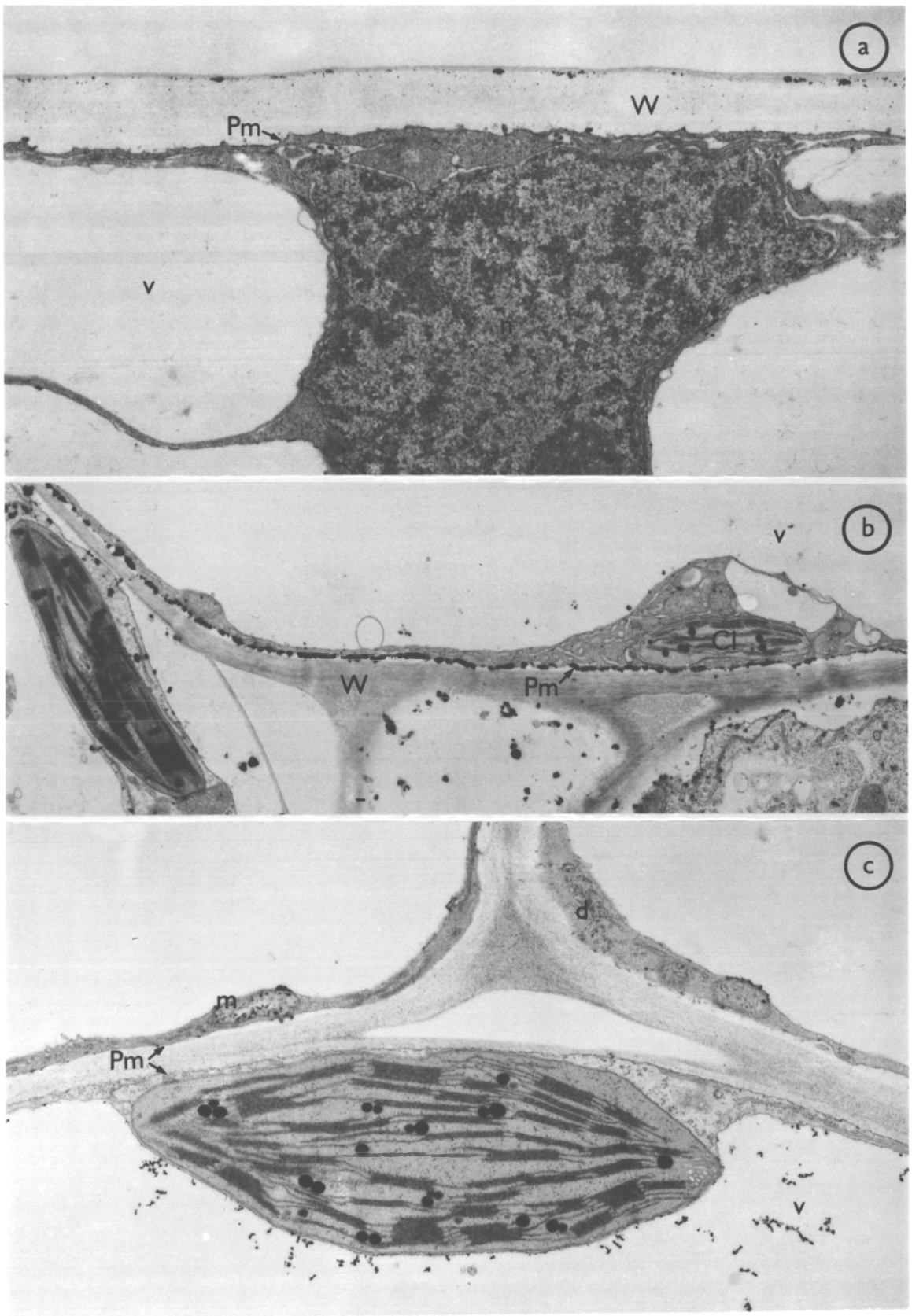

a
W
Pm
v
n
b
v
Cl
W
Pm
c
d
m
Pm
v

Plate 3.10.

a. Section of epidermal cell in leaf of P. sativum infected with Erysiphe pisi prepared from material incubated with β-GP at pH 5.5. Section stained with lead. Dense precipitates indicate enzymic activity at the haustorial plasma membrane of the lobes (hl) and body but no activity is shown at the wall lining (Pm) or extrahaustorial (Em) regions of the host plasma membrane. Ma = extrahaustorial matrix; W = epidermal cell wall. Neg. no. 11438, x 27,900.

b. Section of minor vein in leaf of P. sativum prepared from material incubated with ATP and Mg^{2+} at pH 7.2. Section not post-stained. Flocculent precipitates are most frequent at the plasma membrane of the transfer cell (T) but are also associated with vacuoles (v) and heterochromatin in nuclei (n). Frequent orecipitates characteristically occur throughout areas of cytoplasm that are disrupted (arrowed). P = parenchyma cell; Se = phloem sieve element. Neg. no. 9266, x 7,980.

c. Adjacent section to plate 3.10b, stained with uranyl acetate and lead. At this magnification precipitates are seen associated with plasmodesmata (Pd) and cristae of mitochondria (m) as well as plasma membranes (Pm). n = nucleus. Neg. no. 9263, x 31,300.

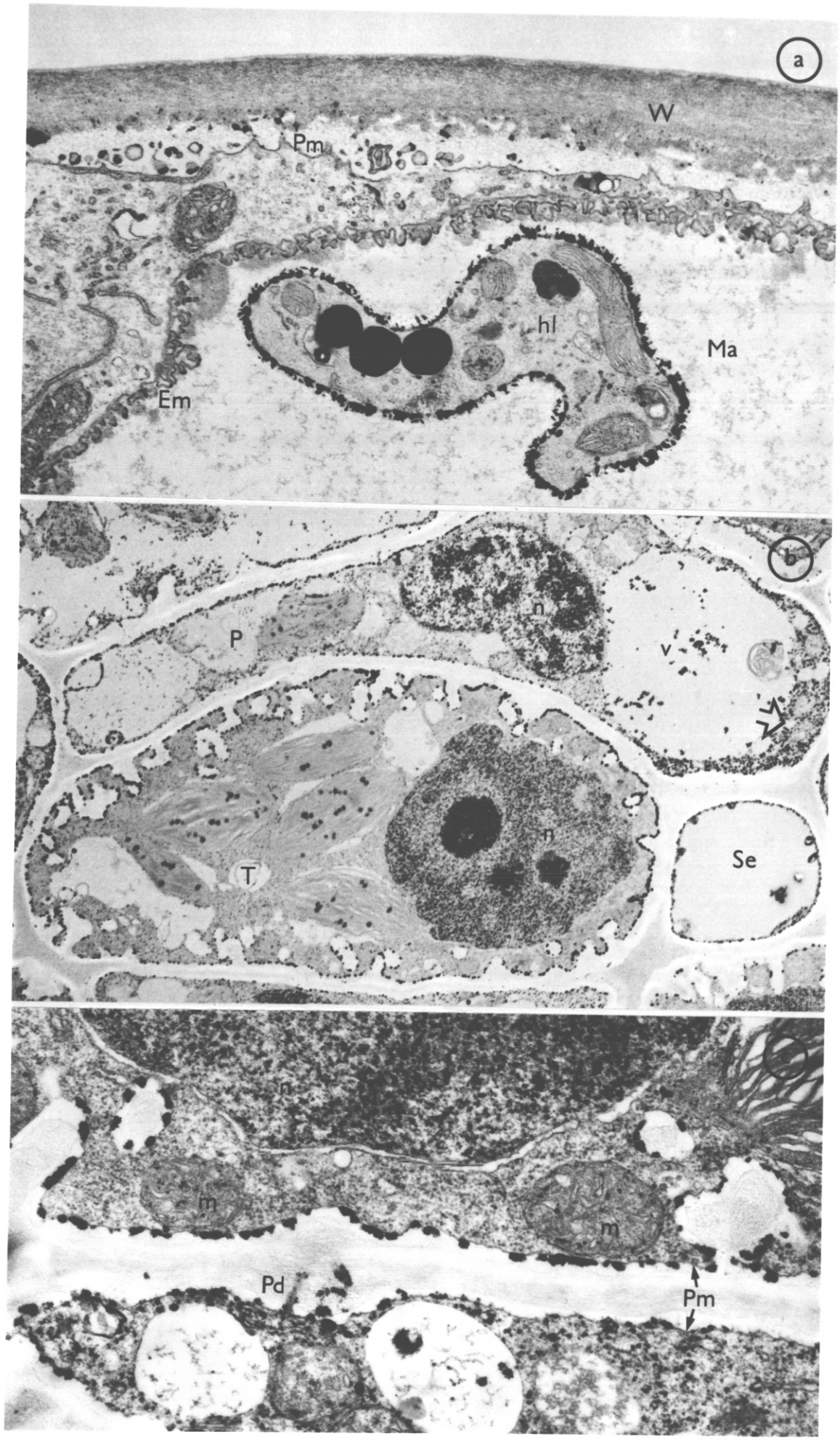

a
W
Pm
hl
Ma
Em
b
n
P
v
n
T
Se
c
n
m
m
Pd
Pm

Plate 3.11.

a. Section of epidermal cell of Pisum sativum infected with Erysiphe pisi prepared from material incubated with medium used for plates 3.12a,b; 3.13 (ATP or β-GP and Mg^{2+} at pH 7.2) but without substrate. The section was stained with lead. Dense osmiophilic staining is shown by the B neck band (B), inclusions in the neck (hn) and haustorial lobes (hl) and some pockets in the extrahaustorial membrane (Em). Fine granular precipitates are present at the cuticle-cell wall boundary (arrow) and in a profile of endoplasmic reticulum (er) in the haustorial neck. A and B = neck bands; ap = appressorium; Ma = extrahaustorial matrix; W = epidermal wall. Neg. no. 13129, x 26,800.

b. Section of epidermal cell of P. sativum infected with E. pisi prepared from material incubated with ATP, Mg^{2+} and NaF at pH 7.2; post-stained with lead. Flocculent precipitates are only associated with the haustorial plasma membrane (hl = haustorial lobe). Em = extrahaustorial membrane; Ma = extrahaustorial matrix. Neg. no. 10231, x 11,500.

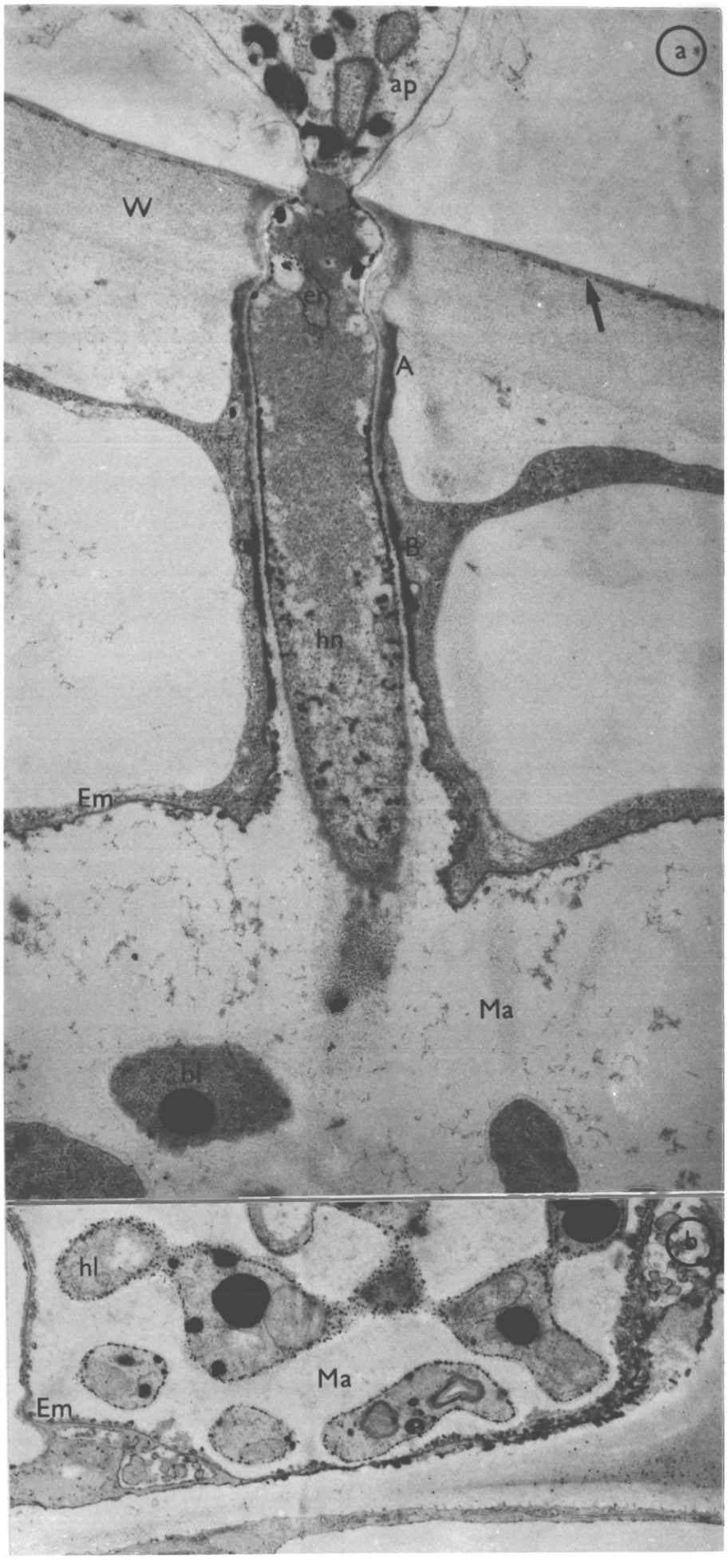

a
ap
W
en
A
B
hη
Em
Ma
hl
b
hl
Ma
Em

Plate 3.12.

a. Section of epidermal cell of Pisum sativum infected with Erysiphe pisi prepared from material incubated with β-GP at pH 7.2. The section was stained with lead. Dense precipitates indicate enzymic activity at the haustorial plasma membrane of the body (hb) and lobes (hl) but no activity is shown at the wall lining (Pm) or extrahaustorial regions (Em) of the host plasma membrane. Fine granular precipitates are present in some profiles of endoplasmic reticulum (er) in the haustorial body. Neg. no. 9536, x 33,800.

b. Section of epidermal cell of Pisum sativum infected by Erysiphe pisi prepared from material incubated with ATP and Mg^{2+} at pH 7.2 and subsequently stained with lead. The epidermal wall (W) is penetrated by the haustorial neck (hn) arising from the appressorium (ap). The septum (s) is perforated (not shown) and the haustorial body (hb) has lobes (hl) seen as separate in the extrahaustorial matrix (Ma). Granular precipitation is particularly frequent at the cuticle-cell wall interface where hyphae are in close proximity with the epidermal cell wall (W). Enzymic activity is indicated by flocculent precipitates at the haustorial plasma membrane in the haustorial lobes, body and adjoining region of the haustorial neck. Neg. no. 9475, x 16,900.

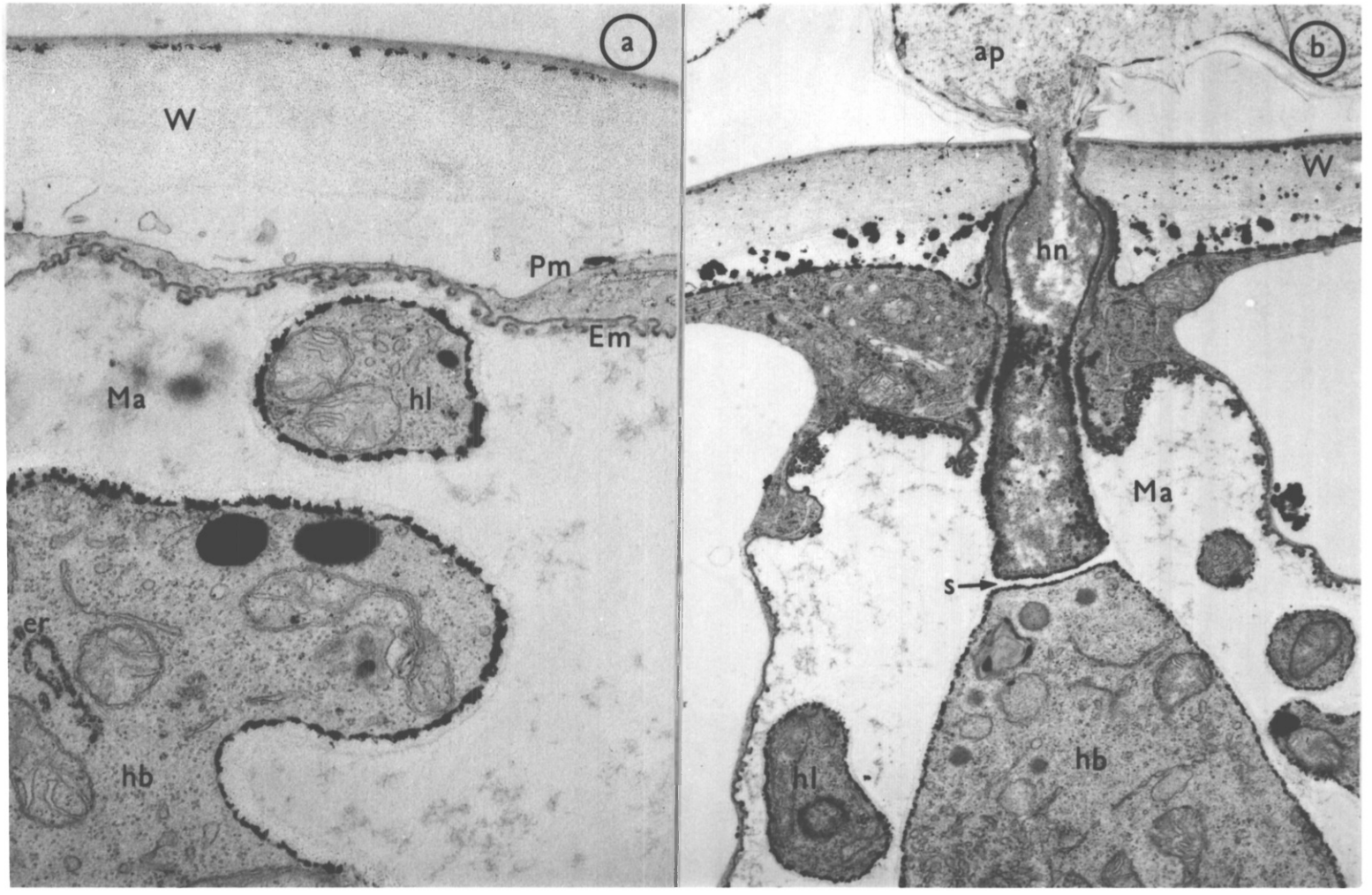

a
W
Pm
Em
Ma
hl
er
hb
b
ap
W
hn
Ma
s
hl
hb

Plate 3.13.

Similar section to plate 3.12b showing that the dense deposits indicating ATPase activity are confined to the wall-lining region of the host plasma membrane (Pm) and are absent from the invaginated domain (Em) surrounding the haustorium. The transition occurs at the point of invagination (arrows). Enzymic activity is also indicated over small islands of membrane (asterisked) sequestered in the collar (C) formed on the host wall (W) around the penetration site. It is absent from the plasma membrane of the upper region of the neck (hn) and the appressorium (ap). A and B = neckbands; Cy = host cytoplasm; Ma = extrahaustorial matrix; pm = plasma membrane; v = host vacuole. Neg. no. 9475, x 172,000.


ap
W
*
C
hn
A
Pm
v
Em
Cy
pm
Ma

Plate 3.14.

a. Section of spongy mesophyll cell of Phaseolus vulgaris infected with Uromyces appendiculatus prepared from material incubated with medium used for plates 3.14b,c, 3.15a,b and 3.16a,b but without substrate or NaF. The section was stained with uranyl acetate and lead. Flocculent precipitation is completely absent from cytoplasms of the host (Cy) and haustorium (hcy). Cl = chloroplast; n = nucleus. Neg. no. 9741, x 14,400.

b. Section of spongy mesophyll cell of P. vulgaris infected with U. appendiculatus prepared from material incubated with ATP, Mg^{2+} and NaF at pH 7.2. The section was stained with lead. The haustorial mother cell (hmc), neck (hn) and body (hb) are sectioned. Dense osmiophilic staining is shown by the neckband (arrowed). Neg. no. 10682, x 11,500.

c. Section of upper epidermal cell of P. vulgaris infected with U. appendiculatus prepared from material incubated with ATP and Mg^{2+} at pH 7.2. Stained with lead. Fine granular precipitates are present in cristae of the mitochondrion (m) in the host cytoplasm. Flocculent precipitates are associated with the tonoplast (t) and vacuole (v) alone. The extrahaustorial membrane (Em) may be invaginated at the point arrowed. hcy = haustorial cytoplasm; Ma = extrahaustorial matrix; pm = haustorial plasma membrane. Neg. no. 10545, x 49,250.

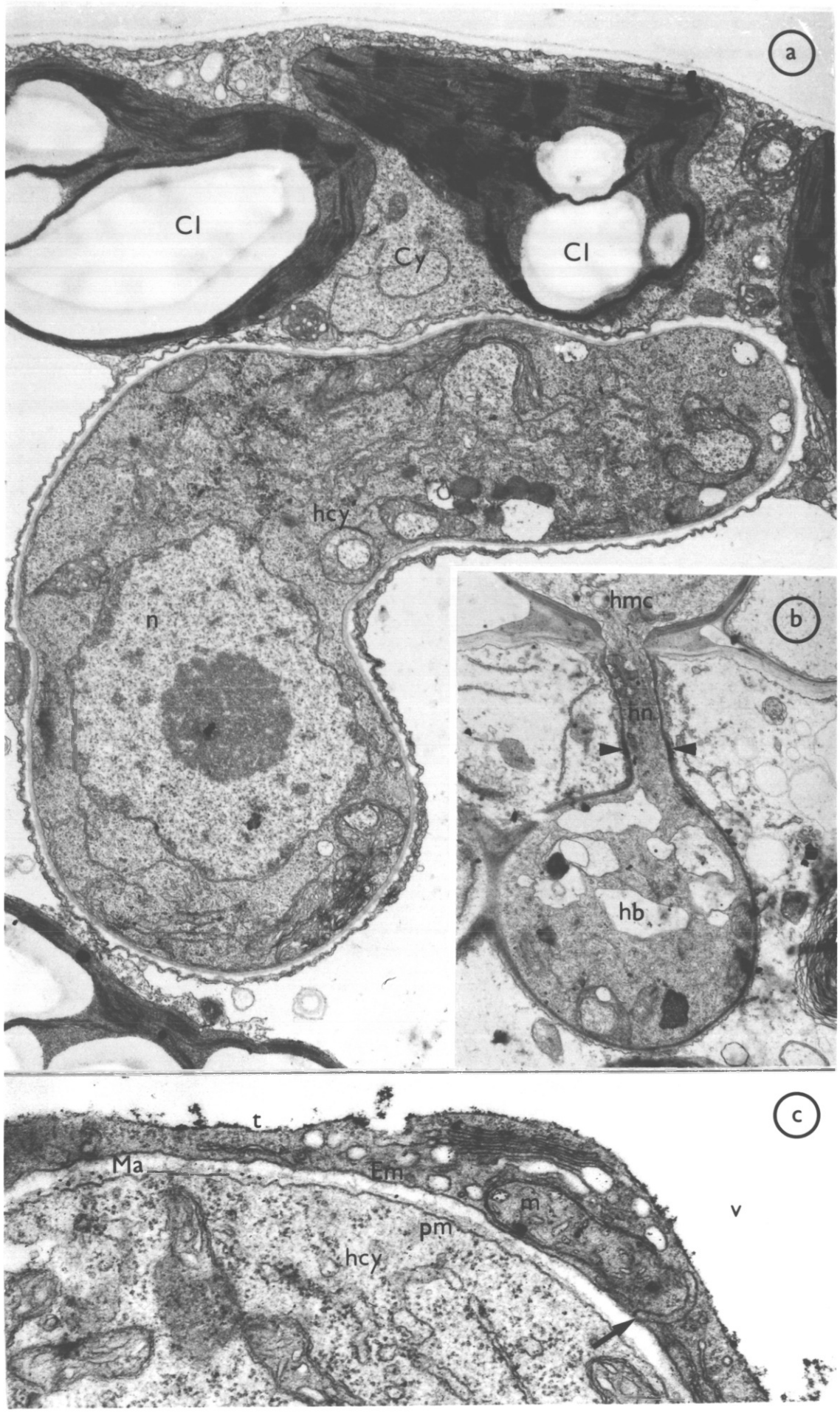

a
Cl
Cy
Cl
hcy
n
b
hmc
hn
hb
c
t
Ma
Em
m
pm
hcy
v

Plate 3.15.

a. Section of spongy mesophyll cell of Phaseolus vulgaris infected with Uromyces appendiculatus prepared from material incubated with ATP and Mg^{2+} at pH 7.2. The section was stained with uranyl acetate and lead. Dense precipitates indicate enzymic activity at the host plasma membrane (Pm) where it lines the cell wall. Precipitates are absent from the extrahaustorial region (Em) of the host plasma membrane and from the haustorial plasma membrane (pm). Invaginations of the extrahaustorial membrane into the host cytoplasm (Cy) are indicated in several places (arrows). hcy = haustorial cytoplasm; Is = intercellular space. Neg. no. 11878, x 37,600.

b. Section of spongy mesophyll cell of P. vulgaris infected with U. appendiculatus prepared from material incubated with β-GP and NaF at pH 7.2. The section was stained with lead. Flocculent precipitates are present in the host nucleus (n) and the outer surface of the cell wall at its boundary with the intercellular space (Is). Granular precipitates are evident in elements of endoplasmic reticulum (er) within the haustorial cytoplasm (hcy). Neg. no. 10697, x 27,900.

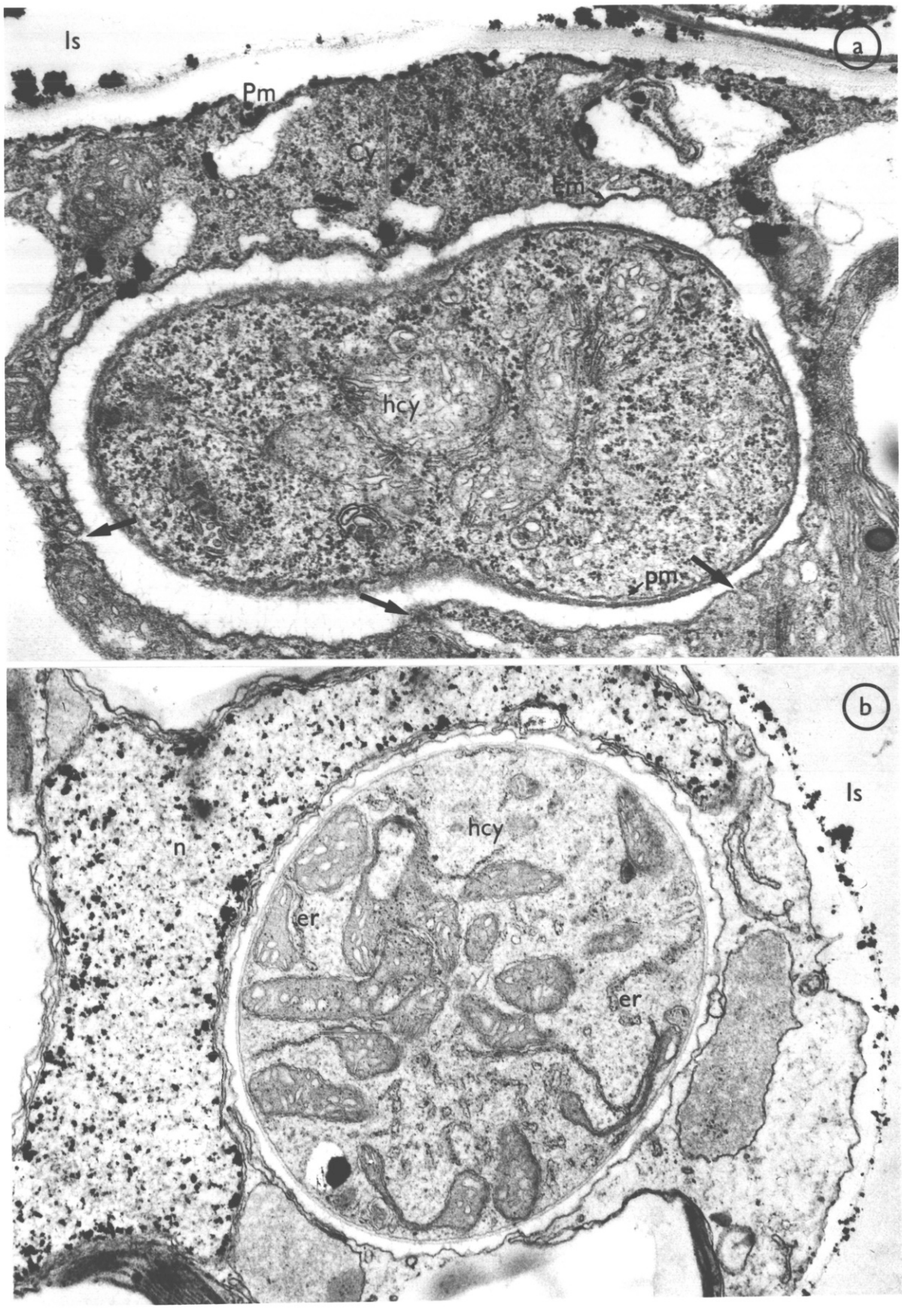

ls
Pm
cy
a
hcy
pm
b
ls
n
hcy
er
er

Plate 3.16.

Serial sections of the neck of an haustorium of Uromyces appendiculatus infecting a mesophyll cell of Phaseolus vulgaris. The material was prepared as for plate 3.15a. Dense precipitates indicating enzymic activity occur at the host plasma membrane (Pm) adjacent to the host wall (W) and in the region over the haustorial neck as far as the neckband (limits arrowed, a). Precipitate is absent from the rest of the extrahaustorial membrane (Em) and from the haustorial and mother cell (hmc) plasma membranes. Note the large frequent precipitates over the plasma membrane of the epidermal cell at the top right of plate 3.16a. Flocculent precipitates are also present in the intercellular space (Is) over cell walls of the haustorial mother cell and host. Granular precipitation occurs throughout the host cell walls (W). a, neg. no. 10533, x 36,250. b, neg. no. 10536, x 54,000.

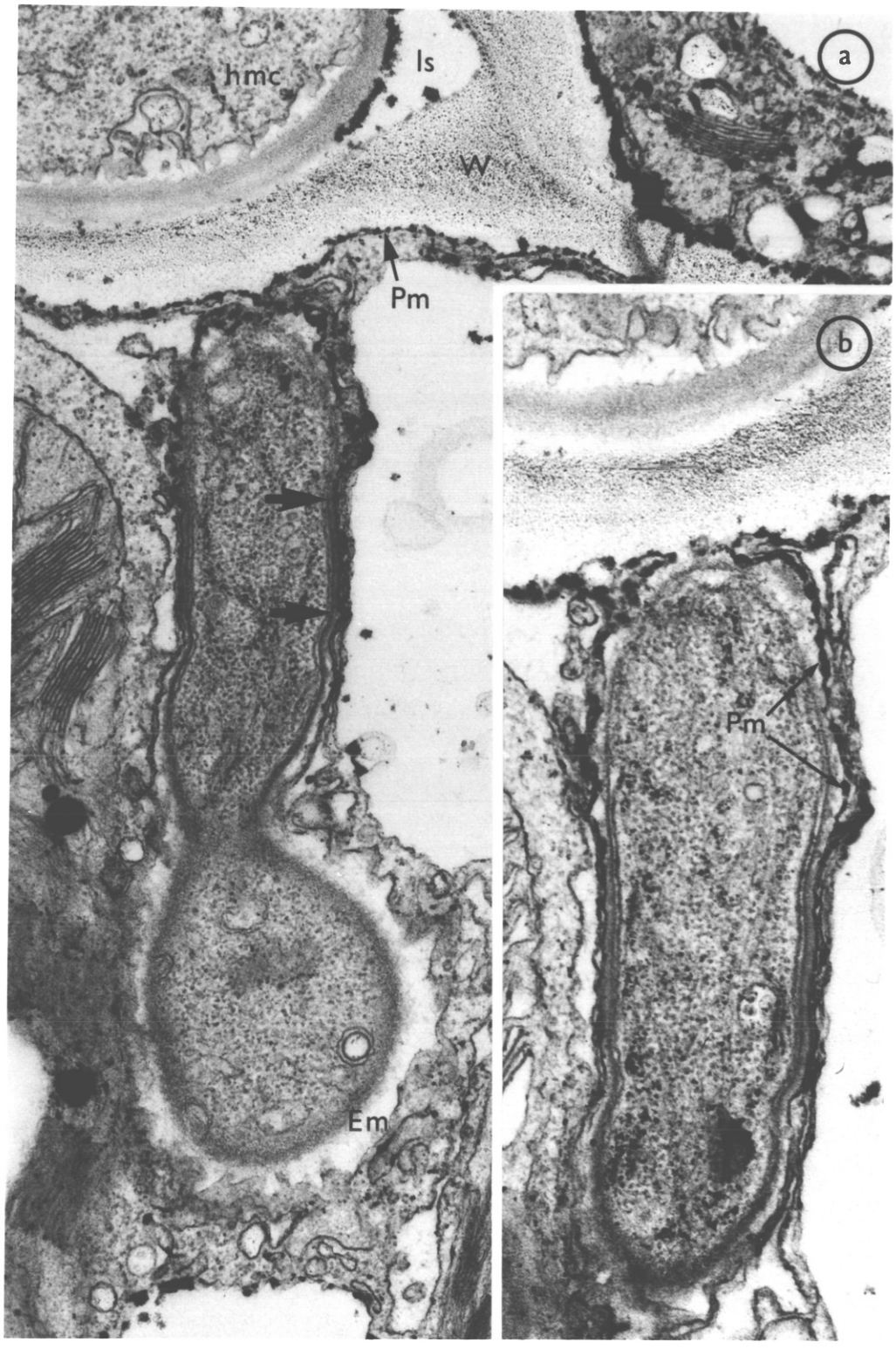

hmc
ls
a
W
Pm
b
Pm
Em

Plate 3.17.

a. Section of mesophyll cell of Pisum sativum infected with Peronospora pisi prepared from material incubated with ATP and Mg^{2+} at pH 7.2 (as used for plate 3.17b) with addition of NaF (10mM). Section post-stained with uranyl acetate and lead. Electron dense precipitates seem to be crystalline and are associated with the plasma membrane (pm) of the haustorial neck and the haustorial mother cell (hmc). No precipitates are located at the plasma membrane of the host cell (Pm). The host cell wall extends as a collar (C) around the point of penetration and along the haustorial neck. Neg. no. 11886, x 20,100.

b. Section of mesophyll cell of Pisum sativum infected with Peronospora pisi prepared from material incubated as for plate 3.17a but without NaF. Stained with lead. Precipitates are typically absent from the wall lining (Pm) and extrahaustorial (Em) regions of the host plasma membrane. Crystalline precipitates are only infrequently associated with the haustorial plasma membrane (pm) and the extrahaustorial matrix (Ma). Neg. no. 11566, x 27,900.

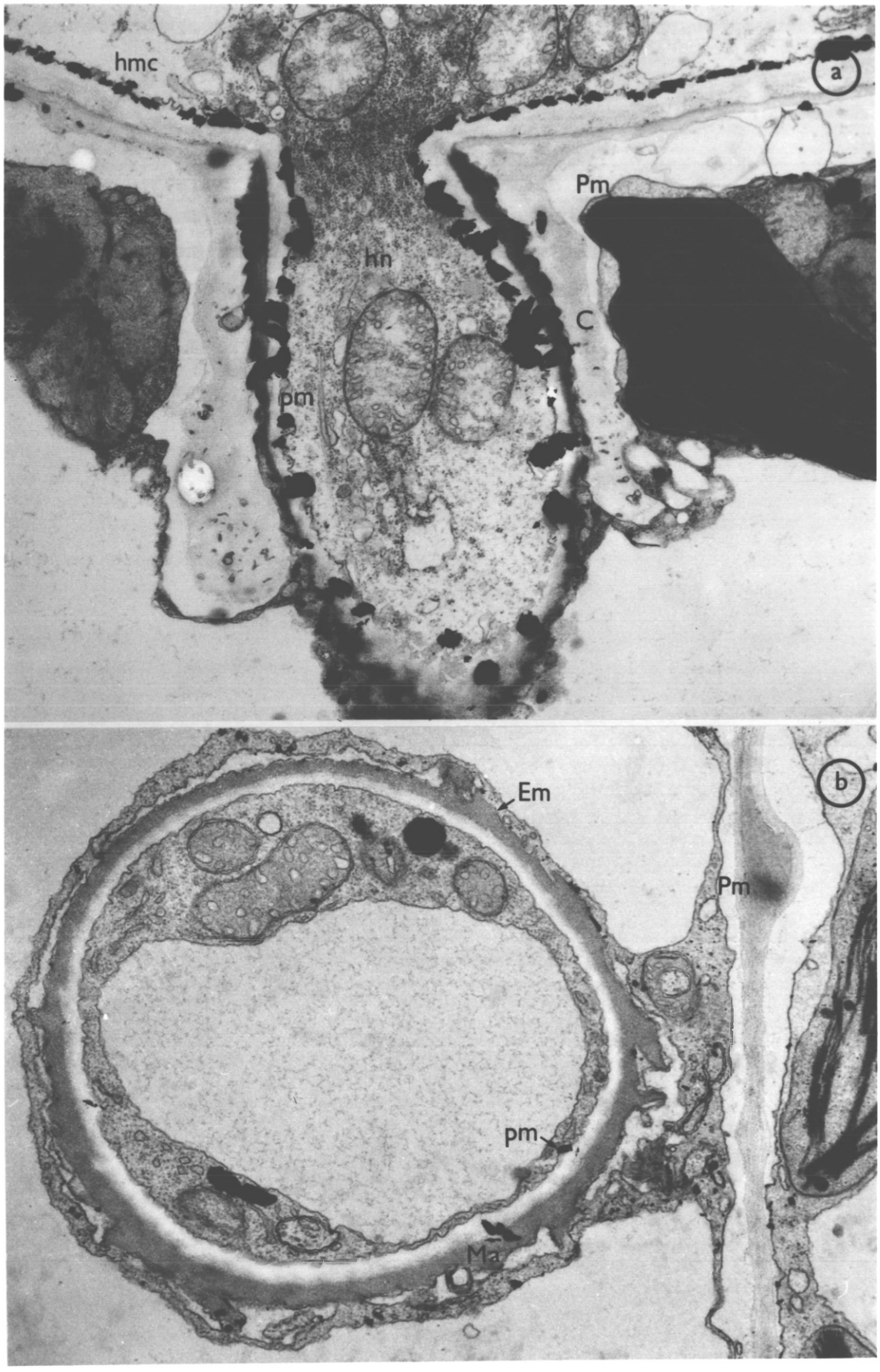

hmc
a
Pm
hn
C
pm
Em
b
Pm
pm
Ma

Plate 3.18.

Sections of necrotic haustorium in mesophyll cell of *P. sativum* infected with *P. pisi* prepared as for plate 3.17b but stained with uranyl acetate and lead. The haustorium (h) has a compressed appearance and its cytoplasm (hcy) is osmiophilic and necrotic. The haustorium and associated structures are encased by an electron lucent deposit (*) which is attached to the host cell wall and contains small islands of membrane; its appearance is similar to the collar around the necks of haustoria (plate 3.17a). Dense crystalline precipitates are distributed over the haustorium and encasing material but are infrequent over the host cytoplasm (Cy). a, neg. no. 11880, x 27,900. b, neg. no. 11879, x 8,850.

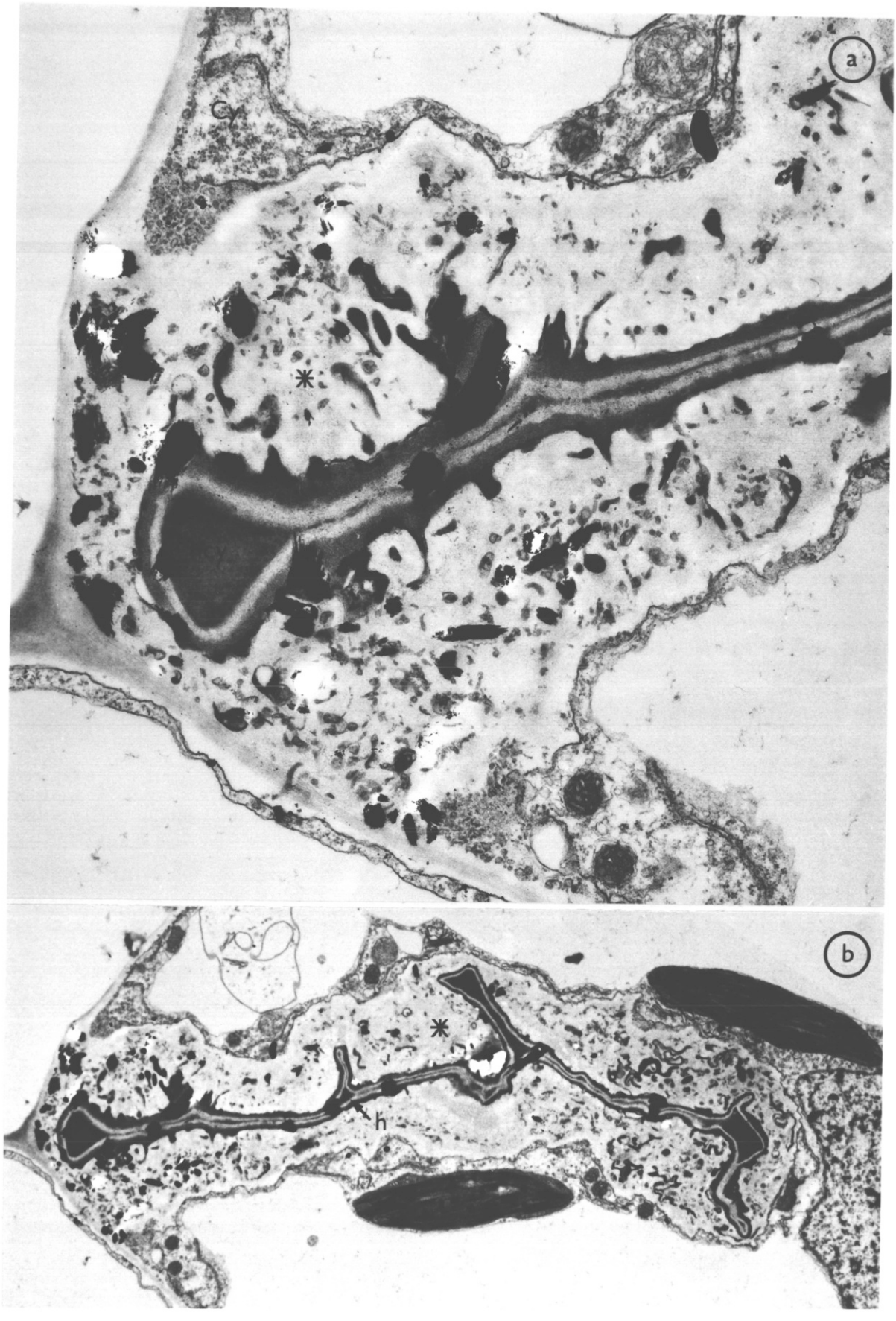

a
Cy
*
b
*
h

Plate 3.19.

a and b. Adjacent sections of epidermal cell of Hordeum vulgare infected with Erysiphe graminis prepared from material incubated with ATP, Mg^{2+} and NaF at pH 7.2. Sections stained with lead. Specific sites of phosphatase activity cannot be distinguished in the epidermal cell as precipitates occur throughout the cytoplasm (Cy) which is disorganised and lines the cell wall (W) and extra-haustorial membrane (Em). Cytoplasms of haustorial lobes (hl) and body (not shown) are well preserved but there is no evidence for phosphatase activity at their plasma membranes (pm) or elsewhere in the cytoplasm (hcy). Similar results were obtained without NaF. Ma = extra-haustorial matrix. a, neg. no. 13122, x 15,400; b, neg. no. 13123, x 48,600.

c. Section of epidermal and mesophyll cells in peel removed with forceps from stem of Pisum sativum infected with Erysiphe pisi. The peel was incubated in medium with ATP and Mg^{2+} at pH 7.2 and sections post-stained with uranyl acetate and lead. The plasma membrane of the epidermal cell (Pm) is fragmented and the cytoplasm of the underlying mesophyll cell (Cy) disorganised. Electron dense precipitates occur throughout the cytoplasms of both cells. Neg. no. 7751, x 20,100.

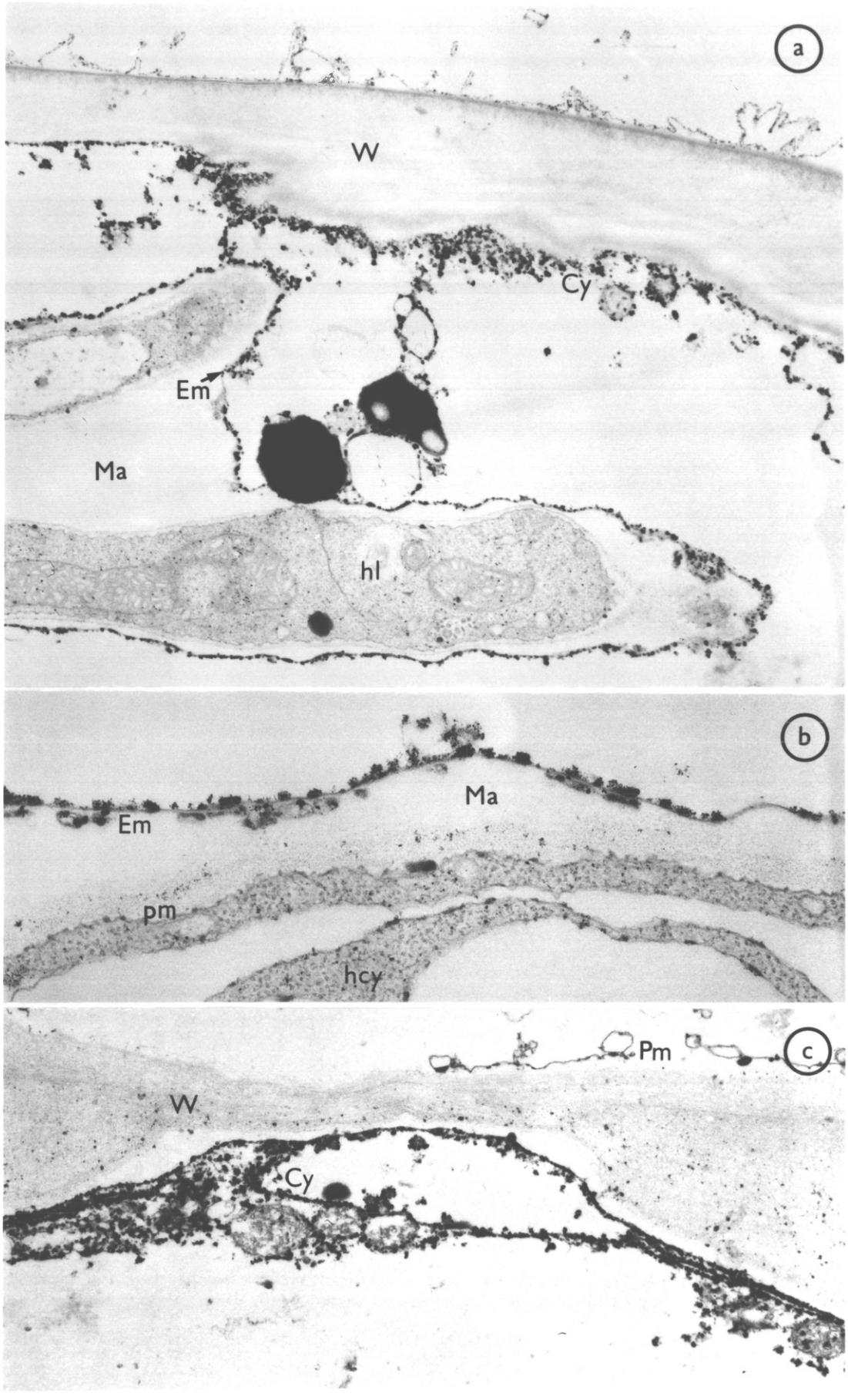

a
W
Cy
Em
Ma
hl
b
Ma
Em
pm
hcy
c
Pm
W
Cy

Plate 3.20.

a. Section of mesophyll and epidermal cells of Hordeum vulgare prepared from material incubated with medium used for plate 3.19a, b but without substrate. Section stained with uranyl acetate and lead. The cytoplasm of the epidermal cell (Cy) is disorganised; although the tonoplast (t) is frequently disrupted the plasma membrane (Pm) is mostly intact. In contrast, cytoplasm of the mesophyll cell (Cl = chloroplast) is well preserved. Neg. no. 13124, x 27,200.

b, c. Sections of cuticle isolated by enzymic digestion from upper epidermal cells of leaf of Pisum sativum. Sections stained with uranyl acetate and lead. The upper surface of the cuticle (Ct) is identified by the outlines of wax crystals in b. The lower surface has a less smooth edge; the projection (plate 3.20c) shows the only recorded deviation in its otherwise uniform appearance. b, neg. no. 8357, x 20,100; c, neg. no. 8361, x 49,250.

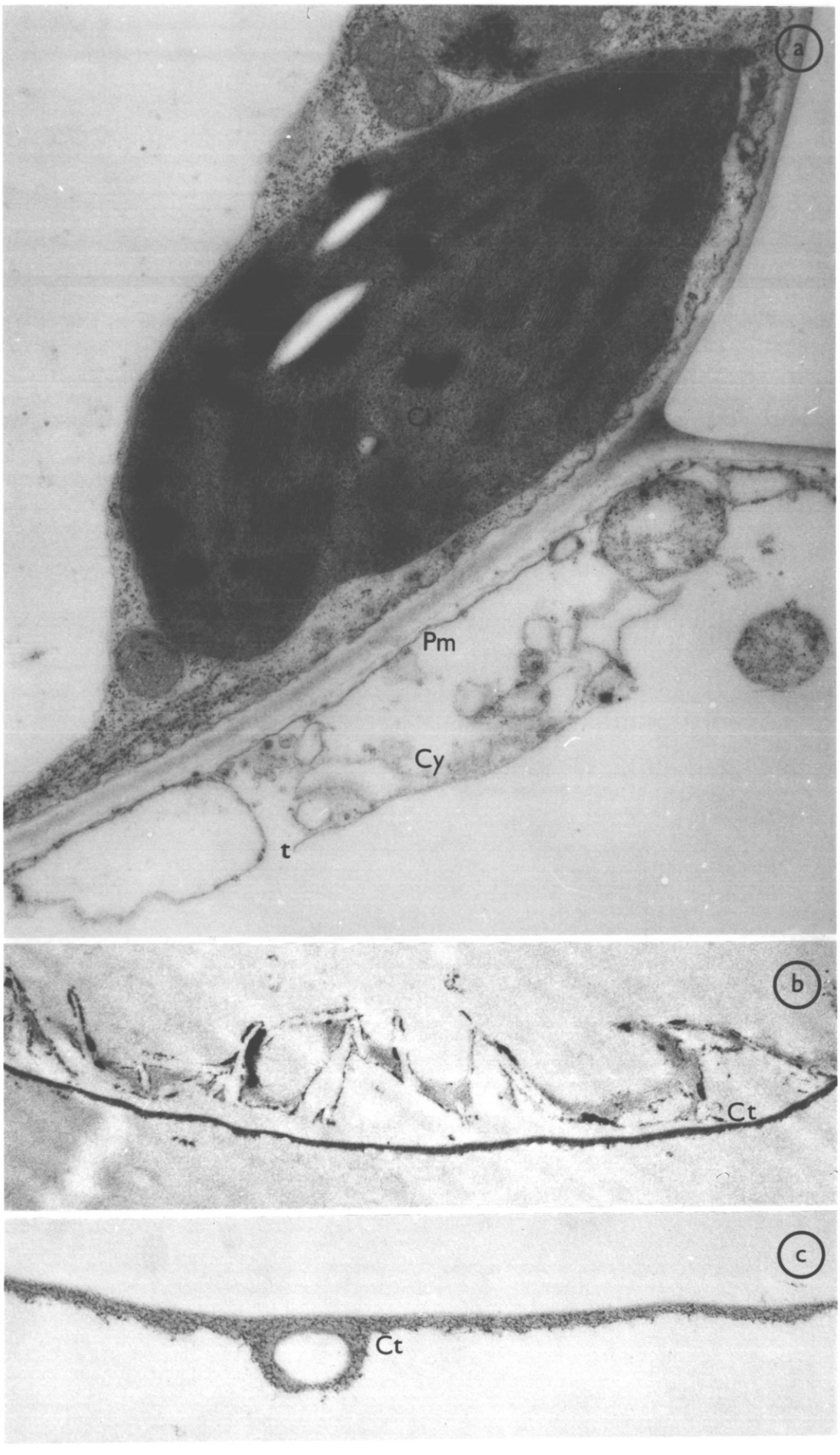

a
Pm
Cy
t
b
Ct
c
Ct

Plate 3.21.

Light micrographs of epidermes peeled from leaves (a) and stems (b,c,d,e,f) of Pisum sativum uninfected or infected with Erysiphe pisi. Viewed with bright field optics.

a. Epidermis from lower surface of uninfected leaf. The specimen was floated on an aqueous solution of neutral red (0.005% w/v) for 5-10 min. and then mounted on a microscope slide in 0.8M KCl. Stomatal guard cells alone have accumulated neutral red and plasmolysed. Neg. no. 1.9, x 800.

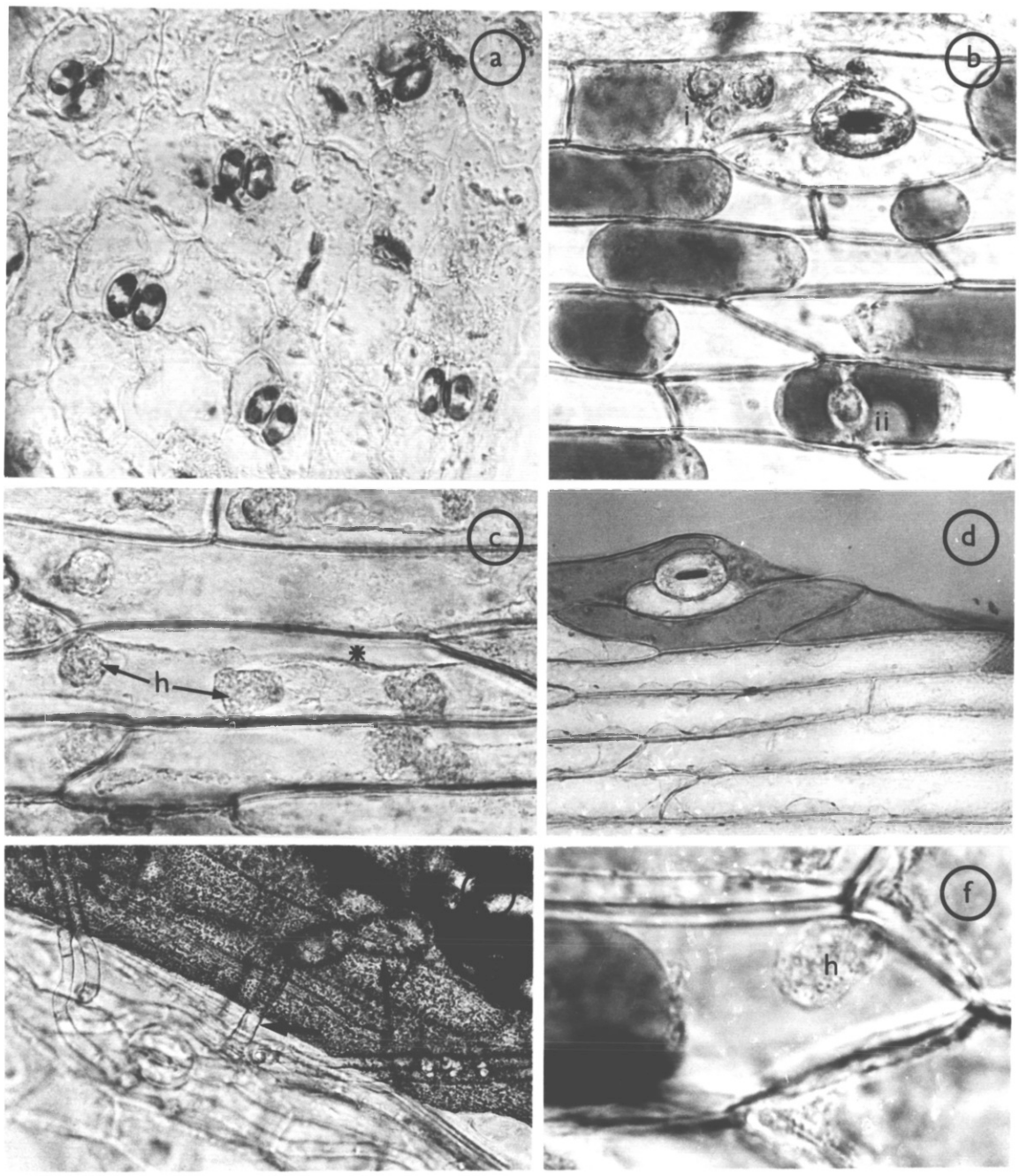
b. Epidermis from infected stem prepared as in (a). Protoplasts of cells containing haustoria (i) usually did not accumulate neutral red or plasmolyse to the same extent as in the uninfected condition. The infected cell (ii) which has accumulated neutral red and plasmolysed is atypical. Neg. no. 6.9, x 800.

c. Epidermis from infected stem; untreated. The space (asterisk) between protoplast and cell wall was typical in cells of this tissue. h = haustorium. Neg. no. 2.5, x 800.

d. Epidermis from uninfected stem; mounted in Evans blue. The stain is excluded from cells with intact plasma membranes. Neg. no. 3.3, x 800.

e. Upper surface of peel of epidermis and mesophyll ten days after removal from uninfected stem; the peel was floated on distilled water immediately after preparation and inoculated with conidia of E. pisi. The conidiophore (arrows) and associated hyphae indicate that infection has been established. Note stippled appearance due to surface waxes of cells in top right portion of micrograph. Neg. no. 5.5, x 800.

f. Epidermis from infected stem prepared as in (a). Unique observation of haustorium (h) detatched from the protoplast of the epidermal cell after plasmolysis. Neg. no. 4.7, x 2000.


a
b
i
ii
c
h
d
f
h

Appendix.

Purity of glutaraldehyde used for phosphatase cytochemistry.

Glutaraldehyde solutions (see Materials and Methods, section 6.1) were examined spectrophotometrically (see figure below) and relative purities estimated by comparing the purification indices calculated from the ratio of absorbance at 235 nm to that at 280 nm (Anderson, 1967). Impurities are associated with an absorption peak at 235 nm and low purification indices are therefore indicative of high purity.

The Taab and EM - scope glutaraldehyde solutions were impure with purification indices of 4.18 and 2.31 respectively. In contrast the index for the glutaraldehyde supplied by Polysciences was 0.26 and this solution was selected as the preferential fixative for phosphatase cytochemistry.

Appendix figure Absorption spectra of glutaraldehyde solutions; A, Taab (EM-grade), 0.8 % (v/v); B, EM-Scope (Ultra-pure), 1.3 % (v/v); C, Polysciences (EM-grade), 8 % (v/v). Concentrations represent the product of dilution factor and concentration as given by the supplier.

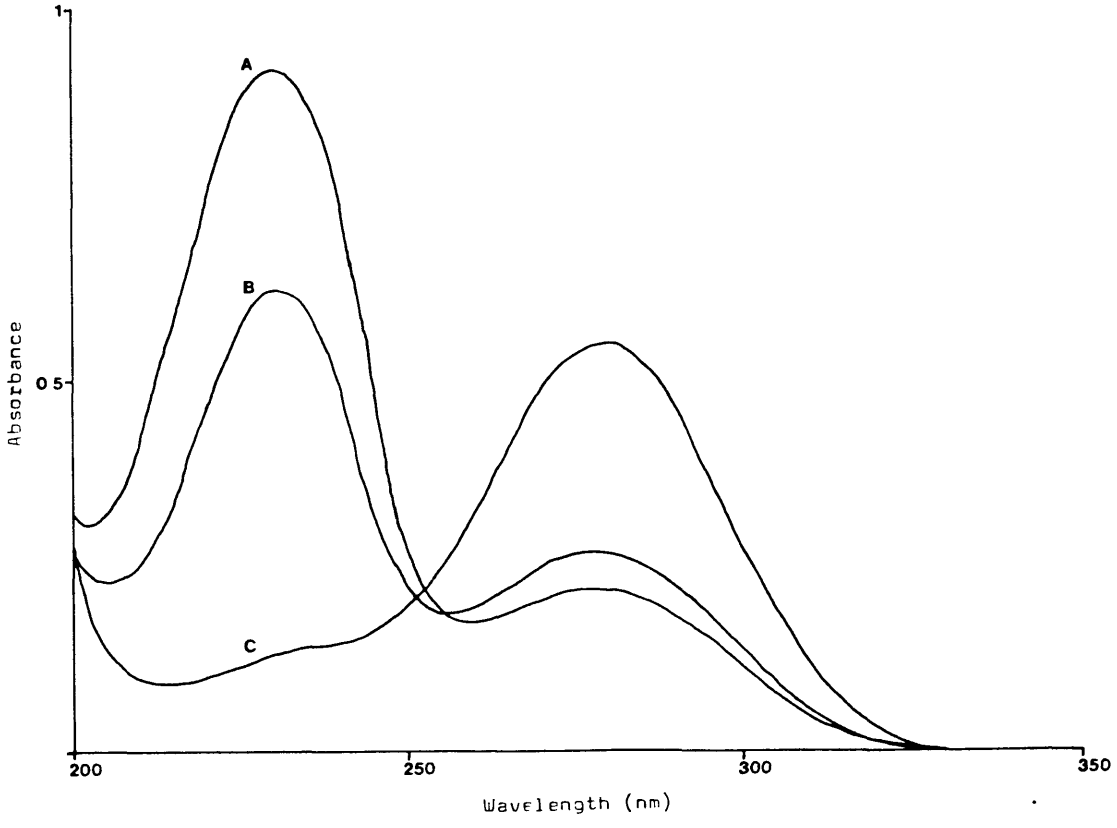


Plate labels.

A = A band
ap = appressorium
B = B band
Bs = bundle sheath cell
C = collar
Cl = chloroplast
Ct = cuticle
Cy = higher plant cytoplasm
cy = fungal cytoplasm
d = dictyosome
Em = extrahaustorial membrane
er = endoplasmic reticulum
h = haustorium
hb = haustorial body
hc = haustorial complex
hcy = haustorial cytoplasm
Hhc = healthy haustorial complex
hmc = haustorial mother cell
hl = haustorial lobe
hn = haustorial neck
hw = haustorial wall
hy = hypha
Is = intercellular space
l = lipid droplet
m = mitochondrion
Ma = extrahaustorial matrix
n = nucleus
Nhc = necrotic haustorial complex
P = parenchyma cell
Pd = plasmodesmata
Phc = pre-necrotic haustorial complex
Pm = host/higher plant plasma membrane
pm = fungal plasma membrane
s = septum
Se = phloem sieve element
T = transfer cell
t = tonoplast
v = vacuole
W = host/higher plant cell wall
w = fungal cell wall
Xy = xylem vessel

REFERENCES.

Abu-Zinada, A.-A. H., Cobb, A. & Boulter, D. (1975). An electron-microscopic study of the effects of parasite interaction between Vicia fabae L. and Uromyces fabae. Physiological Plant Pathology, 5, 113 - 118.

Al-Khesraji, T. O., Losel, D. M. & Gay, J. L. (1980). The infection of vascular tissue in leaves of Tussilago forfara L. by pycnial-aecial stages of Puccinia poarum Niel. Physiological Plant Pathology, 17, 193 - 197.

Allen, T. D. & Haigh, M. V. (1973). Ultrastructural changes in Osmunda regalis prothalli induced by X-irradiation. Journal of Ultrastructural Research, 42, 108 - 120.

Amelunxen, F. & Gronau, G. (1969). Untersuchugen an den Gerbstoffzellen der Niederblätter von Acorus calamus L. Cytobiologie, 1, 58 - 69.

Anderson, J. W. (1968). Extraction of enzymes and subcellular organelles from plant tissues. Phytochemistry, 7, 1973 - 1988.

Anderson, P. J. (1967). Purification and quantitation of glutaraldehyde and its effect on several enzyme activities in skeletal muscle. Journal of Histochemistry and Cytochemistry, 15, 652 - 661.

Andrews, J. H. (1975). Distribution of label from ^{3}H-glucose and ^{3}H-leucine in lettuce cotyledons during early stages of infection with Bremia lactucae. Canadian Journal of Botany, 53, 1103 - 1115.

Arborgh, B., Ericsson, J. L. F. & Helminen, H. (1971). Inhibition of renal acid phosphatase and aryl sulfatase activity by glutaraldehyde fixation. Journal of Histochemistry and Cytochamistry, 19, 449 - 451.

Atkinson, T. G. & Shaw, M. (1955). Occurence of acid phosphatase in association with the haustoria of powdery mildew on barley. Nature, 175, 993 - 994.

Ayres, P. G. (1976). Patterns of stomatal behaviour, transpiration, and CO_2 exchange in pea following

infection by powdery mildew (Erysiphe pisi). Journal of Experimental Botany, 27, 1196 - 1205.

Ayres, P. G. (1978). Water relations of diseased plants. In: Water deficits and plant growth, vol. 2 (Ed. T. T. Kozlowski), pp. 1 - 60. Academic Press; London, New York.

Bachmann, L. & Salpeter, M. M. (1965). Autoradiography with the electron microscope : A quantitative evaluation. Laboratory Investigation, 14, 1041 - 1053.

Bailey, J. A. (1970). Pisatin production by tissue cultures of Pisum sativum L. Journal of General Microbiology, 61, 407 - 415.

Baker, D. A. (1978). Proton co-transport of organic solutes by plant cells. New Phytologist, 81, 485 - 497.

Balke, N. E. & Hodges, T. K. (1975). Inhibition of plasma membrane ATPase by phenolics. Plant Physiology, 56, 5 - 41.

Balke, N. E. & Hodges, T.K. (1979). Inhibition of adenosine triphosphatase activity of the plasma membrane fraction of oat roots by diethylstilbestrol. Plant Physiology, 63, 48 - 52.

Barka, T. & Anderson, P. J. (1962). Histochemical methods for acid phosphatase using hexazonium pararosanilin as coupler. Journal of Histochemistry and Cytochemistry, 10, 741 - 753.

Barnabas, A. D., Butler, V. & Steinke, T. D. (1982). Zostera capensis Setchell: III. Some aspects of wall ingrowth development in leaf blade epidermal cells. Protoplasma, 110, 87 - 94.

Bate-Smith, E. C. & Lerner, N. H. (1954). Leuco-anthocyanins. 2. Systematic distribution of leuco-anthocyanins in leaves. Biochemical Journal, 58, 126 - 132.

Bate-Smith, E. C. & Metcalfe, L. S. (1957). Leuco-anthocyanins. 3. The nature and systematic distribution of tannins in dicotyledonous plants. Journal of the Linnean Society of Botany, 55, 669 - 705.

Baur, P. S. & Walkinshaw, C. H. (1973). Fine structure of tannin accumulations in callus cultures of Pinus elliotti (slash pine). Canadian Journal of Botany, 52, 615 - 619.

Beakes, G. W., Singh, H. & Dickinson, C. H. (1982). Ultrastructure of the host - pathogen interface of Peronospora viciae in cultivars of pea which show different susceptibilities. Plant Pathology, 31, 343 - 354.

Beckman, C. H. & Mueller, W. C. (1970). Distribution of phenols in specialised cells of banana roots. Phytopathology, 60, 79 - 82.

Beckman, C. H., Mueller, W. C. & McHardy, W. E. (1972). The localization of stored phenols in plants hairs. Physiological Plant Pathology, 2, 69 - 74.

Beffagna, N., Cocucci, S. & Marre, E. (1977). Stimulating effect of fusicoccin on K-activated ATPase in plasmalemma preparations from higher plant tissues. Plant Science Letters, 8, 91 - 98.

Bell, A. A. (1981). Biochemical mechanisms of disease resistance. Annual Review of Plant Physiology, 32, 21 - 81.

Bell, A. A. & Daly, J. M. (1962). Assay and partial purification of self-inhibitors of germination from uredospores of the bean rust fungus. Phytopathology, 52, 261 - 266.

Bentwood, B. J. & Cronshaw, J. (1978). Cytochemical localization of adenosine triphosphatase in the phloem of Pisum sativum and its relation to the function of transfer cells. Planta, 140, 111 - 120.

Bergeron, J. J. M., Sikstrom, R., Hand, A. R. & Posner, B. I. (1979). Binding and uptake of ^{125}I-insulin into rat liver hepatocytes and endothelium. An in vivo radio-autographic study. Journal of Cell Biology, 80, 427 - 443.

Blumer, S. (1967). Echte Mehltaupilze (Erysiphaceae). Fischer Verlag; Jena.

Boughey, A. S. (1949). The ecology of fungi which cause economic plant diseases. Transactions of the British Mycological Society, 32, 179 - 189.

Bowles, D. J., Quail, P. H., Marre, D. J. & Hartman, G. C. (1979). Use of markers in plant - cell fractionation. In: Methodological surveys: Biochemistry, vol. 9. Plant organelles. (Ed. E. Reid), pp. 207 - 223. Ellis Horwood; Chichester.

Bracker, C. E. (1968). Ultrastructure of the haustorial apparatus of Erysiphe graminis and its relationship to the epidermal cell of barley. Phytopathology, 58, 12 - 30.

Bracker, C. E. & Littlefield, L. J. (1973). Structural concepts of host - pathogen interfaces. In: Fungal pathogenicity and the plants'response (Eds. R. J. W. Byrde & C. V. Cutting), pp. 159 - 318. Academic Press; London.

Brocklehurst, R., Gardner, D. & Eddy, A. A. (1977). The absorption of protons with ∝-methyl glucoside and ∝-thioethyl glucoside by the yeast N.C.Y.C. 240. Biochemical Journal, 162, 591 - 599.

Brown, F. G. (1968). Pests and diseases of forest plantation trees. Clarendon Press; Oxford.

Browning, A. J., Hall, J. L. & Baker, D. A. (1980). Cytochemical localization of ATPase activity in phloem tissues of Ricinus communis. Protoplasma, 104, 55 - 65.

Budd, G. C. & Pelc, S. R. (1964). The membrane method of electron microscope autoradiography. Stain Technology, 39, 295 - 302.

Burchill, R. T. (1978). Powdery mildews of tree crops. In: The powdery mildews (Ed. D. M. Spencer), pp. 473 - 493. Academic Press; London, New York, San Francisco.

Bushnell, W. R., Dueck, J., & Rowell, J. B. (1967). Living haustoria and hyphae of Erysiphe graminis f. sp. hordei with intact and partly dissected host cells of Hordeum vulgare. Canadian Journal of Botany, 45, 1719 - 1732.

Bushnell, W. R. & Gay, J. L. (1978). Accumulation of solutes in relation to the structure and function of haustoria in powdery mildews. In: The powdery mildews (Ed. D. M. Spencer), pp. 183 - 235. Academic Press; London, New York, San Francisco.

Butt, D. J. (1978). Epidemiology of powdery mildews. In: The powdery mildews (Ed. D. M. Spencer), pp. 51 - 81. Academic Press; London, New York, San Francisco.

Cabantchik, Z. I., Knauf, P. A. & Rothstein, A. (1978). The anion transport system of the red blood cell. The role of membrane protein evaluated by the use of "probes". Biochimica et Biophysica Acta, 515, 239 - 302.

Campbell, C. L., Huang, J-S. & Payne, G. A. (1980). Defense at the perimeter: the outer walls and the gates. In: Plant disease, an advanced treatise. Vol. V (Eds. J. G. Horsfall & E. B. Cowling), pp. 103 - 120. Academic Press; New York, London.

Churchill, K. A. & Sze, H. (1983). Anion - sensitive, H^+-pumping ATPase in membrane vesicles from oat roots. Plant Physiology, 71, 610 - 617.

Colombo, R., DeMichelis, M. I. & Lado, P. (1978). 3-O-Methylglucose uptake stimulation by auxin and fusicoccin in plant materials and its relationship with proton extrusion. Planta, 138, 249 - 256.

Cook, R. (1977). The biology of symbiotic fungi. Wiley; London.

Cornelisse, C. J. & Van Duijn, P. (1973). A new method for the investigation of the kinetics of the capture reaction in phosphatase cytochemistry: I. Theoretical aspects of the local formation of crystalline precipitates. Journal of Histochemistry and Cytochemistry, 21, 607 - 613.

Cronshaw, J. (1980). ATPases in mature and differentiating phloem and xylem. Journal of Histochemistry and Cytochemistry, 28, 375 - 377.

Cullum, F. J. & Webster, J. (1977). Cleistocarp dehiscence in Phyllactinia. Transactions of the British Mycological Society, 68, 316 - 320.

Czaninsky, Y. & Catesson, A. (1974). Polyphenoloxidases (plants). In: Electron microscopy of enzymes: Principles and methods, vol.2 (Ed. M. A. Hayat), pp. 66 - 78. Van Nostrand Reinhold Company; New York, London.

Day, P. R. & Scott, K. J. (1973). Scanning electron microscopy of fresh material of Erysiphe graminis f. sp. hordei. Physiological Plant Pathology, 3, 433 - 435.

De Bary, A. (1870). Beitrage zur Morphologie und Physiologie der Pilze. Dritte; Rheihe.

Dekhuijzen, H. M. (1966). The isolation of haustoria from cucumber leaves infected with powdery mildew. Netherlands Journal of Plant Pathology, 72, 1 - 11.

Delrot, S. (1981). Proton fluxes associated with sugar uptake in Vicia faba leaf tissues. Plant Physiology, 68, 706 - 711.

Dixon, G. R. (1981). Downy mildews of peas and beans. In: The downy mildews (Ed. D. M. Spencer), pp. 487 - 514. Academic Press; London, New York, San Francisco.

Edelman, J., Schoolar, A. I. & Bonner, W. B. (1971). Permeability of sugar cane chloroplasts to sucrose. Journal of Experimental Botany, 22, 534 - 545.

Edwards, H. H. (1975). The ultrastructure of Ml-a-mediated resistance to powdery mildew infection in barley. Canadian Journal of Botany, 53, 2589 - 2597.

Ehrlich, M. A. & Ehrlich, H. G. (1970). Electron microscope radioautography of ^{14}C transfer from rust uredospores to wheat host cells. Phytopathology, 60, 1850 - 1851.

Esau, K. (1953). Plant anatomy. Wiley; New York, London.

Essner, E. (1973). Phosphatases. In: Electron microscopy of enzymes. Principles and methods, vol. 1 (Ed. M. A. Hayat), pp. 44 - 76. Van Nostrand Reinhold; New York.

Etherton, B. & Rubinstein B. (1978). Evidence for amino acid-H^+ co-transport in oat coleoptiles. Plant Physiology, 61, 933 - 937.

Evans, H. E. (1980). A biochemical dissection of the functional polarity of the plasma membrane of the hepatocyte. Biochimica et Biophysica Acta, 604, 27 - 64.

Fahn, A. (1974). Plant anatomy. Pergamon; Oxford.

Faull, J. L. & Gay, J. L. (1983). Phospholipase activity in Erysiphe pisi. Physiological Plant Pathology, 22, 55 - 63.

Ferguson, C. H. R. & Simon, E. W. (1973). Membrane lipids in senescing green tissues. Journal of Experimental Botany, 24, 307 - 316.

Firth, J. A. & Stranks, G. J. (1981). Localization of recently characterised membrane transport adenosine triphosphatases. Histochemical Journal, 13, 517 - 524.

Fiske, C. H. & SubbaRow, Y. (1925). The colorimetric determination of phosphorus. Journal of Biological Chemistry, 66, 375 - 400.

Franz, S. L. & Tattar, T. A. (1981). Effect of sugars and amino acids on membrane potential in two clones of sugar cane. Plant Physiology, 67, 150 - 155.

Freere, R. H. & Weibel, E. R. (1967). Stereological techniques in microscopy. Journal of the Royal Microscopical Society, 87, 25 - 34.

Fric, F. (1975). Influence of powdery mildew (Erysiphe graminis) on the activity of the non-specific phosphatase and ribonuclease in the tissues of susceptible and resistant varieties of barley. Phytopathologische Zeitschrift, 82, 266 - 271.

Fujita, M., Ohta, H., Kawai, K., Matsui, H. & Nakao, M. (1972). Differential isolation of microvillous and basolateral plasma membranes from intestinal mucosa: mutually exclusive distribution of digestive enzymes and ouabain - sensitive ATPase. Biochimica et Biophysica Acta, 274, 336 - 347.

Fulcher, R.G., McCully, M. E., Setterfield, G. & Sutherland, J. (1976). β-1,3-glucans may be associated with cell plate formation during cytokinesis. Canadian Journal of Botany, 54, 539 - 542.

Gaff, D. F. & Okong'O-Ogola, O. (1971). The use of non-permeating pigments for testing the survival of cells. Journal of Experimental Botany, 22, 756 - 758.

Gay, J. L. & Gil, F. (1975). The fungus - host interface. Proceedings of the First Intersectional Congress I.A.M.S., 2, 125 - 130.

Gay, J. L. & Manners, J. M. (1981). Transport of host assimilates to the pathogen. In: Effects of disease on the physiology of the growing plant (Ed. P. G. Ayres), pp. 85 - 100. Cambridge University Press; Cambridge.

Gay, J. L. & Manners, J. M. (1984). Permeability of the parasitic interface in powdery mildews. (In preparation).

Gil, F. (1976). Ultrastructural and physiological properties of haustoria of powdery mildews and their host interfaces. Ph.D. Thesis, University of London.

Gil, F. & Gay, J. L. (1977). Ultrastructural and physiological properties of the host interfacial components of haustoria of Erysiphe pisi in vivo and in vitro. Physiological Plant Pathology, 10, 1 - 12.

Gilula, N. B. (1974). Junctions between cells. In: Cell communication (Ed. R. P. Cox), pp. 1 - 29. Wiley; New York.

Gilula, N. B. (1980). Membrane - membrane interactions. Society of General Physiologists Series, vol. 34. Raven Press; New York.

Gomori, G. (1939). Microtechnical demonstration of phosphatase in tissue sections. Proceedings of the Society for Experimental Biology and Medicine, 42, 23 - 26.

Greenhalgh, J.R. & Mitchell, N.D. (1976). The involvement of flavour volatiles in the resistance to downy mildew of wild and cultivated forms of Brassica oleracea. New Phytologist, 77, 391 - 398.

Gunning, B. F. S. & Steer, M. W. (1975). Ultrastructure and the biology of plant cells. Edward Arnold, London.

Hall, J. L. (1969). Localization of cell surface adenosine triphosphatase activity in maize roots. Planta, 85, 105 - 107.

Hall, J. L., Browning, A. J. & Harvey, D. M. R. (1980). The validity of the lead precipitation technique for the localization of ATPase activity in plant cells. Protoplasma, 104, 193 - 200.

Hall, J. L. & Flowers, T. J. (1976). Properties of membranes from the halophyte Suaeda maritima. I. Cytochemical staining of membranes in relation to the validity of membrane markers. Journal of Experimental Botany, 27, 658 - 671.

Hanssler, G., Maxwell, D. P. & Maxwell, M. D. (1978). Ultrastructure and acid phosphatase cytochemistry of hyphae of Sclerotium rolfsii in hypocotyl tissue of Phaseolus vulgaris. Phytopathlolgische Zeitschrift, 92, 157 - 167.

Harder, D. E., Rohringer, R., Samborski, D. J., Rimmer, S. R., Kim, W. K. & Chong, J. (1979). Electron microscopy of susceptible and resistant near-isogenic (sr6/Sr6) lines of wheat infected by Puccinia graminis tritici. II. Expression of incompatibility in mesophyll and epidermal cells and the effect of temperature on host - parasite interactions in these cells. Canadian Journal of Botany, 57, 2617 - 2625.

Hardwick, N. V., Greenwood, A. D. & Wood, R. K. S. (1971). The fine structure of the haustorium of Uromyces appendiculatus in Phaseolus vulgaris. Canadian Journal of Botany, 49, 383 - 390.

Hayat, M. A. (1975). Positive staining for electron microscopy. Van Nostrand Reinhold; New York, Toronto, London, Melbourne.

Heath, M. C. (1972). Ultrastructure of host and non host reactions to cowpea rust. Phytopathology, 62, 27 - 38.

Heath, M. C. (1974). Light and electron microscope studies of the interactions of host and non host plants with cowpea rust. Physiological Plant Pathology, 4, 403 - 414.

Heath, M. C. (1976). Ultrastructural and functional similarity of the haustorial neckband of rust fungi and the Casparian strip of vascular plants. Canadian Journal of Botany, 54, 2484 - 2489.

Heath M. C. (1979). Partial characterisation of the electron-opaque deposits formed in the non-host plant, French bean, after cowpea rust infection. Physiological Plant Pathology, 15, 141 - 148.

Heath, M. C. (1982). Fungal growth, haustorial disorganisation and host necrosis in two cultivars of cowpea inoculated with an incompatible race of the cowpea rust fungus. Physiological Plant Pathology, 21, 347 - 359.

Heber, U. & Heldt, H. W. (1981). The chloroplast envelope: Structure, function and role in leaf metabolism. Annual Review of Plant Physiology, 32, 139 - 168.

Hickey, E. L. & Coffey, M. D. (1977). A fine-structural study of pea downy mildew fungus Peronospora pisi in its host Pisum sativum. Canadian Journal of Botany, 55, 2845 - 2858.

Higgins, V. J. & Miller, R. C. (1969). Comparative abilities of Stemphylium botryosum and Helminthosporium turcicum to induce and degrade a phytoalexin from alfalfa. Phytopathology, 59, 1493 - 1499.

Hirata, K. (1971). Calcium in relation to the susceptibility of primary barley leaves to powdery mildew. In: Morphological and biochemical events in plant - parasite interaction (Eds. S. Akai & S. Ouchi), pp. 207 - 223. Phytopathological Society of Japan; Tokyo.

Hirata, K & Kojima, M. (1962). On the structure and the sack of the haustorium of some powdery mildews, with some considerations of the significance of the sack. Transactions of the Mycological Society of Japan, 3, 43 - 46.

Hollander, V. P. (1971). Acid phosphatases.In: The enzymes, vol. IV (Ed. P. D. Boyer), pp. 449 - 498. Academic Press; New York, London.

Hoppe, H. H. & Heitefuss, R. (1974). Permeability and membrane lipid metabolism of Phaseolus vulgaris infected with Uromyces phaseoli: I. Changes in the efflux of cell constituents. Physiological Plant Pathology, 4, 5 - 9.

Huber, S. C. & Moreland, D. E. (1981). Co-transport of potassium and sugars across the plasmalemma of mesophyll protoplasts. Plant Physiology, 67, 163 - 169.

Humphreys, T. E. (1973). Sucrose transport at the tonoplast. Phytochemistry, 12, 1211 - 1219.

Humphreys, T. E. (1978). A model for sucrose transport in the maize scutellum. Phyochemistry, 17, 679 - 684.

Hutchings, V. M. (1978). Sucrose and proton co-transport in Ricinus cotyledons. I. H^+ influx associated with sucrose uptake. Planta, 138, 229 - 235.

Ingram, D. S. (1981). Physiology and biochemistry of host - parasite interaction. In: The downy mildews (Ed. D. M. Spencer), pp. 142 - 163. Academic Press; London, New York, San Francisco.

Itai, C. & Meidner, H. (1978). Functional epidermal cells are necessary for abscisic acid effects on guard cells. Journal of Experimental Botany, 29, 765 - 770.

Jennings, D. H. (1976). Transport and translocation in filamentous fungi. In: The filamentous fungi, vol. 2. Biosynthesis and metabolism (Eds. J. E. Smith and D. R. Berry), pp. 32 - 64. Edward Arnold; London.

Jones, G. W. & Bowen, I. D. (1980). Cytochemical characterization of phosphatase activities. In: Abstracts, VI^{th} International Histochemistry and Cytochemistry Congress (Eds. B. D. Lake, O. Bayliss High, S. J. Holt & P. J. Stoward), pp. 188 - 189. Royal Microscopical Society; Oxford.

Jones, M. G. K. & Gunning, B. E. S. (1976). Transfer cells and nematode induced giant cells of Helianthum. Protoplasma, 87, 273 - 279.

Juniper, B. E. & Lawton, J. R. (1979). The effect of caffeine, different fixation regimes and low temperature on microtubules in the cells of higher plants. Evidence

for diversity in their response to chemical and physical treatments. Planta, 145, 411 - 416.

Kasamo, K. (1979). Characterization of membrane-bound Mg^{++}-activated ATPase isolated from the lower epidermis of tobacco leaves. Plant and Cell Physiology, 20, 281 - 292.

Kijne, J. W. (1975). The fine structure of pea root nodules. 2. Senescence and disintegration of the bacteroid tissue. Physiological Plant Pathology, 7, 17 - 21.

Kinne, R. (1976). Properties of the glucose transport system in the renal brush border membrane. In: Current topics in membranes and transport, vol. 8 (Eds. F. Bonner & A. Kleinzeller), pp. 209 - 267. Academic Press; London.

Kiraly, Z. (1980). Defenses triggered by the invader: hypersensitivity. In: Plant disease, an advanced treatise. Vol. V (Eds. J. G. Horsfall & E. B. Cowling), pp. 201 - 224. Academic Press; New York, London.

Kosuge, T. (1969). The role of phenolics in host response to infection. Annual Review of Phytopathology, 7, 195 - 222.

Kramer, D. (1980). Transfer cells in the epidermis of roots. In: Plant membrane transport: Current conceptual issues (Eds. R. M. Spanswick, W. J. Lucas & J. Dainty), pp. 393 - 394. Elsevier/North - Holland; Amsterdam, New York, Oxford.

Kramer, D. (1983). The possible role of transfer cells in the adaptation of plants to salinity. Physiologia Plantarum, 58, 549 - 555.

Kuc, J. (1972). Phytoalexins. Annual Review of Phytopathology, 10, 207 - 232.

Kunoh, H. & Ishizaki, H. (1976). Accumulation of chemical elements around penetration sites of Erysiphe graminis hordei on barley leaf epidermis: (III) Micromanipulation and X-ray microanalysis of silicon. Physiological Plant Pathology, 8, 91 - 96.

Kunoh, H., Ishizaki, H. & Nakaya, K. (1977). Cytological studies of early stages of powdery mildew in barley and wheat leaves: (II) Significance of the primary germ tube of Erysiphe graminis on barley leaves. Physiological Plant Pathology, 10, 191 - 199.

Lawton, J. R. & Harris, P. J. (1978). Fixation of senescing plant tissues: sclerenchymatous fibre cells from the flowering stem of a grass. Journal of Microscopy, 112, 307 - 318.

Leath, K. T. & Rowell, J. B. (1969). Thickening of corn mesophyll cell walls in response to invasion by Puccinia graminis. Phytopathology, 59, 1654 - 1656.

Ledbetter, M. C. & Porter, K. R. (1970). Introduction to the fine structure of plant cells. Springer - Verlag; Berlin, Heidelberg, New York.

Leonard, R. T. & Hodges, T. K. (1973). Characterization of plasma-membrane-associated adenosine triphosphatase activity of oat roots. Plant Physiology, 52, 6 - 12.

Lin, W. (1981). Inhibition of anion transport in corn root protoplasts. Plant Physiology, 68, 435 - 438.

Littlefield, L. J. & Bracker, C. E. (1972). Ultrastructural specialisation at the host - pathogen interface in rust-infected flax. Protoplasma, 74, 271 - 305.

Littlefield, L. J. & Heath, M. C. (1979). Ultrastructure of rust fungi. Academic Press; New York, San Francisco, London.

Loomis, W. D. & Battaile, J. (1966). Plant phenolic compounds and the isolation of plant enzymes. Phytochemistry, 5, 423 - 438.

Lowry, O. H., Rosebrough, N. J., Farr, A. L. & Randall, R. J. (1951). Protein measurement with the Folin phenol reagent. Journal of Biological Chemistry, 193, 265 - 275.

Luft, J. H. (1961). Improvements in epoxy resin embedding methods. Journal of Biophysical and Biochemical Cytology, 9, 409 - 414.

Lupu, R., Grossman, S. & Cohen, Y. (1980). The involvement of lipoxygenase and antioxidants in pathogenesis of powdery mildew on tobacco plants. Physiological Plant Pathology, 16, 241 - 248.

MacLean, D. J., Sargent, J. A., Tommerup, I . C. & Ingram, D. S. (1974). Hypersensitivity as the primary event in resistance to fungal parasites. Nature, 249, 186 - 187.

Macri, F & Vianello, A. (1979). Inhibition of K^+ uptake, H^+ extrusion and K^+-activated ATPase, and depolarisation of transmembrane potential in plant tissues treated with Cercospora beticola toxin. Physiological Plant Pathology, 15, 161 - 170.

Maddy, A. H. (1964). A fluorescent label for the outer components of the plasma membrane. Biochimica et Biophysica Acta, 88, 390 - 399.

Manners, J. M. (1979). Physiology of fungal haustoria (Erysiphales). Ph. D. Thesis, University of London.

Manners, J. M. & Gay, J. L. (1977). The morphology of haustorial complexes isolated from apple, barley, beet, and vine infected with powdery mildews. Physiological Plant Pathology, 11, 261 - 266.

Manners, J. M. & Gay, J. L. (1978). Uptake of ^{14}C-photosynthates from Pisum sativum by haustoria of Erysiphe pisi. Physiological Plant Pathology, 12, 199 - 209.

Manners, J. M. & Gay, J. L. (1980). Autoradiography of haustoria of Erysiphe pisi. Journal of General Microbiology, 116, 529 - 533.

Manners, J. M. & Gay, J. L. (1982). Transport, translocation and metabolism of ^{14}C-photosynthates at the host - parasite interface of Pisum sativum and Erysiphe pisi. New Phytologist, 91, 221 - 244.

Manocha, M. S. (1975). Autoradiography and fine structure of host - parasite interface in temperature-sensitive combinations of wheat stem rust. Phytopathologische Zeitschrift, 82, 207 - 215.

Mansfield, J. W. & Sexton, R. (1974). Changes in the localization of β-glycerophosphatase activity during the infection of Phaseolus vulgaris by Colletotrichum lindemuthianum. Annals of Botany, 38, 711 - 717.

Marre, E. (1979). Fusicoccin: a tool in plant physiology. Annual Review of Plant Physiology, 30, 273 - 288.

Marre, M. T., Ballarin-Denti, A. & Cocucci, M. (1980). Effectes of Helminthosporium maydis T toxin on the ATPase activity of maize root membrane preparations and its sensitivity to diethylstilbestrol. Plant Science Letters, 18, 7 - 12.

Martin, T. J. & Ellingboe, A. H. (1978). Genetic control of ^{32}P transfer from wheat to Erysiphe graminis f. sp. tritici during primary infection. Physiological Plant Pathology, 13, 1 - 11.

Marx, C., Dexheimer, C. M., Gianinazzi-Pearson, V. & Gianinazzi, S. (1982). Enzymatic studies on the metabolism of vesicular-arbuscular mycorrhizas. IV. Ultracyto-enzymological evidence (ATPase) for active transfer processes in the host - arbuscule interface. New Phytologist, 90, 37 - 43.

Mendgen, K. (1977). Reduced lysine uptake by bean rust haustoria in a resistant reaction. Naturwissenschaften, 64, S.438.

Mendgen, K. & Heitefuss, R. (1975). Microautoradiographic studies on host - parasite interactions. I. The infection of Phaseolus vulgaris with tritium labeled uredospores of Uromyces phaseoli. Archiv für Mikrobiologie, 105, 193 - 199.

Mitchell, P. (1967). Translocations through natural membranes. Advances in Enzymology, 29, 33 - 87.

Mueller, W. C. & Beckman, C. H. (1974). Ultrastructure of the phenol-storing cells in the roots of banana. Physiological Plant Pathology, 4, 187 - 190.

Mueller, W. C. & Beckman, C. H. (1976). Ultrastructure and development of phenolic-storing cells in cotton roots. Canadian Journal of Botany, 54, 2074 - 2082.

Mueller, W. C. & Beckman, C. H. (1978). Ultrastructural localization of polyphenoloxidase and peroxidase in roots and hypocotyls of cotton seedlings. Canadian Journal of Botany, 56, 1579 - 1587.

Mueller, W. C. & Greenwood, A. D. (1978). The ultrastructure of phenolic-storing cells fixed with caffeine. Journal of Experimental Botany, 29, 757 - 764.

Mueller, W. C. & Rodehorst, E. (1977). The effect of some alkaloids on the ultrastructure of phenolic-containing cells in the endodermis of cotton roots. In: 35th Annual Proceedings of the Electron Microscopy Society of America (Ed. G. W. Bailey), pp.544 - 545. Electron Microscopy Society of America; Boston.

Nadler, N. J. (1971). The interpretation of grain counts in electron microscope radioautography. Journal of Cell Biology, 49, 877 - 882.

Nir, I., Klein, S. & Poljakoff-Mayber, A. (1969). Effect of moisture stress on submicroscopic structure of maize roots. Australian Journal of Biological Sciences, 22, 17 - 33.

Northcote, D. H. & Pickett-Heaps, J. D. (1966). A function of the golgi apparatus in polysaccharide synthesis and transport in the root cap cells of wheat. The Biochemical Journal, 98, 159 - 167.

Novacky, A., Ullrich-Eberius, C. I. & Luttge, U. (1978). Membrane potential changes during transport of hexoses in Lemna gibba Gl. Planta, 138, 263 - 270.

Obukowicz, M. & Kennedy, G. S. (1981). Phenolic ultracytochemistry of tobacco cells undergoing the hypersensitive reaction to Pseudomonas solanacearum. Physiological Plant Pathology, 18, 339 - 344.

Ogle, H. J. & Brown, J. F. (1971). Quantitative studies of the post-penetration phase of infection by Puccinia graminis tritici. Annals of Applied Biology, 67, 309 - 319.

Parham, R. A. & Kaustein, H. M. (1977). On the site of tannin synthesis in plant cells. Botanical Gazette, 138, 465 - 467.

Pate, J. S. & Gunning, B. E. S. (1972). Transfer cells. Annual Review of Plant Physiology, 23, 173 - 196.

Pearce, R. S. & McDonald, I. (1977). Ultrastructural damage due to freezing followed by thawing in shoot meristem and leaf mesophyll cells of tall fescue (Festuca arundinacea Schreb.). Planta, 134, 159 - 168.

Pegg, G. F. & Mence, M. J. (1970). The biology of Peronospora viciae on pea: laboratory experiments on the effects of temperature, relative humidity and light on the production, germination and infectivity of sporangia. Annals of Applied Biology, 66, 417 - 428.

Perera, R. & Gay, J. L. (1976). The ultrastructure of Sphaerotheca pannosa (Wallroth ex Fries,)Leveille and changes in infected and associated cells of rose. Physiological Plant Pathology, 9, 57 - 65.

Peters, T. & Ashley, C. A. (1967). An artefact in radio-autography due to binding of free amino acids to tissues by fixatives. Journal of Cell Biology, 33, 53 - 60.

Pitt, D. & Galpin, M. (1973). Role of lysosomal enzymes in pathogenicity. In: Fungal pathogenicity and the plants' response (Eds. R. J. W. Byrde & C. V. Cutting), pp. 449 - 465. Academic Press; London, New York.

Poole, R. J. (1978). Energy coupling for membrane transport. Annual Review of Plant Physiology, 29, 437 - 460.

Preistley, D. A. & Woolhouse, H. W. (1980). The chloroplast envelope of Phaseolus vulgaris L. II. Enzymic characteristics. Plant and Cell Physiology, 21, 709 - 717.

Pueppke, S. G. & Van Etten, H. D. (1976). The relation between pisatin and the development of Aphanomyces euteiches in diseased Pisum sativum. Phytopathology, 66, 1174 - 1185.

Quail, P. H. (1979). Plant cell fractionation. Annual Review of Plant Physiology, 30, 425 - 484.

Rasi-Caldogno,F., De Michelis, M. I. & Pugliarello, M. C. (1981). Evidence for an electrogenic ATPase in microsomal vesicles from pea internodes. Biochimica et Biophysica Acta, 642, 37 - 45.

Raven, J. A. & Smith, F. A. (1980). The chemiosmotic viewpoint. In: Plant membrane transport: Current conceptual issues (Eds. R. M. Spanswick, W. J. Lucas, J. Dainty), pp. 161 - 180. Elsevier/North-Holland; Amsterdam, New York, Oxford.

Reynolds, E. S. (1963). The use of lead citrate at high pH as an elctron opaque stain in electron microscopy. Journal of Cell Biology, 17, 208 - 212.

Robards, A. W. & Kidwai, P. (1969). Cytochemical localization of phosphatase in differentiating secondary vascular cells. Planta, 87, 227 - 238.

Robb, J., Harvey, A. E. & Shaw, M. (1975a). Ultrastructure of tissue cultures of Pinus monticola infected by Cronartium ribicola. I. Prepenetration host changes. Physiological Plant Pathology, 5, 1 - 8.

Robb, J., Harvey, A. E. & Shaw, M. (1975b). Ultrastructure of tissue cultures of Pinus monticola infected by Cronartium ribicola. II. Penetration and post-penetration. Physiological Plant Pathology, 5, 9 - 18.

Rosenthal, A. S., Moses, H. L., Beaver, D. L. & Schuffman, S. S. (1966).Lead ion and phosphatase histochemistry. I. Non-enzymatic hydrolysis of nucleoside phosphates by lead ions. Journal of Histochemistry and Cytochemistry, 14, 698 - 701.

Sabnis, D. D., Gordon, M. & Galston, A. W. (1970). Localization of adenosine triphosphatase activity in the chloroplast envelope in tendrils of Pisum sativum. Plant Physiology, 45, 25 - 32.

Salpeter, M. M. & Bachmann, L. (1972). Autoradiography. In: Principles and techniques of electron microscopy: Biological applications, vol. 2 (Ed. M. A. Hayat), pp.

221 - 278. Van Nostrand Reinhold; New York, London.

Sargent, C. & Gay, J. L. (1977). Barley epidermal apoplast structure and modification by powdery mildew contact. Physiological Plant Pathology, 11, 195 - 205.

Scarborough, G. A. (1976). The Neurospora plasma membrane ATPase is an electrogenic pump. Proceedings of the National Academy of Sciences (USA), 73, 1485 - 1488.

Schlösser, E. W. (1980). Preformed internal chemical defenses. In:Plant disease, an advanced treatise. Vol. V (Eds. J. G. Horsfall & E. B. Cowling), pp. 161 - 177. Academic Press; New york, London.

Schnathorst, W. C. (1965). Environmental relationships in the powdery mildews. Annual Review of Phytopathology, 3, 343 - 366.

Schnepf, E. (1974). Gland cells. In: Dynamic aspects of plant ultrastructure (Ed. A. W. Robards), pp. 331 - 357. McGraw - Hill; London.

Schnepf, E. & Pross, F. (1976). Differentiation and redifferentiation of a transfer cell; development of septal nectaries of Aloe and Gasteria. Protoplasma, 89, 105 - 115.

Schonherr, J. (1976). Water permeability of isolated cuticular membranes. The effect of cuticular waxes on diffusion of water. Planta, 131, 159 - 164.

Scott, K. J. (1976). Growth of biotrophic parasites in axenic culture. In: Encyclopedia of plant physiology; new series vol. 4. Physiological plant pathology (Eds. R. Heitefuss & P. H. Williams), pp. 719 - 742. Springer - Verlag; Berlin, Heidelberg, New York.

Sexton, R. & Hall, J. L. (1978). Enzyme cytochemistry. In: Electron microscopy and cytochemistry of plant cells (Ed. J. L. Hall), pp. 63 - 147. Elsevier/North Holland; Amsterdam.

Sheldon, H., Zetterquist, H. & Brandes, D. (1955). Histochemical reactions for electron microscopy: acid phosphatase. Experimental Cell Research, 9, 592 - 598.

Shiraishi, T., Oku, H., Isono, M. & Ouchi, S. (1975). The injurious effect of pisatin on the plasma membrane of pea. Plant and Cell Physiology, 16, 939 - 942.

Shiraishi, T., Oku, H., Ouchi, S. & Tsuji, Y. (1977). Local accumulation of pisatin in tissues of pea seedlings infected by powdery mildew. Phytopathologische Zeitschrift, 88, 131 - 135.

Simon, E. W. (1974). Phospholipids and plant membrane permeability. New Phytologist, 73, 377 - 420.

Singer, S. J. & Nicholson, G. L. (1972). The fluid mosaic model of the structure of cell membranes. Science, 175, 720 - 731.

Singh, J. (1979). Ultrastructural alterations in cells of hardened and non-hardened winter rye during hyperosmotic and extracellular freezing stresses. Protoplasma, 98, 329 - 341.

Slayman, C. L. (1974). Proton pumping and generalised energetics of transport: a review. In: Membrane transport in plants (Eds. U. Zimmerman & J. Dainty), pp. 107 - 119. Springer - Verlag; Berlin.

Slayman, C. W. & Slayman, C. L. (1975). Energy coupling in the plasma membrane of Neurospora: ATP-dependent proton transport and proton-dependent sugar co-transport. In: Molecular aspects of membrane phenomena (Eds. H. R. Kaback., H. Neurath, G. K. Radda, R. Schwyzer & W. R. Wiley), pp. 233 - 248. Springer Verlag; Berlin.

Slesinski, R. S. & Ellingboe, A. H. (1971). Transfer of ^{35}S from wheat to the powdery mildew fungus with compatible and incompatible parasite/host genotypes. Canadian Journal of Botany, 49, 303 - 310.

Smith, G. (1900). The haustoria of the Erysiphaceae. Botanical Gazette, 29, 153 - 184.

Smith, M. M. & McCully, M. E. (1978a). Enhancing aniline blue fluorescent staining of cell wall structures. Stain Technology, 53, 79 - 85.

Smith, M. M. & McCully M. E. (1978b). A critical evaluation of the specificity of aniline blue induced

fluorescence. Protoplasma, 95, 229 - 254.

Smith, F. A. & Raven, J. A. (1979). Intracellular pH and its regulation. Annual Review of Plant Physiology, 30, 289 - 311.

Spanswick, R. M. (1981). Electrogenic ion pumps. Annual Review of Plant Physiology, 32, 267 - 289.

Spencer-Phillips, P. T. N. & Gay, J. L. (1980a). Electron microscope autoradiography of ^{14}C photosynthate distribution at the haustorium-host interface in powdery mildew of Pisum sativum. Protoplasma, 103, 131 - 154.

Spencer-Phillips, P. T. N. & Gay, J. L. (1980b). Autoradiography, ATPase localization and transport in a plant-pathogen interface. Proceedings of the Royal Microscopical Society, 15, 112.

Spencer-Phillips, P. T. N. & Gay, J. L. (1980c). Transport into fungal haustoria. In: Abstacts, VIth International Histochemistry and Cytochemistry Congress (Eds. B. D. Lake, O. Bayliss High, S. J. Holt & P. J. Stoward), p. 352. Royal Microscopical Society; Oxford.

Spencer-Phillips, P. T. N. & Gay, J. L. (1981). Domains of ATPase in plasma membranes and transport through infected plant cells. New Phytologist, 89, 393 - 400.

Spurr, A. R. (1969). A low-viscosity epoxy resin embedding medium for electron microscopy. Journal of Ultrastructural Research, 26, 31 - 43.

Stanton, M. G. (1968). Colorimetric determination of inorganic phosphate in the presence of biological material and adenosine triphosphate. Analytical Biochemistry, 22, 27 - 34.

Staples, R. C. (1965). Acid phosphatases from healthy and rust infected pinto bean leaves. II. Effect of removing apical meristem. Contributions of the Boyce Thompson Institute, 23, 83 - 91.

Staples, R. C. & Stahman, M. A. (1964). Changes in protein and several enzymes in susceptible bean leaves after infection by the bean rust fungus. Phytopathology, 54, 760 - 764.

Stavely, J. R., Pillai, A. & Hanson, E. W. (1969). Electron microscopy of the development of Erysiphe polygoni in resistant and susceptible Trifolium pratense. Phytopathology, 59, 1688 - 1693.

Sullivan, T. P., Bushnell, W. R. & Rowell, J. B. (1974). Relations between haustoria of Erysiphe graminis and host cytoplasm in cells opened by microsurgery. Canadian Journal of Botany, 52, 987 - 998.

Swain, T. (1977). Secondary compounds as protective agents. Annual Review of Plant Physiology, 28, 479 - 501.

Syrop, M. (1975a). Leaf curl disease of almond caused by Taphrina deformans (Berk.)Tul. I. A light microscope study of the host/parasite relationship. Protoplasma, 85, 39 - 56.

Syrop, M. (1975b). Leaf curl disease of almond caused by Taphrina deformans (Berk.)Tul. II. An electron microscope study of the host/parasite relationship. Protoplasma, 85, 57 - 69.

Sze, H. & Churchill, K. A. (1981). Mg^{2+}/KCl-ATPase of plant plasma membranes is an electrogenic pump. Proceedings of the National Academy of Sciences (U.S.A.), 78, 5578 - 5582.

Takahashi, K., Inaba, T. & Kajiwara, T. (1977). Distribution of ^{14}C assimilated from $^{14}C\ O_2$ in cucumber leaves infected with downy mildew. Physiological Plant Pathology, 11, 255 - 259.

Thatcher, F. S. (1942). Further studies of osmotic and permeability relations in parasitism. Canadian Journal of Research, C21, 283 - 311.

Toyoda, H., Yano, T. & Shishyama, J. (1979). Delay of hypersensitive necrosis by thermal treatment and fungal development in powdery-mildewed barley leaves. Canadian Journal of Botany, 57, 1414 - 1417.

Tribe, H. T. (1955). Studies in the physiology of parasitism. XIX. On the killing of plant cells by enzymes from Botrytis cinerea and Bacterium aroideae. Annals of Botany, 19, 351 - 371.

Vance, C. P., Kirk, T. K. & Sherwood, R. T. (1980). Lignification as a mechanism of disease resistance. Annual Review of Phytopathology, 18, 259 - 288.

Verma, D. P. S., Kazazian, V., Zogbi, V & Bal, A. K. (1978). Isolation and characterization of the membrane envelope enclosing the bacteroids in soybean root nodules. Journal of Cell Biology, 78, 919 - 936.

Wachstein, M. & Meisel, E. (1957). Histochemistry of hepatic phosphatases at a physiologic pH with special reference to the demonstration of bile caniculi. American Journal of Clinical Pathology, 27, 13 - 23.

Ward, E. W. B., Unwin, C. H. & Stöessl, A. (1973). Post-infectional inhibitors from plants. VII. Tolerance of capsidol by fungal pathogens of pepper fruit. Canadian Journal of Botany, 51, 2327 - 2332.

Wardrop, A. B. & Cronshaw, J. (1962). Formation of phenolic substances in the ray parenchyma of angiosperms. Nature, 193, 90 - 92.

Washitani, I. & Sato, S. (1976). On the reliability of the lead salt precipitation method of acid phosphatase localization in plant cells. Protoplasma, 89, 157 - 170.

Weibel, E. R., Kistler, G. S. & Scherle, W. F. (1966). Practical stereological methods for morphometric cytology. Journal of Cell Biology, 30, 23 - 38.

West, I. C. (1980). Energy coupling in secondary active transport. Biochima et Biophysica Acta, 604, 91 - 126.

Wheeler, H. & Hanchey, P. (1968). Permeability phenomena in plant disease. Annual Review of Phytopathology, 6, 331 - 350.

Williams, P. H. & Staples, R. C. (1964). Acid phosphatases from healthy and rust infected pinto bean leaves. Contributions of the Boyce Thompson Institute, 22, 269 - 282.

Winter-Sluiter, E., Läuchli, A. & Kramer, D. (1977). Cytochemical localization of K^+-stimulated adenosine triphosphatase activity in xylem parenchyma cells of barley roots. Plant Physiology, 60, 923 - 927.

Withers, L. A. (1976). Studies on the growth in culture of plant cells. XXI. Fine structural features of Acer pseudoplatanus L. cells responding to 2,4-dichlorophenoxyacetic acid withdrawal in turbidostat culture. Journal of Experimental Botany, 27, 1073 - 1084.

Woods, A. M. & Gay, J. L. (1983). Evidence for a neckband delimiting structural and physiological regions of the host plasma membrane associated with haustoria of Albugo candida. Physiological Plant Pathology, 23, 73 - 88.

Wylie, R. B. (1952). The bundle sheath extension in leaves of dicotyledons. American Journal of Botany, 39, 645 - 651.